

Department of Biomedical Engineering

University of Strathclyde



The development of an adaptive and reactive interface system for lower limb prosthetic application

Jake Bagwell

2022

A thesis presented in fulfilment of the
requirements for the
degree of Engineering Doctorate in Medical
Devices

Supervisors: Dr Arjan Buis, Dr Mario Giardini

Declaration

This thesis is the result of the author's original research. It has been composed by the author and has not been previously submitted for examination, leading to the award of a degree.

The copyright of this thesis belongs to the author under the terms of the United Kingdom Copyright Acts as qualified by the University of Strathclyde Regulation 3.50. Due acknowledgement must always be made of the use of any material contained in, or derived from, this thesis.

Signed:

A handwritten signature in black ink, appearing to read "B. Bagwell", is written on a light-colored rectangular background.

Date: 29/10/2022

Acknowledgements

I would like to recognise the valuable help provided to me throughout the duration of my research. Firstly, my supervisor Dr Arjan Buis for his support and assistance in putting forward ideas and suggesting avenues to explore whilst allowing me the freedom to progress the project independently. Secondly, I to Dr Mario Giardini for providing invaluable technical advice throughout my time at the university.

A special thank you is reserved for the Engineering and Physical Sciences Research Council (EPSRC) for providing the support and funding required to make this research possible (EP/L015595/ with further thanks to the Centre of Doctoral Training (CDT) for their excellent service and encouragement throughout the project.

I am also incredibly grateful to those who have supported me throughout my academic career. I am fortunate to have family and friends that provide stability and push me towards my goals.

List of Figures

Figure 1: Computational model of the magnitude of von Mises stresses evident around the residual limb of a below-knee amputee (S. Portnoy Z. N.-M.-N., 2008)	21
Figure 2: An overview of the initial proof of concept study for tibial stabilisation and subsequent reduction in the risk of DTI.....	24
Figure 3: outline of the expected feedback loop for stabilisation mechanism.....	25
Figure 4: Chronic ulcerations identified in stump skin (K. Wolff, 2011).....	31
Figure 8: The relationship with cell survival when loaded over time (A. Gefen B. v., 2008).	35
Figure 9: The average simulated Von-mises stresses generated from walking over different terrains (S. Portnoy, 2010).....	39
Figure 10: F-Scan sensor pressure sensor array for sole pressure monitoring	47
Figure 5: the displacements of the tibia ends of 7 patients as identified by X-ray (M. Lilja, 1993), showing oscillation about the mean mid-stance position during various stages of stance and swing.	50
Figure 6: Ultrasound imaging allowed for the monitoring of residual femur oscillation about its average position during walking, showing significant movement in every plane of motion (P. Convery K. D., 2001)	51
Figure 7: Moments measured about the centre of mass of a residual limb socket complex of a below-knee amputee, showing the direction and point of reaction likely to occur on the user during gait (T. Kobayashi, 2016).....	54
Figure 11: the Hero Arm utilises a proportional actuator control based on the magnitude of muscle movement detected by EMG sensors (Bionics, 2018)	60
Figure 12: Step wise process to produce a variable impedance prosthetic socket based on tissue stiffness measurements at the skin's surface (D. M. Sengeh H. H., 2013).....	62

Figure 13: Basic block diagram illustrating how positional data from the limb will be responded to by an effector in a feedback loop.....	75
Figure 14: Pugh's matrix example (Ullman, 2006).....	76
Figure 15: Signal generation using a Hall effect sensor (AspenCore, 2014).....	78
Figure 16: Arduino UNO.....	87
Figure 17: Left) SLA Resolution and surface finish, Right) FDM Resolution and surface finish.	99
Figure 18: Vectors generated by a simplified marker configuration.	104
Figure 19: Magnetic field line orientations tested to establish which produced measurable changes in input over the largest range.....	109
Figure 20: Experimental set-up, using digital callipers to measure the displacement between the Hall effect sensor and magnet.....	109
Figure 21: Graph showing the difference in sensor measurement for the same magnet depending on its orientation.....	111
Figure 22: Graph showing the difference in sensor measurement for different magnet sizes	111
Figure 23: shows the difference in measured gauss depending on the direction of the magnet.	112
Figure 24: A diagram of the stilt like orthotic designed for able-bodied experimentation, complete with how the design would allow similar moments about the participants shank during gait.....	115
Figure 25: A custom socket liner for use with the open-ended socket to increase comfort and fit of the overall orthotic	116
Figure 26: Completed socket pre-machining.....	116

Figure 27: Final, machined, open ended socket used to develop the initial prototype orthotic device for trials	117
Figure 28: A cam designed to apply 25mm extension at full rotation.....	118
Figure 29: In-built collar to allow simple attachment to servo rotor.....	118
Figure 30: piston housing and servo housing mount	119
Figure 31: In-built bearing housing to allow low friction conversion of torque to linear motion.	119
Figure 32: Piston complete with pin holes for bearing connectors to be fitted	120
Figure 33: The piston housing was shaped to fit comfortably with the participant's shank, the socket, and the shape of the piston.....	120
Figure 34: The piston housing was combined with the structure to carry the servo housing.	121
Figure 35: Detachable housing for the Futaba Servos	122
Figure 36: Underside of the servo housing mount, showing in more detail the space for the electromagnet attachment.	122
Figure 37: Assembly of the 3D printed components.	123
Figure 38: The underneath of the servo housing	123
Figure 39: 3D-printed components assembled in conjunction with a Futaba servo.....	124
Figure 41: Completed orthotic device for initial able-bodied trials.....	125
Figure 42: Open-ended socket mounted with Futaba servos and associated 3D-printed components.	125
Figure 43: Alignment of the connecting bar was important in reducing obstruction of the shank.	127
Figure 44: Circuit design, showing connections between the Hall effect sensing circuit, Arduino Uno and Futaba servos.	128

Figure 45: Diagram visualising the vector angles that were compared with the CAREN device.
..... 137

Figure 46: Initial magnetic field measurements taken by two initial walks for system characterisation and troubleshooting. 138

Figure 47: A misstep in the second walk, showing clear differences from the norm. 139

Figure 48: Walk 3 separated to better visualise the Hall effect measurement of a slip and the attempt at recovery made by the participant. 141

Figure 49: Magnetic field measurements taken during initial trials with the servos engaged.
..... 141

Figure 50: 33 suitable gait cycles as measured by the Hall effect sensor without servo engaged.
..... 143

Figure 51: 32 individual gait cycles as measured by the Hall effect sensor. 143

Figure 52: Representation of all off cycles corrected to ensure each walk was measured as a percentage of a full gait cycle. 144

Figure 53: Box plot showing the Gauss measurement at HC with the device disengaged versus engaged. 145

Figure 54: Box plot showing the full spread of the Gauss measurement with the device disengaged versus engaged. 145

Figure 55: Average gauss measurements with the stabilisation device off versus on 145

Figure 56: Box plot showing the Gauss measurement during Swing with the device disengaged versus engaged. 146

Figure 57: Box plot showing the Gauss measurement at TO with the device disengaged versus engaged. 146

Figure 58: Box plot showing the Gauss measurement at Midstance with the device disengaged versus engaged. 146

Figure 59: The general pattern of anterior and posterior angle with servos disengaged.	148
Figure 60: Shows the range of measured angle change of both the anterior (Top set) and posterior (Bottom set) vectors against the centre line of the orthotic	150
Figure 61: Shows the range of measured angle change of both the anterior (Top set) and posterior (Bottom set) vectors against the centre line of the orthotic.	150
Figure 62: Anterior and Posterior vector angles calculated from data derived from the Motek CAREN system while the servos were engaged.	151
Figure 63: gait cycles compared as a gait percentage to allow greater comparison of gait stages.	152
Figure 64: Average gait cycles vector angle for anterior CAREN data Top) device disengaged, Bottom) device engaged.	153
Figure 65: Distribution of Anterior Disengaged Data	155
Figure 66: Distribution of Anterior Engaged Data	155
Figure 67: Distribution of Posterior Disengaged Data	156
Figure 68: Distribution of Posterior Engaged Data	156
Figure 69: Top) Average anterior angles with servos engaged versus disengaged, Bottom) Average posterior angles.	157
Figure 70: Vector angle averages corrected about the median values of each data set.	158
Figure 71: Box plot showing the full spread of the posterior vector angle measured with the device off versus on.	159
Figure 72: Box plot showing the full spread of the anterior vector angle measured with the device off versus on.	159
Figure 73: Left) Anterior vector angles at Mid-Stance, Right) Posterior vector angles at Mid-Stance.	160
Figure 74: Left) Anterior vector angles at HC, Right) Posterior vector angles at HC	160

Figure 75: Left) Anterior vector angles at Swing, Right) Posterior vector angles at Swing. 161

Figure 76: Left) Anterior vector angles at TO, Right) Posterior vector angles at TO..... 161

Figure 77: Hall Effect data superimposed with Caren Vector Angle for reference..... 164

Figure 78: Circuit design, showing connections between the Hall effect sensing circuit, Arduino Uno and Futaba servos220

Abstract

Deep tissue injury (DTI) is a known problem correlating to the use of a prosthetic by a transtibial amputee (TTA), causing ulcer-like wounds on the residual limb caused by stress-induced cell necrosis. The magnitude of these stresses at the bone tissue interface has been identified computationally, far exceeding those measured at the skin's surface. Limited technology is available to directly target and reduce such cellular loading and actively reduce the risk of DTI from below-knee use.

The primary aim of this project was to identify whether a bespoke prosthetic socket system could actively stiffen the tissues of the lower limb. Stabilising the residual tibia during ambulation and reducing stress concentrations on the cells. To achieve this, a proof-of-concept device was designed and manufactured, a system that allowed the change in displacement of a magnet to be responded to by counterbalancing load. The device was evaluated through experimentation on an able-bodied subject wearing an orthotic device designed to replicate the environment of a prosthetic socket. The chosen sensor effector system was validated against vector data generated by the Motek Medical Computer Assisted Rehabilitation Environment (CAREN.)

The project explored a new concept of reactive loading of a below-knee prosthesis to reduce tibial/socket oscillation. The evaluation of the device indicated that external loading of the residual limb in such a manner could reduce the magnitude of rotation about the tibia and therefore minimise the conditions by which DTIs are known to occur. Efforts were made to move the design to the next iteration, focusing on implementing the target demographic.

Table of Contents

Declaration.....	1
Acknowledgements.....	2
List of Figures.....	3
Abstract.....	9
1.1 Background.....	18
1.2 Motivations and Objectives.....	21
1.3 Device Outline.....	22
1.4 Thesis Outline.....	26
Chapter 2 – Background Literature Review.....	26
Chapter 3 – Methodology and Initial System Design.....	26
Chapter 4 – Detailed Design.....	26
Chapter 5 – Experimentation on Participant.....	27
Chapter 6 – Discussion of Future Work Considerations.....	27
Chapter 7 – Conclusions.....	27
2.1 Introduction.....	28
2.2 Historical Background.....	29
2.2.1 Transtibial Prosthetics.....	29
2.2. Research Relevant Physiology.....	30
2.2.1 Deep Tissue Injury.....	30
2.2.1.1 Soft Tissue Deformation.....	34
2.2.1.2 Tissue Morphology and Mechanical Properties.....	42

2.2.1.3 Ischemia and Reperfusion	43
2.2.1.4 Sensory Impairment	43
2.2.1.5 Socket Design	44
2.2.1.6 Prosthetic Make Up.....	44
2.2.1.7 Prosthetic Liner	45
2.3. Socket and Residual Limb Environment	47
2.3.1. Residual Limb Volume Change	47
2.3.2. Variations in Socket Casting Techniques	48
2.3.3. Residual Bone Movement and Moments About Below-Knee Amputees	49
2.4. Bone Movement Identification	55
2.4.1. Magnetic Resonance Imaging	55
2.4.3. Computed Tomography	56
2.4.4. Near-Infrared Spectroscopy	57
2.4.5. Ultrasound Imaging	57
2.5. Control Systems in Prosthetics	58
2.5.1 Natural Control Systems	59
2.5.2 Control Systems in Prosthetics	59
2.6. Technological Advances in Prosthetic Sockets	61
2.6.1 Stress Mitigation in Lower Limb Prosthetics	62
2.6.2 Adjustable Sockets.....	63
2.7. Hall Effect.....	64

2.7.1. Hall Effect in Prosthetics	65
2.7.2. Implantation	66
2.8. Conclusions.....	68
3.1 Introduction.....	71
3.2 Task Clarification.....	71
3.2.1 Problem Statement.....	71
3.2.2 Research-Defined Requirements	72
3.2.3 Device Demands	72
3.2.4 Device Wishes	73
3.2.5 Device Design Specification (Arranging and Checking of Requirements).....	74
3.3 Concept Components, Materials and Processes.....	74
3.3.1 Component Evaluation.....	75
3.3.2 Displacement Sensor.....	77
3.3.2.1 Hall Effect.....	78
3.3.2.2 Light.....	79
3.3.2.3 Pressure	79
3.3.2.4 Ultrasound.....	80
3.3.2.5 Tissue Stiffness	80
3.3.2.6 Electromyography.....	81
3.3.2.7 Pugh’s Comparison.....	83
3.3.2.8 Conclusion	86

3.3.3 Microcontroller	86
3.3.4 Actuator.....	88
3.3.4.1 Hydraulic.....	88
3.3.4.2 Pneumatic.....	88
3.3.4.3 Electrical Linear.....	89
3.3.4.4 Electrical Rotary	89
3.3.4.5 Comparison	89
3.3.4.6 Conclusion	91
3.3.5 Socket Manufacture	91
3.3.5.1 Hands-On	91
3.3.5.2 Hands-off	92
3.3.5.3 3D Printing.....	93
3.3.6 Structural Component Manufacture.....	94
3.3.6.1 Computer-Aided Design	94
3.3.6.2 Additive Layer Manufacturing Techniques	95
3.3.7 Device Testing Methods	101
3.3.7.1 Sensor Feedback	101
3.3.7.2 Motek Computer-Assisted Rehabilitation Environment.....	101
3.3.7.3 Participant Survey	104
3.4 Discussion.....	105
4.1 Introduction.....	107

4.2 Detailed Design.....	107
4.2.1 Actuator System.....	107
4.2.2 Hall Effect Sensor Configuration.....	109
4.2.2.1 Results.....	111
4.2.2.2 Conclusions.....	113
4.2.3 Socket Manufacture	114
4.2.4 Structural Components.....	117
4.2.4.1 Computer-Aided Design	118
4.2.4.2 Manufacture	125
4.2.5 Circuitry	128
4.2.5.1 Required Servo Angle against Measured Magnetic Field Density	129
4.2.6 Coding and Control Systems	129
4.2.7 Control Systems	130
4.3 Conclusion	131
5.1 Introduction.....	134
5.2 Methodology	135
5.2.1. Experimental Procedure.....	135
5.2.2 Data Acquisition and Feedback	136
5.2.2.1 Initial Magnetic Field Measurements (stabilisation disengaged)– Trial Troubleshooting	138
5.2.2.2 Initial magnetic field Measurements (stabilisation engaged)– Trial Troubleshooting	140

5.3 Results.....	142
5.3.1 Hall Effect Data Acquisition.....	142
5.3.1.1 Magnetic Field Measurements.....	142
5.3.2.1 Anterior and Posterior Vector Angles – No Servo Engaged	148
5.3.2.2 Anterior and Posterior Vector Angles – Servo Engaged	151
5.3.2.3 Data Correction for Comparison.....	152
5.4 Discussion.....	165
5.4.1 System Performance	165
5.4.2 Angle Change.....	168
Anterior Vector	169
Posterior Vector	170
5.4.3 Contribution to Knowledge.....	171
5.4.4 Mitigation Criteria for Future Design and Experimental Iterations.....	172
5.5 Conclusions.....	172
6.1 Introduction.....	174
6.2 Discussion.....	174
6.2.1 The Need.....	174
6.2.2 The Design.....	175
6.2.3 Hall Effect Sensing	175
6.2.4 Arduino Controlled Rotary Actuation	175
6.2.5 Structural Components.....	176

6.2.6 The Design Process.....	177
6.2.6 Confidence in Scoring Matrix Methods.....	178
Benefits	178
Limitations	178
6.2.7 Testing and Validation.....	179
6.2.8 Able-Bodied Trial	180
6.2.9 Design Enhancement Based on Trial Feedback.....	181
6.2.10 Device Implications	181
6.3 Future Work and Development.....	182
6.3.1 Electrostatic Materials	182
6.3.2 Shear Stress Measurement	183
6.3.3 Magnet Implantation.....	184
6.3.4 Embodiment for Productisation	185
Further Device Development.....	186
Alternative routes of control	186
Clinical Implementation.....	187
7.1 Introduction.....	190
7.3 Conclusions.....	190
Bibliography	192
Appendix - A.....	219
Circuit diagram for proof of concept device.....	220

Appendix – B221

 Ethics application for participant trialling221

Appendix - C.....229

 Open CV Code.....229

Chapter 1 Introduction

1.1 Background

Lower limb prosthetics have reportedly been used for 3500 years (Fliegel, 1966), with archaeological finds dating back to the peak of the Egyptian empire. However, examples found were often solely used as cosmetic replacements rather than functional equivalents, with a shift towards functional prostheses occurring much later. The shift change in design allowed a better fit and essential ambulation (Vanderwerker, 1976), which was thought to be directly linked to the growth in the knowledge and understanding of amputation surgery. As developments in prosthetics progress to meet the wants and needs of users, such as device comfort, efficiency, and a lifelike appearance (Marks, 2001), it is well known that modern prosthetics are far from perfect. Risks such as skin conditions in the form of pressure ulcers (PUs) and deep tissue injury (DTIs) are still evident.

Often categorised alongside PUs, DTIs refer to ulcers that originate at the tissue-bone interface rather than the socket-skin interface (Gefen 2013) and will act as the primary focus problem being targeted in the work demonstrated in this document.

DTIs are defined as tissue damage at which the tissue loses its ability to recover. This inability to naturally recover through primary healing is caused by the progression of cell necrosis in the tissue (Stroncek, 2008). A demographic at particular risk is prosthetic-wearing trans-tibial amputees (TTAs), as damage migrates towards the skin's surface from the bone tissue interface (Graser, 2020). This damage can only be accurately diagnosed up to two weeks after its propagation through the tissue, with the traditional treatments requiring limb immobilisation, immediate wound care management and potential hospitalisation to save further damage or the possible need for further amputation. Removing their ability to ambulate with their prosthesis for significant periods is a scenario that could harm the amputee's quality of life.

The conditions under which cell necrosis occurs are directly linked to stresses exerted upon them reaching excessive magnitudes or where lower pressures are endured over sustained periods. The cells' resistance is overcome in both situations, stimulating their death (Wu, 2016). Previous studies have indicated that if a cell experiences a strain of 0.5 (65%) for an hour or more, it is likely to become necrotic. These studies highlighted the risks of significant strains on muscle tissues, which have been identified in the residuum of below-knee amputees while walking (Gefen 2008). Further to compressive strains, DTIs have been identified to result from other conditions, most notably shear strains. Shear strains are a risk for TTAs, with shear strains generated by tissue flow over a bony prominence, such as the tibia end, common (Gefen, 2007). The computational simulation found that significant differences can be seen at the muscle-bone interface compared to the skin-socket interface, with additional issues being found when the TTAs were ambulating over different terrains (S. Portnoy J. v.-N., 2010). Results indicate peak heel contact (HC) stresses, mainly when the participant walked downhill. Studies of tibial movement during gait have confirmed significant tissue flow about the tibial end, particularly at HS (~10mm from normal mid-stance position) and TO (Lilja, 1993). Further, x-rays of a TTA at the significant stages of gait have revealed the extent to which the tibia position is altered when coupled with a lower limb prosthetic. This factor was mirrored by a real-time ultrasound study of trans-femoral amputees, with the femur angle being recorded to vary $\pm 8^\circ$ from its mid-stance position in both its sagittal and coronal planes (Convery, 2001).

It is possible to introduce the potential for a medical device to aid in alleviating the risks posed by the flow of tissue around the tibial end of a below-knee prosthetic user. A system designed to detect the displacement of the tibial end and provide a counterbalancing influence on the entire environment, reducing the risk of DTIs whilst being integrated into a lower limb prosthesis. Allowing the wearers to carry out their typical day-to-day activities with reduced risk. An attempt at reducing stress localisation on the residual limb of below-knee amputees

was carried out by Sengeh, focusing on targeting the reduction of stress at the surface of the skin. He produced a variable stiffness socket that reduced the peak stresses measured at the skin's surface (Sengeh 2013). It was designed to allow identified areas of the lower limb to be carried by a correspondingly stiff material, allowing universal distribution of load across the limb and, thus, reducing localised stress concentration. Despite the successful approach of the study, evidence generated by FEA has indicated that despite stresses at the skin's surface, far more severe and, therefore, significant stresses occur at the distal end of the tibia in TTAs (up to four times larger than the skin interface levels as shown Figure 1 (S. Portnoy, 2008).

Estimating the true prevalence of DTIs in below-knee amputees is currently difficult. The wide range of prevalence rates can be attributed to the differences in study populations, methodologies, and definitions of DTI used in various studies. Although with, it is estimated that up to 65% of people with amputation experience dermatologic issues such as ulcers and pressure sores (Highsmith, 2016). It needs to be confirmed to what extent DTIs are more or less prevalent than PUs due to the similarity in appearance and overall classification.

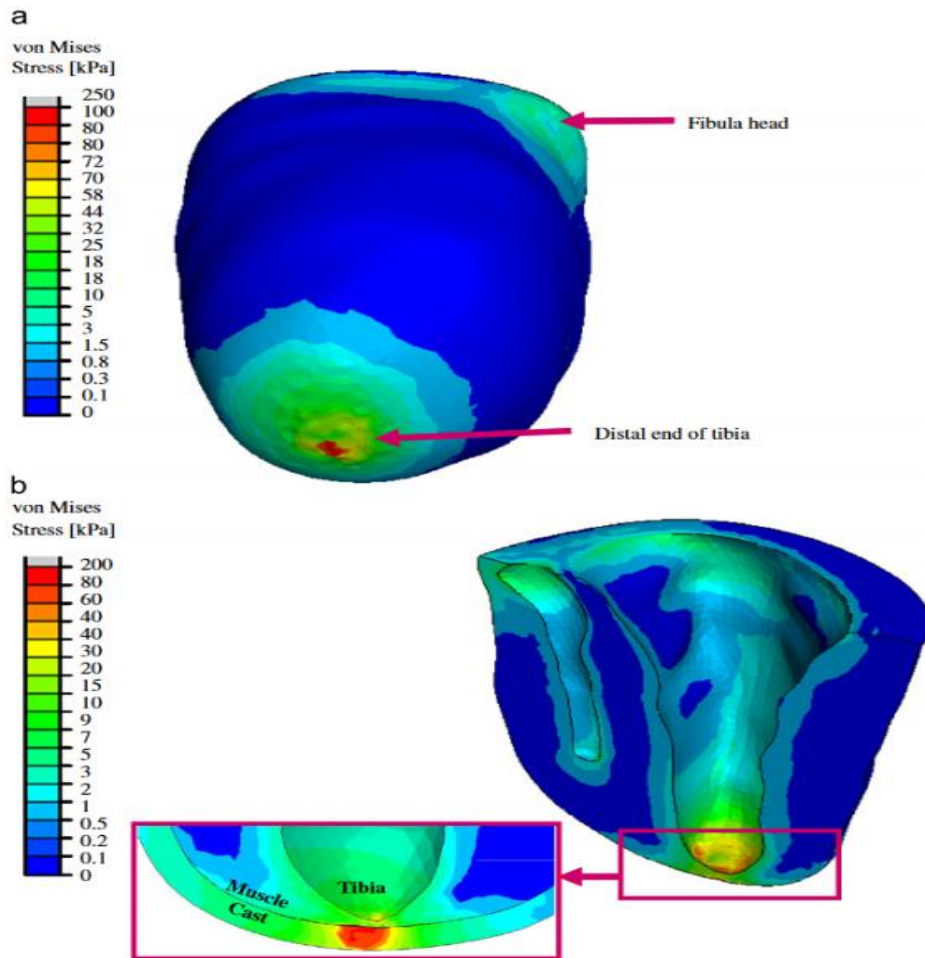


Figure 1: Computational model of the magnitude of von Mises stresses evident around the residual limb of a below-knee amputee (S. Portnoy Z. N.-M.-N., 2008)

1.2 Motivations and Objectives

Given this, the work presented in this thesis aims to evaluate whether a bespoke prosthetic socket system could actively stiffen the tissues of the lower limb, stabilising the residual tibia during ambulation, by building on the concept of adjustable panel prosthesis and exploring the potential for providing powered panels to antagonistically load the tissues of the limb during gait. It is hypothesised that the technology employed that the additional loading would stiffen the tissues surrounding the bony prominence of the tibial end, a reduce its flow about the point limiting the development of shear strains a key factor in the development of DTI.

To prove the concept proposed. A method was devised to detect tibial movement and identify the magnitude of displacement away from its mid-stance position. Providing the information by which an effector response could be generated, allowing external loading to be generated at both the anterior and posterior of the shank during walking.

Conceptualise, design, and manufacture a prototype device and validate its performance through trialling, data acquisition, and analysis. Making it possible to compare its output and envision further enhancements.

It was also preferable to identify how technology could be integrated and tested with a TTA while identifying whether the techniques chosen for the initial system design could be successfully upgraded to allow significant tests on the target demographic without requiring invasive procedures.

1.3 Device Outline

With the objectives outlined, a summary of the final concept is provided. With the initial device designed as a proof of concept for verification with a non-disabled participant, a bespoke orthotic was manufactured to emulate the environment of a below-knee prosthesis as closely as possible. Allowing the socket wall to revolve around the shank in the same manner expected from a prosthetic user, as shown in Figure 2.

The sensor actuator system forms a simple feedback loop with an Arduino microcontroller stimulating the response from the actuators based on the movement of the magnet placed on the participant's shank relative to the orthotic prosthetic wall, as represented in Figure 3. It is thought that applying antagonistic loading at the skin surface would allow the compression and stiffening of the tissues surrounding the bony prominence, limiting the potential for dangerous cellular shear stresses to occur during ambulation.

Bespoke stilt orthotic allowing a participant to walk generating oscillations about the shank as would be expected from a prosthetic user.

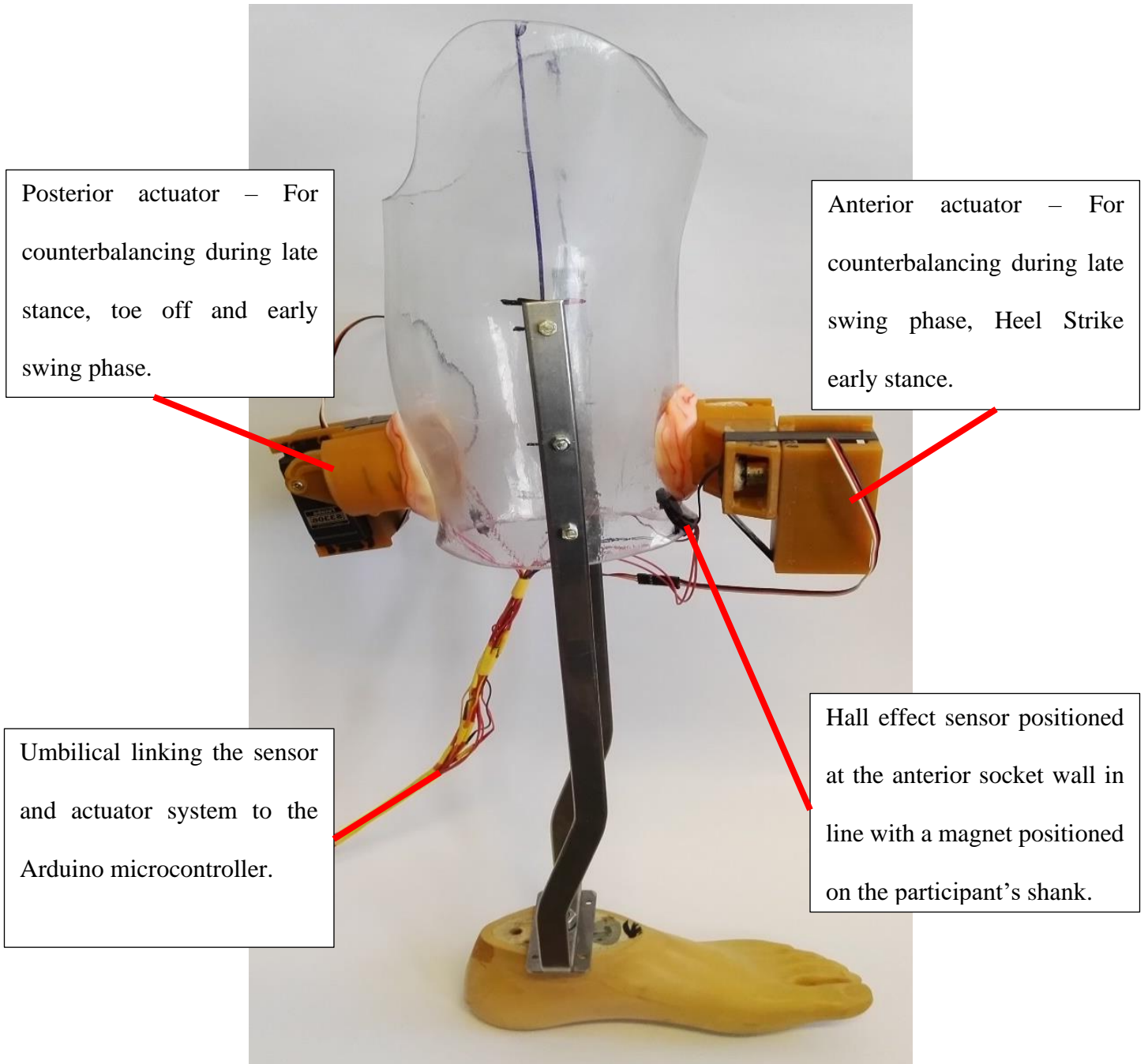


Figure 2: An overview of the initial proof of concept study for tibial stabilisation and subsequent reduction in the risk of DTI.

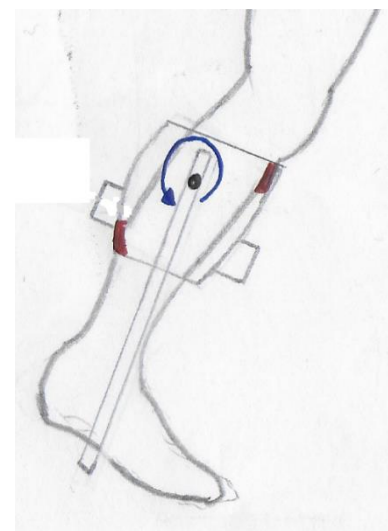
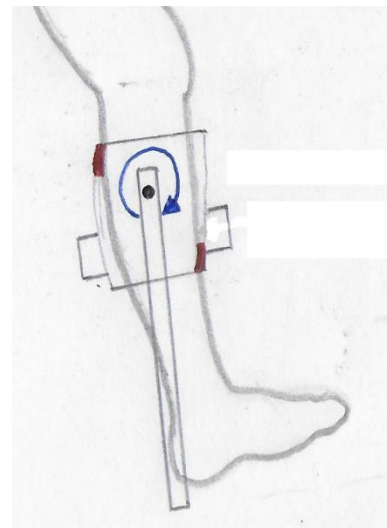
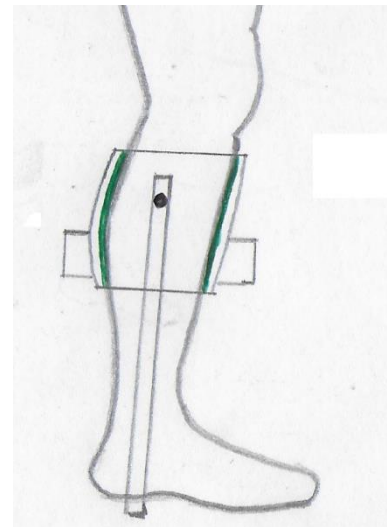
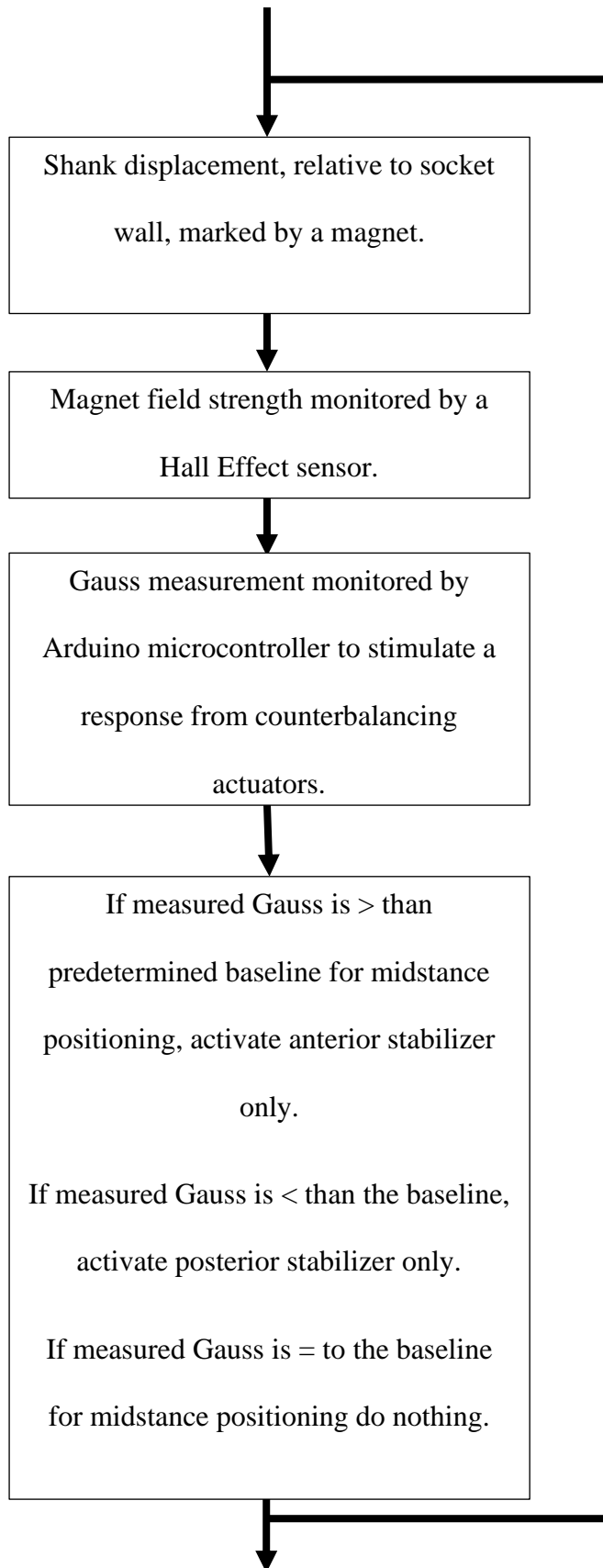


Figure 3: outline of the expected feedback loop for stabilisation mechanism.

1.4 Thesis Outline

Chapter 2 – Background Literature Review

A review of the background literature was undertaken, exploring deep tissue injury in greater detail, evaluating the information concerning its causation in prosthetic users, as well as in the broader wound care field, while highlighting research that has explored the mechanisms by which cell necrosis is found to occur (namely shear and compressive stresses and strains.) Further details of how residual limb composition is developed at amputation and represented in finite element studies will be considered before contributing project factors, such as control system methodologies and sensor types for bone movement application, will be reviewed.

Chapter 3 – Methodology and Initial System Design

Chapter 3 draws on the knowledge gathered from the literature review, identifying critical characteristics allowing the strategic development of a product design template to be created and followed. This process allowed the heuristic design and evaluation of potential concepts into a final detailed design, followed by proof by concept testing and interpretation of the subsequent results. Finally, the final detailed design was taken through clinical trials, accompanied by a review of the total design process and results.

Chapter 4 – Detailed Design

Chapter 4 gives a breakdown of the components and technology used to develop the first-generation prototype for the device, with an introduction of how the techniques and methods mentioned in previous chapters were utilised to manufacture and combine the various technologies to produce a functioning device.

Chapter 5 – Experimentation on Participant

Following the initial device's design and manufacture, it was possible to explore its performance in a verification trial, utilising the Computer-Assisted Rehabilitation Environment (CAREN) motion tracking software to help validate the data gathered and respond to the stabilisation system. MOTEK Entertainment is a company based on the motion capture and animation of real-world activities in film, television, and video games. Their use of body tracking cameras makes it possible to record the movement of people carrying out specific activities to create an enhanced and realistic representation in Computer-generated Imagery (CGI). In an offshoot of this work, MOTEK Medical uses similar techniques for physically and mentally rehabilitating patients suffering from problems ranging from Post-Traumatic Stress Disorder (PTSD) to stroke (VICON, 2013). The chapter details the trial's design and purpose, including an analysis of the results and a discussion of their implications before evaluating the significance of the data and how future iterations of its design could be developed.

Chapter 6 – Discussion of Future Work Considerations

Chapter 6 provides a succinct discussion of the project could be progressed in further iterations of the design. Highlight how the device might differ due to design greater for further clinical implementation and trialling.

Chapter 7 – Conclusions

Chapter 7 reviews the work carried out during the project's timeline, highlighting the contributions made towards completing the initial statements of intention made in Chapter 1, with a comprehensive review of the results generated from the previous chapters, followed by concluding statements drawn from the findings.

Chapter 2 Literature Review

2.1 Introduction

This chapter explores the potential of a lower limb prosthetic stabilisation system to sense and identify the residual tibia's movement trajectory during a TTA's ambulation. Utilising a control system, it was hypothesised that significant stabilisation of tibial movement could reduce the development of shear and compressive strains within the tissues of the residual limb, reducing the risks of conditions such as DTI. The following sections of this chapter aim to provide information on available scientific work conducted by researchers and research groups that have influenced the subject area.

Section 2.2 details the broader areas of the topic, focusing on defining DTI and its causes. Before understanding its prevalence in prosthetic users and how the socket limb environment influences the known contributing factors. Followed by a review of previously developed systems and their mechanisms of reducing stress concentrations on the lower limb. Section 2.3 will focus on the theoretical studies that are more directly linked to the subject and the main aims and objectives of the thesis, exploring the methods and theories designed to identify specific causes of DTI and cell necrosis. Next, the document will summarise studies designed to monitor and measure stress concentrations on the residual limb of lower limb amputees. The following sections will look at device-related topics, such as the issue of sensing bone movement and suitable control and effector response mechanisms that could be applied to help stabilise tibial movement. Finally, information on amputee-related experiments will be reviewed, identifying how investigations have been designed in the past to achieve suitable data and whether changes should be made.

2.2 Historical Background

2.2.1 Transtibial Prosthetics

Prosthetic socket design has long been a focus of research and development, especially with the shift from cosmetic to functional prosthetics seen in more recent years. Laing et al. highlights how transtibial prosthetic sockets have changed dramatically, from early cone-shaped varieties to the total surface bearing (TSB) versions available today (Laing, 2011). The review of articles from the past five decades details the shift in prosthetic socket design, with key developments in sensor technology and computational modelling being significant contributing factors. These changes have allowed for better mapping of stresses on the skin's surface and within the tissues of the residual limb. Meanwhile, pressure casting has allowed for a more significant redistribution of stresses across the limb's surface, making for more comfortable sockets. Differing from the traditional patellar tendon bearing (PTB) sockets that focus on shifting high stresses to more tolerant regions of the residuum. Laing et al. concluded that the evidence suggests hydrostatic sockets (produced from pressure casting) may provide a more comfortable fit; however, more studies are required to confirm that they can supersede PTB sockets (Laing, 2011).

FEA use in socket design presents difficulties, particularly regarding modelling a residual limb. Each limb is unique, not only in terms of geometry but also in the composition of the limb itself, with residual limbs comprising varying tissue thicknesses and tissue makeups (percentage of muscle, fat, or scar tissue.) The measurement requires a scan of an individual's residual limb, such as Magnetic Resonance Imaging (MRI). This makes it challenging to extrapolate FEA data to the general prosthetic-using community. However, the ability to predict stresses within the residual limb is becoming of greater interest, with the identification of DTI as a significant problem in the lower limb prosthetic using community. Faustini et al.

confirmed the difficulties of manufacturing prosthetic sockets based on FEA designs in their experimental socket manufacture using selective laser sintering (SLS) based on computational modelling (Faustini, 2006). The indication was that the critical difficulty of producing prosthetic sockets through computational techniques was due to the variability in different amputees' residual limbs. A full 3D scan of their residual limb would be required before a socket could be customised for an individual, a concept that is impossible for many lower limb amputees. However, it was suggested that the technique had benefits, including reduced manufacturing time and less pressure exerted on prosthetists. Designing and manufacturing sockets in this manner shows potential for improving the supply against the increasing need for prosthetics, with population increases and the prevalence of vascular diseases seeing, on average, 185,000 amputations per year in America alone (Coalition, 2017), likely further exacerbating the stress on available prosthetists. England alone saw over 5000 major leg amputations a year, referring to amputations below the knee, with a large proportion also contributing to arterial disease (Ahmad, 2014). With such large numbers, there is a need to produce lower-risk prosthetics capable of returning amputees to their day-to-day activities as soon as possible.

2.2. Research Relevant Physiology

2.2.1 Deep Tissue Injury

To be able to produce a prosthetic and, more specifically, a prosthetic socket, it is essential to understand the factors, biological or mechanical, that contribute to the generation of DTIs in lower limb amputees, with the knowledge gained making it possible to begin planning how such factors could be manipulated to reduce the dangers and to benefit the prosthesis user. The literature review has focused more on conditions that exacerbate previously mentioned conditions.

It is common practice to categorise DTI alongside PUs, although there are differences in their cause and effects, despite their similar outward appearance. Studies have investigated the efficient diagnosis of the two wound types to allow more efficient planning and treatment, as

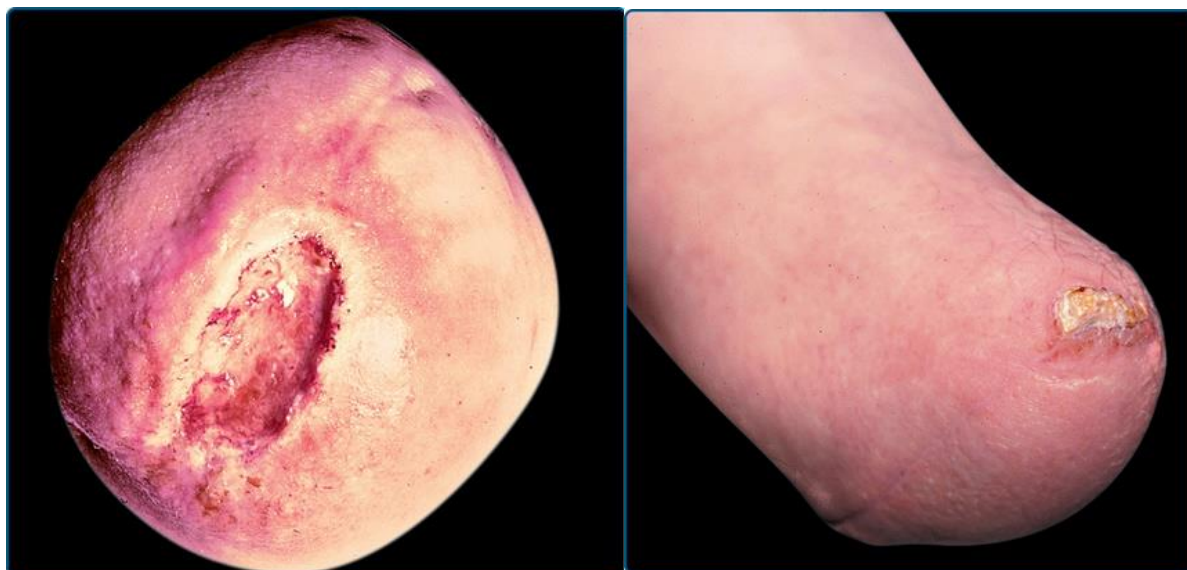


Figure 4: Chronic ulcerations identified in stump skin (K. Wolff, 2011)

it has been revealed that the treatment plan for PUs is not always compatible with the treatment of DTIs. This follows progress in the re-classification of DTIs under a new, more well-defined classification scale, rather than the wound type being classified as severe PU, as previously done. Figure 4 illustrates the size and location of chronic ulceration around residual limb tissue.

A critical factor in understanding the differences between PUs and DTIs can be seen in a comparison between healing procedures. It is usually thought that it is best to prevent further ulceration and damage by reducing the level of prosthetic use of the patient, reducing stress on the limb and further damage, and allowing for healing to occur. However, a contrasting opinion was formulated by Salawu et al., whose research indicated that this was not necessarily true for the treatment of standard low-level residual limb ulceration (stage 1 and 2 PUs) (Salawu, 2006). A study of 102 patients with ulceration caused by prosthetic use found that with suitable

treatment techniques, 89% of the patients experienced either complete or partial healing of any ulcers without the need to de-load the limb for an extensive period. This indicated that the dangers of stage 1 and 2 ulcers could be stopped with effective treatment without restricting prosthetic use, providing detection is early enough to prevent further deterioration. However, as summarised in a review by Highsmith et al., the complexity of the healing process is high, with individual patients needing to be assessed on a case-by-case basis as conditions such as acute pain and rapid volume and weight change all have a considerable impact on the increase of PUs, necessitating less prosthetic use (Highsmith, 2016). Therefore, excluding more severe cases (whereby the ulcer extends through nearly the entire residual tissue), it is possible for PU healing to continue. In contrast, the prosthetic user continues their typical day-to-day activities if regular check-ups of the wound are maintained.

The primary concern with DTI is that the treatment required to counteract the damage is more drastic. By the time the wound becomes diagnosable, it is likely to have been present for up to two weeks, meaning significant damage has occurred to the tissues of the residual limb (Gefen 2013). Gefen et al. highlighted how, in the case of DTI without the immediate removal of a prosthesis, 61% of DTI wounds progressed to a full-thickness wound (a wound that spans from the bone surface to the skin surface (Therapy, 2013)). This is a stage in the wound's life cycle that is difficult to treat, with effects of the injury resulting in a long-term reduction in mobility, potential hospitalisation, further amputation and, in the worst-case scenarios, death (Gefen, 2013). Due to such dramatic consequences and the relative inability for early detection and treatment, it was considered that a shift in research focus on preventative measures for DTI would be beneficial. Research regarding detection and treatment is being undertaken, with biomarker monitoring, ultrasound treatment, and intermittent electrical stimulation showing promise (Twist, 2012). However, prevention remains the best course of action, mainly as early-stage detection is still relatively novel and limited in its availability and application.

Berlowitz et al. showed that four main factors contribute to DTI development, one of which being the prolonged deformation of tissue over bony prominences, with large stresses in these regions triggering the cell necrosis that precedes the development of deep tissue-related injuries (Berlowitz, 2007). Such stresses are commonly associated with a poorly fitting prosthetic socket or cyclic loading from walking, although similar activities can also be responsible for the generation of DTIs. An information brochure provided by MIST defines DTI as a "purple, or a maroon localised area of discoloured intact skin or blood-filled blister due to damage of underlying soft tissue from pressure and shear" (Therapy, 2013). Damage to the underlying tissue identifies the critical difference between DTIs and PUs, with the origin of the DTI occurring beneath the skin's surface, unlike PUs, which originate at the skin's surface. Originating from the bone tissue interface damage, DTI (usually in the form of cell necrosis) spreads out from the bone surface towards the skin, with a DTI on or visibly near the skin's surface traditionally classified as either a level 3 or 4 PU (the worst possible levels) on the National Pressure Ulcer Advisory Panel (NPUAP) scale of PU assessment. By this time, the wound has damaged the full thickness of the tissue between the bone and skin's surface, making a far more difficult-to-treat injury than a standard ulcer (NPUAP, 2007) and with the possibility of further amputation a genuine concern, particularly in a situation where a shorter than ideal residual limb is already present.

One factor of consideration is the overall cost of DTIs in amputees to healthcare networks such as the NHS. Although difficult to calculate accurately, the cost of DTI to the NHS will likely be considerable. Ulcer healing costs increase with its grade, with a stage 4 wound costing the NHS in the region of £10500 and approximately £1000 for a stage 1 (Bennett, 2004). Although the paper does not specifically refer to PU/ DTIs caused by prosthetic use, the overall cost of recovery is likely to be similar, if not worse, for each case due to the addition of prosthetic adaptation to help reduce the likelihood of repeated incidents. To help estimate a possible cost

of wound healing alone, data collated by a review of 805 prosthetic users were collected to understand better the range of skin problems experienced. A skin condition was reported one month before the questionnaire completion, revealing 57% (463) participants had PUs, with 31% (246) noting wounds (Meulenbelt, 2009). Suppose the prevalence of such injury is in the region of 50%. In that case, the proportion of the estimated £60 million (NHS, 2023) spent by the NHS (England) on prosthetic-related rehabilitation is likely to be significant.

To be able to produce a prosthetic and, more specifically, a prosthetic socket, it is essential to understand the factors, biological or mechanical, that contribute to the generation of DTIs in lower limb amputees, with the knowledge gained making it possible to begin planning how such factors could be manipulated to reduce the dangers and to benefit the prosthesis user. The literature review has focused more on conditions that exacerbate previously mentioned conditions.

Graser et al. highlight the limited availability of known risk factors for amputees, despite correlations between factors known to cause DTIs in immobilised patients (Graser, 2020). However, the review highlighted several themes available regarding the aetiology of DTI and both non-prosthesis and prosthesis-related risk factors. Forming the framework by which information was reviewed for this project.

2.2.1.1 Soft Tissue Deformation

Exploring the effects of pressure is also essential to understanding the mechanisms through which cell necrosis and DTI occur, as this is widely regarded as one of the leading causes of such injury, not only in prosthetic users but in patients affected by paralysis, diabetes, and vascular diseases. Studies have been carried out to determine how resilient muscle cells are in coping with sustained periods of pressure. One such study, by Gefen et al., involved groups of normal-sized muscle cells being compressed and assessed by the levels of necrosis seen at

different time intervals, with results indicating an increase in the rate of cell death over time (Gefen, 2008). Taking readings every 15 minutes for four hours and 45 minutes, it was determined that the cultured muscle cells could survive engineering strains of 65% for approximately one hour, as shown in Figure 8, while lower strains of 40% could be tolerated for the full four hours and 45 minutes. However, the tolerance dropped away rapidly between one and three hours.

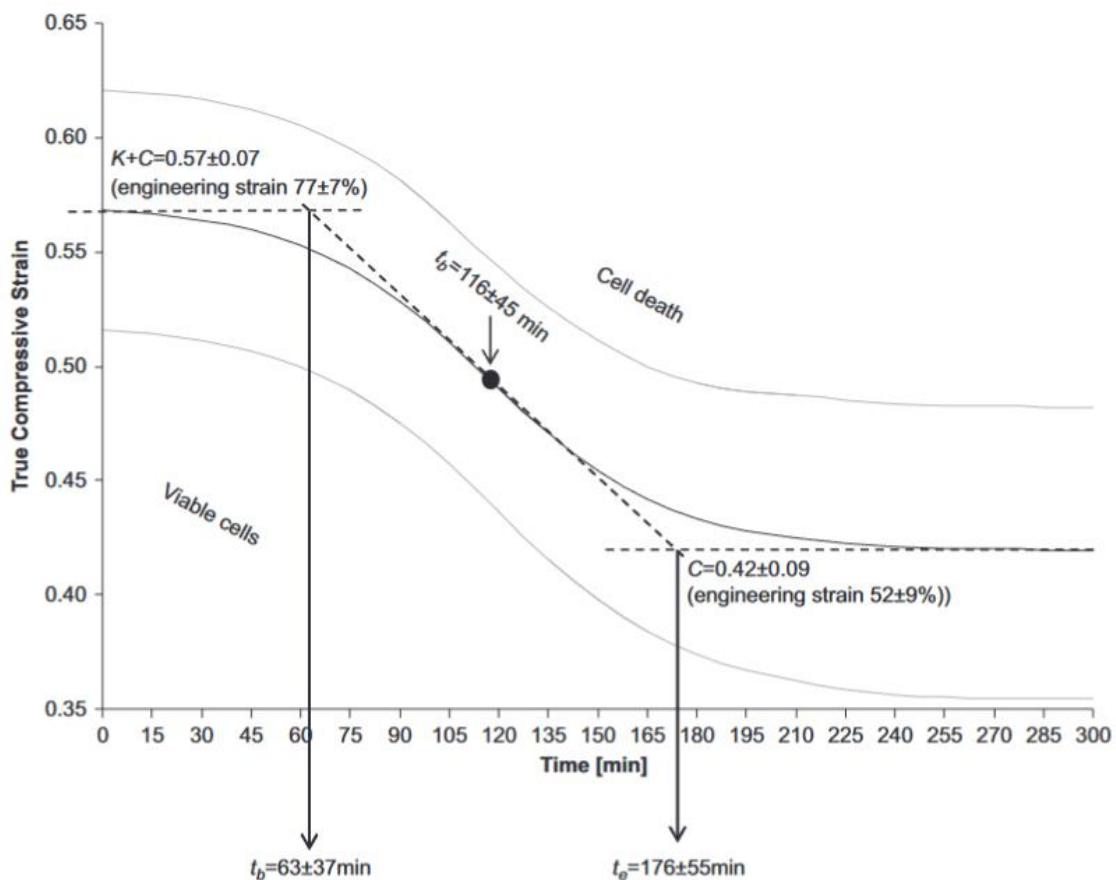


Figure 5: The relationship with cell survival when loaded over time (A. Gefen B. v., 2008)

A mechanism that causes cell death was researched by Wu et al. using a compression system while monitoring the activations of different compounds within the cell. The study, lasting 24 hours, concluded that compression caused the activation of MAP Kinase enzymes responsible for breaking the cell's cytoskeleton. Manipulation of the pathways regarding these enzymes falls out of the project's scope; however, it is important to understand how cells are likely to react to compression on a cellular level (Wu, 2016). Although TTAs are unlikely to experience

continuous strains for this period, it was also found that engineering strains over 70% could kill the muscle cells instantly, a consideration that was considered during other stages of this research.

Alongside compression and temperature, the literature suggests that the most significant danger for increasing the risk of DTI is the generation of shear stress. Shear stress refers to the lateral deformation of a material where changes in dimension are known as shear strains. These conditions are very easy to produce when tissues slide over bony surfaces. A review by Gefen et al. regarding the development, identification, and methods of reducing the risk of DTIs emphasised that areas that commonly experience DTI undergo movements likely to generate considerable levels of shear (Gefen, 2013). One such region is the sacrum in bedridden patients required to sit up with back support. In this scenario, skin is pulled across the bony prominence of the sacrum and stressed under the patient's body weight, with body load through the bone acting antagonistically to the friction between the skin and back support and generating the dangerous conditions mentioned. Similar effects are caused by typical prosthetic-residual limb interaction, such as pistoning and abduction of the bone within the residual limbs while confined by the socket walls.

Further covered by Gefen's review is the weakness of muscle tissue to shear forces due to the normal inline orientation of the cells, arranged in a manner allowing them to slide over one another in extension and contraction. Shear causes a deformation in the cell membranes that disrupts the function of the cell to the point that the cell contents can be leaked into the extracellular matrix, causing cell death. Detecting this leakage has begun to be studied as a method for the early detection of dangerous shear conditions; however, it is still in the early stages of development and has yet to be introduced into a clinical setting.

Understanding the dangers of shear stress, this research assumes that producing a mitigation system for below-knee amputees would be beneficial. This system could identify and monitor dangerous levels of tissue flow and respond in a counteractive manner. One of the first studies focusing on the coefficient of friction between bone and muscle tissue was carried out by Shacham et al. Using porcine muscle tissue and ulnas to provide the raw materials for the experiment, results showed a coefficient of friction between 0.36 and 0.29, with a mean plateau of 0.3 for loads exceeding 4N (Shacham, 2010), supplying a suitable average to carry forward in calculations and computational models. However, the measured values may vary in accuracy compared to the true value as perfect limb conditions could not be replicated.

Many studies have been carried out to record the stresses experienced around the residual limb, whether at the skin-socket interface or those visualised within the tissue of the residuum. In a review paper published by Al-Fakih et al., the process of understanding what and how research into interface stress measurement was investigated. Tracking the changes over the last 50 years, Al-Fakih et al. highlighted how the development of socket fit has changed, with developments in the manufacturing processes and more patient-specific varieties aiming to reduce high-stress distribution on the limb. Essential systems, like prosthetic suspension, have seen dramatic changes as technology has improved the original suspension systems, such as in the thigh corset designs, replaced by the patellar tendon bearing (PTB) bar in the 1950s (Al-Fakih, 2016). Designed to redistribute the load to regions of the limb with a higher tolerance, the PTB socket became a standard for prosthetic socket comfort. It fits before later being updated to produce a total surface bearing (TSB) socket where, as the name suggests, loads are redistributed across the entire socket surface area, minimising stress concentrations at specific locations.

In a similar manner of evolution, the measuring of the stresses at the socket interface has developed rapidly over a short time. Initial attempts used socket-mounted transducers to measure stress values; these would remain in contact with the skin at key locations through

small holes drilled through the socket wall. Internally mounted sensors placed between the liner and the skin are more common today, giving more accurate results. It is evident from Al-Fakih's review that attempts to measure both static and dynamic pressures accurately are challenging as high-accuracy techniques, such as externally mounted transducers, are limited to the area of measurement, with holes in the socket potentially changing the standard conditions of the residual limb, while internal sensors, such as strain gauges, have shown too much variability and hysteresis.

Producing stress distribution results for a residual limb, both experimentally and computationally, is extremely difficult for the reasons stated above, with studies over the last two decades shifting towards utilising data produced from the FEA of residual limbs to enhance the new prosthetic design. One such analysis was carried out by Portnoy et al., where a detailed three-dimensional map of changes in the strain of cells within the residual limb was visualised using an MRI scanner. A volunteer would load the stump by imposing weight bearing through a ledge which allowed the displacement of the tibia within the stump to be visualised in a standing scenario, the intention of which was to "characterise the mechanical conditions in the muscle flap of the residual limb of a TTA patient after donning the prosthetic socket" (Portnoy, 2008). Using FEA, the results indicated peak tensile, compressive and shear strains of 85%, 129% and 106%, respectively, which can be used better to understand the cause of DTIs in individual patients. However, limitations of the technique were exposed as the muscle flap was modelled as a single material throughout. This limited the model as this was not an accurate representation of the tissue comprising the stump, which would be a combination of muscle, scar, fat, and other tissue types throughout its thickness. The paper shows that with a best practice approach to the problem, to produce the best results, a level of estimation and simplification must be implemented due to the complexity of the system and the limitations of the technology available to carry out the analysis. In an extension to their work, Portnoy et al.

attempted to look at how pressure densities would change in the residuum when walking over different terrains, including level ground, grass, stairs, and slopes. Using a newly designed portable monitor, it was possible to estimate peak stresses within the residual limb of multiple patients individually while better understanding how different terrains may cause variations in stress distribution throughout the limb. The device was calibrated using data collected from a phantom limb compromised of a silicone residuum and prosthetic socket, with stress data being

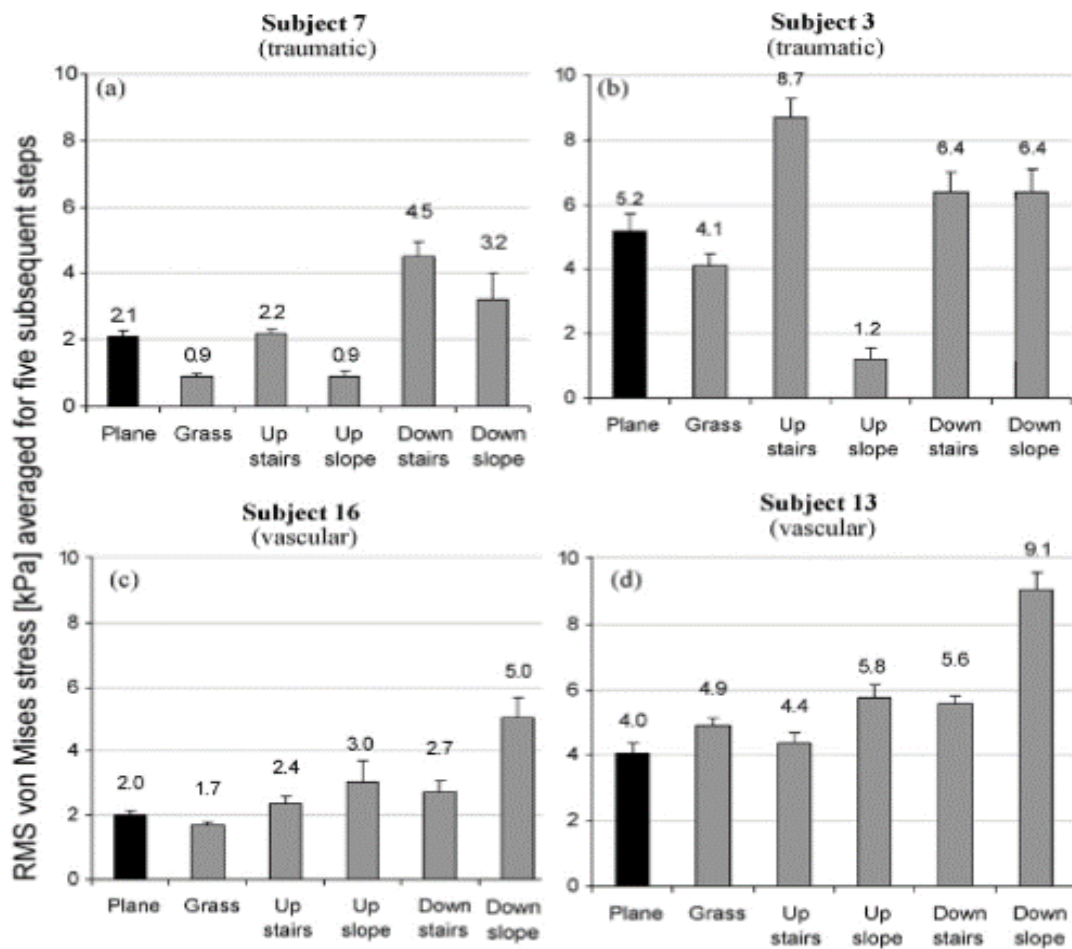


Figure 6: The average simulated Von-mises stresses generated from walking over different terrains (S. Portnoy, 2010)

collected from implanted sensors responding to external loading of the limb, with the device designed to estimate bone tissue interface stresses, measured from the phantom limb experiment, based on measured skin-socket interface pressures. Initial results showed that for body weights greater than 70 kg, the device produced accurate results with negligible errors and was, therefore, carried forward for human study.

Further to the development of the device, further results were generated to evaluate how different terrains caused differences in the region and the magnitude of stresses acting on the limb compared to walking on flat ground. The results showed that significantly greater stresses (between 40 – 50% greater) could be seen in some volunteers descending a slope, as shown in Figure 9 (Portnoy, 2010). The study highlighted the benefits of combining computational and experimental data to benefit the patients best while also effectively showing that different terrains are a large factor and risk in the development of possibly dangerous levels of stress in the residual limb.

With the knowledge of DTI gathered alongside the initial understanding of how transtibial amputees may experience conditions that pose a greater risk of causing such complications, it is necessary to focus further on which scenarios are of most concern, specifically on research carried out to identify DTI-causing situations that could potentially be mitigated in the future by enhancing lower limb prosthetic design.

One such concerning scenario to lower limb prosthetic users occurs during sitting (Portnoy, 2010). As mentioned in a previous section, one cause of DTI stems from the consistent loading of body tissues for extended periods without any adjustment and redistribution of the load. Portnoy et al. verified that sustained loading (of 1 - 3 hours) could be experienced during everyday sitting, with TTA individuals keeping their residual limb confined within the socket during activities such as watching television or at a desk while maintaining a consistent loading pattern on the limb. This may be so, especially in patients with reduced limb sensitivity, as making position adjustments and load distribution would be less likely to occur. Portnoy's study, involving an FE analysis of a residual limb in a sitting position with knee flexions of 30° and 90° running for 75 minutes, concluded that sitting posed a not insignificant risk of DTI, with a volume of tissue damage over ten times greater for knee flexion at 90° occurring rapidly within the first 30 minutes of the simulation.

Researching socket interface pressures was an initial focus of numerous studies. It provided measurable patient-specific data regarding prosthetic fit and comfort that could be collected relatively quickly before being extrapolated using finite element techniques. A review by Pirouzi et al. identified many past methods for collecting skin surface data while also considering the positives and negatives of the techniques to help solve the socket fit conundrum. Broad issues include the preferences of the model maker in developing a finite element model, meaning different model makers with equivalent data may produce different results (Pirouzi, 2014). However, it has been shown that surface-mounted sensors have proved beneficial to prosthetic adjustment for fast and statistically adequate evaluation. Rajtukova et al. described one such example, where TACTILUS tactile pressure sensors were used to return data on prosthetics for improving transtibial prosthesis socket fit (Rajtukova, 2014). It was confirmed by statistical tests that despite some small errors in interface modelling, data could be used to adapt prosthetics providing small improvements for the user. With such a complicated problem being posed by lower limb prostheses, the issue cannot be solved in its entirety by targeting one specific area, with all the components in the prosthesis having some bearing on the result.

Dumbleton et al. carried out a significant advance in interface pressure mapping in a comparison experiment designed to understand better differences in surface pressures of IceCast sockets and hand-cast PTB sockets. Differing from traditional hand-cast sockets, IceCast sockets are produced using pressure casting systems, producing an even pressure distribution across the surface of the residual limb, in contrast to the targeted selection of support tissue used in hand-casting techniques (Goh, 2003). A Tekscan F-Scan transducer formed from an array of pressure sensors arranged into a flexible mat was used, which allowed pressure maps to be built up against time, like that shown in Figure 10 (Tekscan, 2020). The dynamic pressure maps were evaluated throughout the volunteer's day-to-day activities, with

a comparison between each socket type evaluated for its performance in various standard activities in a real-world setting (Dumbleton, 2009). The evaluations of both data sets showed that stress concentrations frequently changed during walking, suggesting that prosthetic adaptations introduced from static studies, although beneficial, may not be as effective as a solution that would account for these dynamic changes.

2.2.1.2 Tissue Morphology and Mechanical Properties

The tissue morphology of the residuum of below-knee amputees will vary wildly from person to person. Traumatic injury is somewhat random, leaving unique limb dimensions and tissue layering. Despite common or standardised amputation methods for those suffering from vascular disease, differences will be present for like-for-like amputated limbs based on several factors. A residuum's post-amputation showed muscle atrophy and increased stiffness, meaning the limb's tolerance to loading will have changed. It is also known that greater adipose infiltration into the tissue of the lower limb can significantly influence the limb's resistance to further damage due to the lower tolerance of mechanical loading (Bramley, 2021). A particular concern for amputations caused by vascular disease in diabetic patients, who are much more likely to have more significant intramuscular fat content.

Diabetic patients form a large percentage of below-knee amputees and have been categorised into several groups: those with polyneuropathy (without vascular disease), those with polyneuropathy (with vascular disease) and those with vascular disease (without polyneuropathy) (Larsson, 1995). In particular, those suffering from peripheral vascular disease lead to impaired blood flow, which puts them at high risk of amputation (Morley, 2018). The tissue morphology in diabetic amputees often exhibits skin thinning, reduced elasticity, and decreased subcutaneous fat, making the residual limb more vulnerable to injury (Goulding, 2015), such as pressure and shear-related injury correlated with DTI.

Although comparatively less frequent, below-knee amputation resulting from trauma (accident or injury) can have a significant influence on the overall tissue morphology of the residual limb when it is fully established, it has been noted that in some cases, traumatic amputation leaves a less-than-ideal residuum, with the primary focus of the procedure often being focused on wound closure rather than long-term functionality (Ertl, 2018). Thus, leaving the limb with a nonideal structure regarding muscle flap thickness, bone shape and overall skin integrity. Without being able to predict how the limb will condition in terms of scarring, atrophy, and overall stiffening.

2.2.1.3 Ischemia and Reperfusion

The restriction of blood flow, more commonly referred to as ischaemia, and subsequent reperfusion, the return of blood flow to the tissue, is a risk to prosthetic users whereby blood vessel restriction is a common issue. Although a full description of what cellular activity is disrupted, a study by Cui et al. identified that ischemia-reperfusion (I/R) was a risk factor in the cause of DTI when cycled (2 hours of compression with half an hour release) (Cui, 2016). Results indicate higher levels of endoplasmic reticulum stress proteins exhibited in the compressed tissue cells compared to the control samples, indicating the potential onset of pressure-related injury. Although unconfirmed specifically on prosthetic users, the study infers an inherent risk of I/R-related events, particularly in tissue that has already endured the trauma of amputation. Although not a mechanism to be targeted by the medical device proposed, greater knowledge could and should be gained regarding the potential causes, effects and mitigation for I/R-related issues for below-knee amputees.

2.2.1.4 Sensory Impairment

With a known cause of DTI being the exposure to continuous tissue loading, there is an inherent risk in prosthetic users unknowingly maintaining an excessive limb loading due to sensory impairment. A study by Kosasih et al. attempted to determine what modalities of sensory

impairment were present in correlation to participant demographics. Results indicated superficial pain and light touch impairment were a risk for prosthetic users in the elderly demographic (over 60) or those who have used a prosthesis for 20 years or more (Kosasih, 1998). Although minimal impairment of deep pressure sensation was identified, the study highlights the significant differences in participant results based on variables of prosthetic use but also the need for up-to-date knowledge of how residual limbs will change morphologically over time.

2.2.1.5 Socket Design

As described in section 2.2.3.2, socket design, when related to DTI, most commonly refers to TSB and PTB sockets. However, current knowledge is limited to identifying differences in interface loading magnitudes; more needs to be concluded on differences in internal loading conditions generated by the two different suspension methods (Graser, 2020). Finite element analysis studies, like those carried out by Portnoy et al., show a full view of potential internal loading conditions of the residual limb (Portnoy, 2008). However, the methodology is limited by model input parameters, model material determination, vast patient-to-patient variation in residual limb composition and large simplifications in model element meshing at sites of specific interest.

2.2.1.6 Prosthetic Make Up

A link was found between the interaction of specific prosthetic components influenced the potential for pressure generation around a participant's residual limb. This was described by Sanders et al., in which surface pressures were analysed for three subjects with different configurations of lower limb prosthetics. It was found that prosthetic design, such as an aluminium pylon with a SACH foot compared to a pneumatic type shank with a Seattle Lightfoot, produced peak stresses at different stages of gait (Sanders, 2000), thus indicating

that all things should be considered, for what is a complicated problem that does not have a blanket solution for all subjects involved.

2.2.1.7 Prosthetic Liner

Similarly, the coefficient of friction between human skin and its encompassing material when confined within a socket is highly important. Looking at multiple materials and areas of the body, Zhang et al. calculated an average coefficient of friction for a broad range of materials encompassing several areas of interest, one of these areas being the region of the lower limb prosthetic. In the study, the coefficient of friction between the skin of the leg and silicone, the material used for socket liners, was carried out, with results showing a coefficient of friction between 0.47 – 0.48 (Zhang, 1999). It was noted that the experiment proved challenging due to the difficulty of repeating it under similar conditions and the presence of many variables that could affect the results, including the mechanical properties of the skin, the ambient air conditions (involving the moisture content of the air and temperature), and maintaining a sweat-free environment, thus, highlighting that if a computational study was to be undertaken, specific knowledge of the liner was essential. This was shown by Saunders et al., where a review of 15 commercially available silicone liners indicated vastly different friction coefficients between the socket liners. The study, designed to compare the mechanical properties of the different liners, showed that coefficients could vary from 0.42 to 0.79 (Saunders, 2004), both highlighting the weaknesses in Zhang's study (using silicone is not necessarily applicable to all commercially available liners) and the considerable variation in the coefficient of friction that, it was concluded, resulted from differences in the manufacturing method. This indicates a lack of knowledge regarding the dangers of shear stresses in prosthetic sockets. Other results have shown the critical differences between silicone gel type and silicone elastomer type liners, with the level of cross-linking present in the polymer being of direct importance to the performance of the liner in the other mechanical tests they were subjected to.

From this, it can be deduced that for theoretical or computational analysis, it would be necessary to have a specific liner in mind to ensure valid comparisons can be drawn between any data generated computationally and experimentally, as a significant range in properties exists between liners, despite similar materials being used.

A research collaborative published information regarding this (OWM, 2014), and one of the papers discussed the correlation between ulcer formation and the differences between pressure and temperature. The study used healthy pigs with metal discs applied to the skin for five hours at pressures ranging between 10 – 50 mmHg and 100 – 150 mmHg at temperatures varying between 25 - 53°C (Ialzzo, 2004). The results showed that elevated temperatures (50°C) at low pressures (10mmHg) caused more significant epidermal necrosis of tissue than high pressure at low temperatures, with normal conditions of 50mmHg at 35°C showing necrosis occurring primarily in muscle layers rather than other tissue layers, indicating a critical region at which DTIs could occur in a relatively short period. The temperatures were similar to the values recorded by Peery et al. (Peery, 2005) in a study monitoring the skin surface temperature within transtibial sockets during rest and brief periods of walking. Here, 15 minutes of rest (sitting comfortably) saw a skin surface temperature increase of 0.8°C, from approximately 31.7°C to 32.6°C, while a 10-minute walk caused an average temperature increase of 1.7°C. It was noted that this increase in temperature was linked to increased irritation and discomfort for the amputee, while (as indicated by Lalzzo et al.) it may have also promoted conditions indicative of deep tissue ulceration. This condition should also be considered when reducing the potential of DTIs in a transtibial amputee. A paper published by Gefen (2011), reporting on a mathematical modelling study, also confirmed the benefits of maintaining a low temperature in reducing the risk of conditions such as PUs. However, it should be known that there are difficulties in generating accurate results connected to the skin and a socket liner due to the problems regarding the implantation of sensors, liner breakdown and sensor positioning, as

described by Mathur et al. (Mathur 2014). Therefore, values should be viewed with tolerance, even though the trend is clear and repeatable.



Figure 7: F-Scan sensor pressure sensor array for sole pressure monitoring

This complex and unpredictable variation amputee to amputee makes predicting the risk of further injury for below-knee amputees very difficult. With the variables being present not only person to person but correlation also present in prosthetic componentry being likely to cause further pressure related injury. Further highlighting the need for greater in-depth research to understand better the mechanisms by which DTI might be influenced so that more preventive measures can be established.

2.3. Socket and Residual Limb Environment

2.3.1. Residual Limb Volume Change

A characteristic that acts independently of prosthetic design and shape, although still has a considerable impact on comfort and fit, is the fluctuation in the volume of the residual limb. Many factors affect volume change in mature limbs, both postoperatively and daily. Common factors such as muscle atrophy and fluid collection cause limb volume fluctuation. This factor

must be stabilised post-amputation before prosthetic fitting can occur to ensure the best results. However, in daily activities, the limb can experience massive changes in volume due to interstitial fluid flow (Sanders, 2011). Zachariah et al. used a short walking experiment in an initial study of six participants and found that in as little as 35 minutes, stump volume could change an average of 6%, with a range of 2.4 to 10.9% in this small sample size (Zachariah, 2004). The volume change was determined by optical scanning of the residual limb following incremental changes in the time of prosthetic use. The result shows that with such a considerable variation in volume change, pain and discomfort mitigation techniques are likely to be only sometimes successful. Whilst further varying depending on pain severities and from patient to patient. While consideration of volume changes should be considered for the project of bone stabilisation, the changes in the residuum mechanics will alter the required performance of the system for an equivalent response, particularly as increasing the stiffness of the tissue is likely to be a key mechanic employed to allow for tibial stabilisation to take place. Thus, as concluded by Sanders et al., volume control measures are relatively subjective as effectiveness remains to be seen at best (Sanders, 2011).

2.3.2. Variations in Socket Casting Techniques

There has been a rise in a new method of producing sockets instead of conventional hand-cast sockets, which are cast on a loaded limb using constant pressure across its surface.

(Shikh, 2008). Hydrostatic casting was introduced to alleviate the demand for skilled prosthetists, especially in more impoverished regions. It has been suggested that this method holds certain advantages over the standard hand-cast techniques, offering the potential to produce multiple casts, with the differences generated between a different prosthetist and the inaccuracies caused by the execution being negated (Buis, 2017). This makes the system viable in areas where facilities and trained professionals are at a premium. With the casting on a loaded stump, the limb is at its most deformed shape and state, allowing constant pressure

across the limb throughout the gait cycle. This process aids in reducing pistoning and similar residual limb movement within the socket, theoretically reducing the risks of stump damage and increasing comfort. However, a comparison study between PTB and hydrocast system sockets has indicated greater patient satisfaction with the more traditional PTB variety, despite pressure sensor data indicating a smoother pressure variation in the hydrocast variants. This is not seen as a critical point of contention for the project as the investigation primarily explores the potential behind a stabilisation system and how it could benefit. Furthermore, as an extension to the study, particularly with hydrostatic casting becoming more prevalent in research and industry, it may be the right decision to apply the system to both hand-cast and hydrocast sockets to identify whether there is any significant difference in the stabilisation results. Building on a proof-of-concept study by Buis et al. in assessing transfemoral stability during gait of both socket designs (Buis, 2017).

2.3.3. Residual Bone Movement and Moments About Below-Knee Amputees

It is prevalent for the residual limb of a lower limb amputee, whether that is above or below the knee, to be analysed in a manner that assumes the residual bone remains in a fixed position while confined within a socket such that it is modelled as remaining perpendicular to the reaction plane when in a mid-stance position, throughout the stages of gait. Despite this, studies by Lilja et al. have demonstrated that this is not always the case for below-knee amputations, with a study by Convery et al. also suggesting femoral movement in above-knee amputations. Using X-ray and ultrasound scanning, respectively, it was identified that oscillation of the tibia could reach $\pm 1\text{cm}$ at HS TO (Lilja, 1993), as shown in Figure 5, while femoral movement, recorded in degrees of offset, peaked at approximately $\pm 8^\circ$ from its mid-stance position in both its sagittal and coronal planes (Convery, 2001).

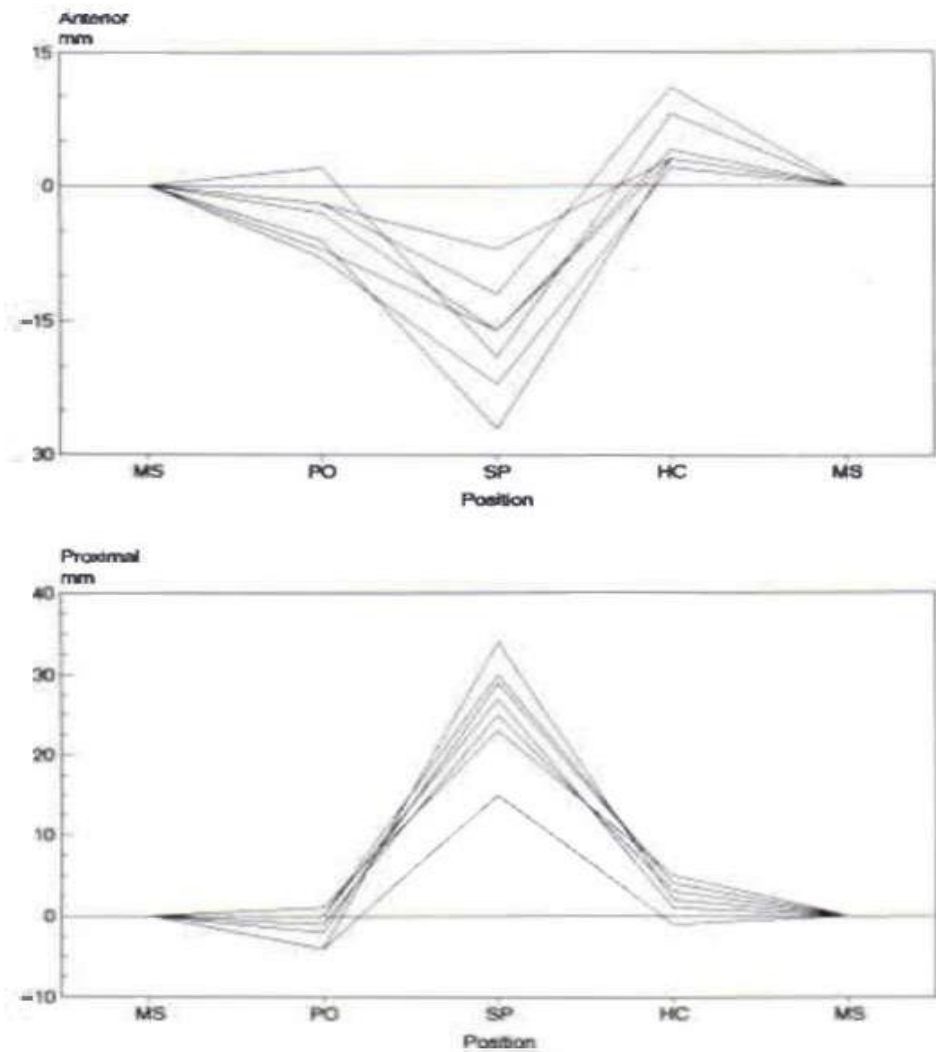


Figure 8: the displacements of the tibia ends of 7 patients as identified by X-ray (M. Lilja, 1993), showing oscillation about the mean mid-stance position during various stages of stance and swing.

The specific oscillation significantly impacts FEA studies, for example, the review carried out by Dickson et al. However, many examples need to include the dynamic relationship associated with bone oscillation and instead choose to simplify the study to a fixed orientation, as mentioned previously (Dickinson, 2017). Such an approach would likely produce inaccurate results for stress generation at both the skin's surface and the limb's internal tissues. Alongside tibial movement, another essential and linked mechanism that was thought to influence the stress development in the residual limb was that of moments about the prosthesis.

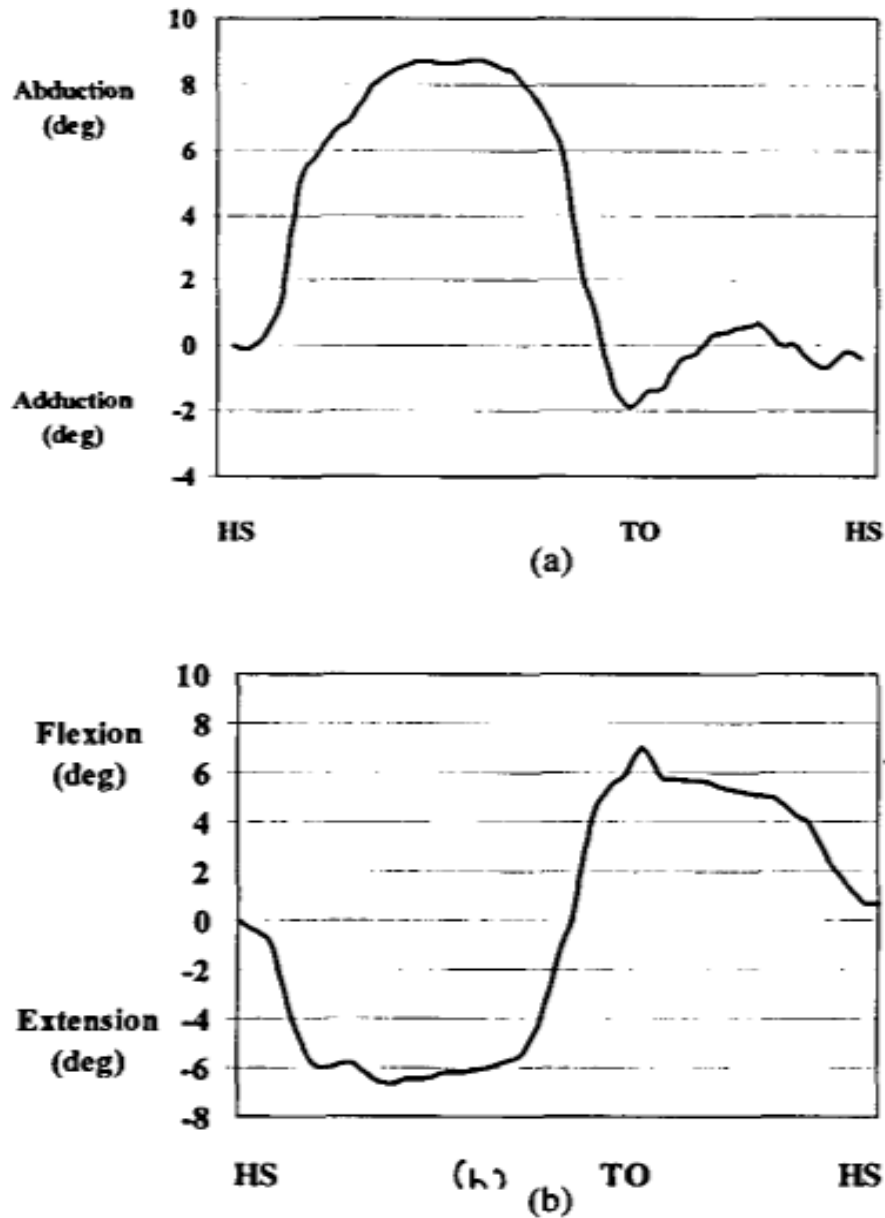


Figure 9: Ultrasound imaging allowed for the monitoring of residual femur oscillation about its average position during walking, showing significant movement in every plane of motion (P. Convery K. D., 2001)

With the research aim to understand the magnitude of moments and forces acting about the prosthesis, meaning a suitable counterbalancing system could be designed, the research focus was shifted to understanding the variations in below-knee amputee gait.

The gait differences between below-knee amputees and non-amputees have been studied over several years, with force plate data often being used to estimate joint forces about the ankle, knee and, to a lesser extent, the hip. It has been found that, in general, forces at HS are significantly reduced in below-knee amputees, a trend that continues throughout mid-stance.

However, the peak reaction force recorded at the TO of an amputee is often around the same magnitude, if not larger, than the TO of a non-amputee, although the peak occurs at an earlier percentage of the mid-stance position (Hurley, 1990),

which has been confirmed by a more modern study by Kovac et al. A similar response was seen with ground reaction forces in the region of 1N/kg rather than 1.5N/Kg, as seen by Hurley (Kovac, 2009). There is also a similar response seen in TTAs during running tests; with data collected from children with single lower limb amputation, Engsborg et al. showed that during running, the ground reaction force at HS was greater in magnitude than that of the non-disabled volunteers. However, they much reduced at TO, with a considerable compensation of this difference evident in the subsequent reaction forces measured in the non-amputated limb of the amputee (Engsborg, 1993).

Many factors can affect the distribution of loads. It is possible to assume that the reduced reaction forces measured by Kovac et al. indicate that as the technology implemented in prosthesis has improved, the unnatural imbalances in limb loading have been reduced as the reaction forces measured will move more and more towards the profile of a normal limb of a non-disabled person. Similarly, factors such as prosthetic alignment or the chosen silicone, polyurethane or polymer liner material can influence the moments represented about the knee and other joints, with a study by Xiaohong et al. showing a -10Nm offset of moments measured about the knee with a silicone liner rather than the polyurethane equivalent (Xiaohong, 2008). Furthermore, to better understand the magnitude of moments about a lower limb prosthesis, it is essential to understand the magnitude around the stump socket complex to design and implement an appropriate counterbalancing system.

In a series of articles, Boone, Kobayashi et al. developed a device capable of measuring the moments of a below-knee amputee, experimenting with socket alignment. The authors were

able to understand how detrimental malalignment of the prosthesis could be to ease of walking, with as little as 3° adduction and abduction, showing moment offsets of over 0.05Nm/Kg over the various stages of stance (Boone, 2013). Meanwhile, a further study of the mechanism with a variety of volunteers using the medically designed alignment indicated an average moment about the prosthesis of -0.15Nm/Kg at HS and a peak value of 0.72Nm/kg at TO in the sagittal plane, as shown in Figure 7. Although there were ranges of peak extension, the most massive moments seen varied between 0.512 and 0.993Nm/Kg , indicating a large variability across the 11 volunteers studied. This measurement of moments is highly significant for the investigation moving forward as it provides a base value by which a stabilisation load could be calculated. However, it was thought that the necessary load for suitable tissue stiffening and socket stabilisation would likely be less due to the damping nature of stiffening tissue on the overall system.

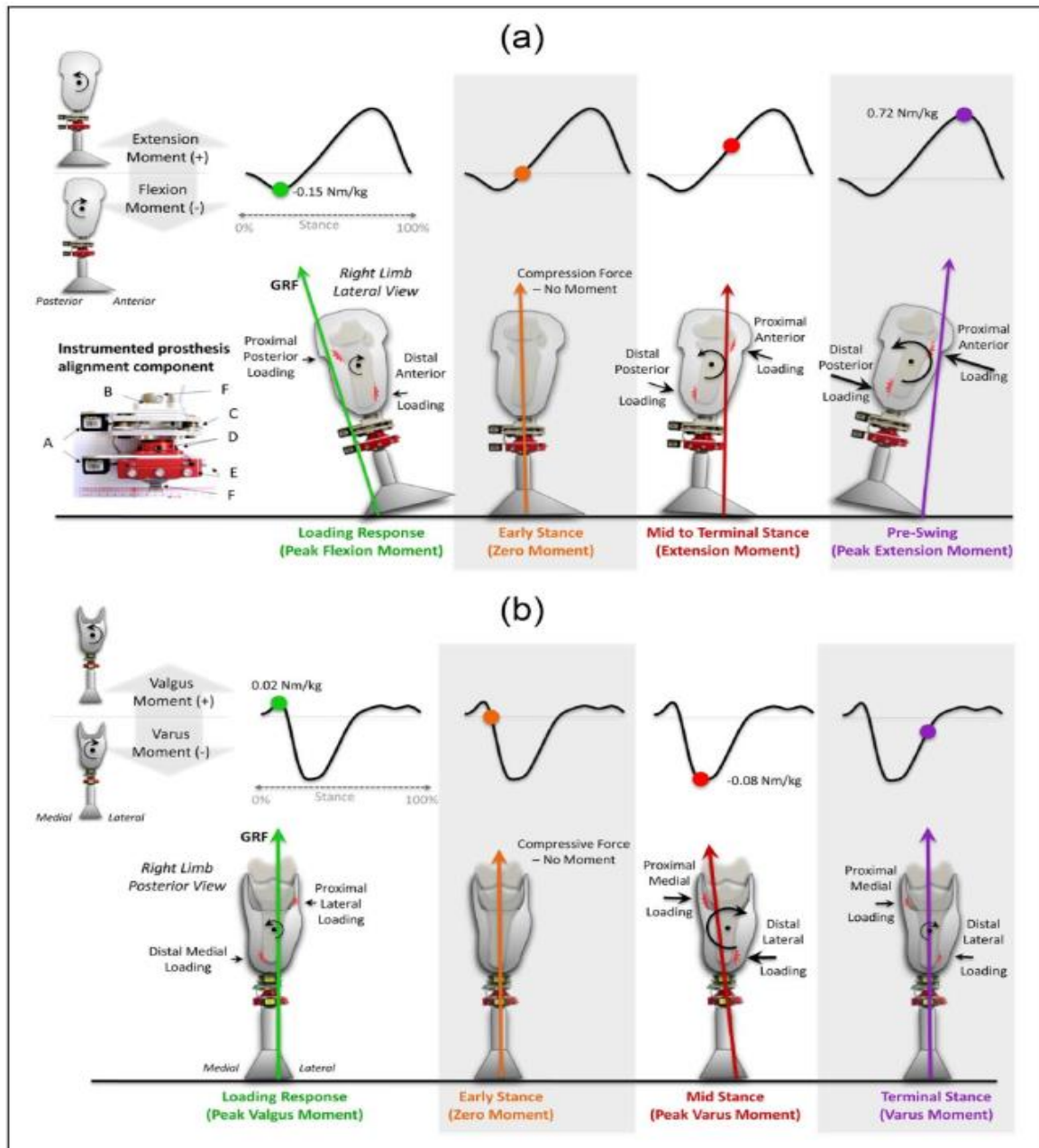


Figure 10: Moments measured about the centre of mass of a residual limb socket complex of a below-knee amputee, showing the direction and point of reaction likely to occur on the user during gait (T. Kobayashi, 2016).

2.4. Bone Movement Identification

As already discussed, within the residual limb, the tibia (and fibula to a lesser extent) moves away from its normal mid-stance position during the different stages of gait; a result made evident by the work of Lilja et al., while the concept was also visualised in the residual femur (in above-knee amputees) by Convery et al. in a dynamic ultrasound study. It was important to identify the possible methods capable of dynamically scanning the residual limb for bone movement, providing data on levels of displacement throughout gait. This research assessed the possibility of implementing dynamic scanning in a below-knee prosthetic. While a wide variety of possible systems are available, the search was limited to quickly identifying the most suitable system, with choices limited to MRI, X-ray, computed tomography (CT), near-infrared (NIR), and ultrasound. The following sections will provide some necessary background on these techniques before focusing on dynamic studies that have been carried out in the past and their potential. A thorough selection comparison is given in subsequent sections.

2.4.1. Magnetic Resonance Imaging

Magnetic resonance imaging (MRI) uses non-ionising electromagnetic radiation to align the hydrogen molecules within the body before detecting the energy released as the atom nuclei spin to produce cross-sectional images of the body with high tissue contrast capabilities. Traditional MRI requires the patient to remain still after being moved into a confined scanning space, and a 3D image of the body is built up layer by layer. The technique was not initially designed for dynamic study; however, developing new open-bore systems with a double doughnut configuration has opened the possibility of high-resolution dynamic imaging.

Specifications for the device were reviewed by (Shapiro, 2012), with details later used to compare suggested techniques. With highly detailed scans, the technique would be widely suited to studying various body movements. The difficulty for gait analysis, especially for

transtibial amputees, revolves around MRI scanners needing to be compatible with any form of metal, making the choice of prosthetic problematic. Furthermore, the scanners are currently unsuited to be paired with a treadmill, although developments in the future may enable this.

2.4.2. X-ray

X-ray images are produced as emitted x-rays are blocked by denser materials in the body, creating contrast images. The body is positioned between the emitter and the receiver. Traditionally a static technique, X-ray, has been developed over the last several decades to be compatible with dynamic studies, although clinical acceptance has yet to be achieved. Animal studies have been conducted to determine the accuracy of dynamic X-ray techniques, with high-quality results consistently produced (Tashman, 2003). The method has been used to study the knee joint of canines while on a treadmill, suggesting potential for TTA gait analysis. However, limitations do exist regarding radiation and the possible need for implants to ensure an accurate representation of rotation in 2D images. An improvement to the technique, which did not require invasive markers, was detailed by Bey (2008), in which highly accurate 3D scans were taken of the knee joint during motion. The technique proved successful, although concerns were raised regarding validation testing for each joint and increased exposure times. As with all radiation-based techniques, there is some exposure risk, while the availability of the technique is also a concern as it is not widely available.

2.4.3. Computed Tomography

Computed tomography (CT) is an advanced X-ray version involving rotating an X-ray source and receiver around the body to build up cross-sectional images with high-density materials easily differentiated from other tissues. With this technique, there are widespread concerns regarding greater exposure times to radiation (Brenner, 2007). Dynamic studies (4D, 3D against time) have been carried out on cadaveric hands to understand better wrist joint stability

(Leung, 2011). The technique provides high-contrast images, making it easy to measure bone movements to high degrees of precision; however, the technique has yet to be adapted to gait studies, making it a difficult concept to implement for TTA studies. Furthermore, with the radiation concerns, there may be better choices for the application required.

2.4.4. Near-Infrared Spectroscopy

Near-infrared fluorescence has been used in previous studies to produce contrast images. Bone-targeting substances are injected, and, over time, an image can be generated from the fluorescence generated by near-infrared light energy (Harmatys, 2013). Reacting strongly with calcium ions in the bone, the contrasting agent allows distinct images to be taken, although the technique has only been used on animal subjects. The technique has been used for dynamic bone movements, while it also monitors chemical penetration through regions of the body, such as the skull (Crespi, 2016). Therefore, the technique is versatile for a wide range of applications and can be used for the dynamic study of bone movement after the injected matter has successfully adhered to the bone.

2.4.5. Ultrasound Imaging

The final possibility is an ultrasound scanning technique, whereby sound waves between 2MHz-20MHz are emitted in bursts, with the reflected signals being regathered by a receiver before a second burst is released (Ali, 2008). Dynamic scanning using ultrasound is made possible by monitoring the Doppler effect. Material such as bone, when moving, will cause a slight distortion in the frequency of the received bursts comparable to the rate of change of displacement of the bone from its neutral position. Several studies have used Doppler imaging techniques to measure bone movement within the body; one such example studied the small movements of the hyoid bone during the swallowing process (Sonies, 1996). The technique

proved very successful, with scans as accurate as X-rays providing movement data and the benefit of no radiation exposure to patients.

Further, a study involving trans-femoral amputees was conducted using a similar method to understand the motion of the residual femur within a socket during everyday activities (Convery 2001). Once more, it was found that bone movement results were repeatable, with an accuracy of around 1mm. At the same time, the scanning method allowed for additional video imagery to be taken, allowing any compensation from all over body movement being considered that may have affected the results during the scanning. In a non-invasive technique, ultrasound was also used for bone motion analysis of the knee (Masum,2014). In this case, a skin-mounted sensor could image the bone within the knee, with later frames being compared to an initial control frame. This allowed bone movement vectors to be calculated and bone position to be found. Masum et al. reported "sub-millimetre precision", while the system also allowed for flexibility for the user to move without restriction. The primary reported issue of the technique during dynamic imaging involved relatively severe motion blurring, which could create potential analysis problems.

2.5. Control Systems in Prosthetics

There are multiple scenarios where either reactive, predictive or both control system types are utilised. Control systems are used to generate the best output for a given input or stage of the cycle, with systems such as power converters (Cortes, 2008) and flight control of uncrewed aerial vehicles (UAVs) (Kim, 2003) being just two examples of how predictive control can be used. Reactive control has also been used in scenarios such as telerobotic systems (Arkin, 1991) and architecture control of autonomous mobile robots (Baklouti, 2017). Both system types can carry out tasks in vast areas and fields that often overlap, making it difficult to pinpoint when either system holds a distinct advantage. A more thorough focus on each system and its

advantages and disadvantages was carried out, with thought given to how each system could be applied to a tibial controlling prosthetic socket as the process progressed.

2.5.1 Natural Control Systems

It is worth noting that control systems are not solely based on electro-mechanical systems but are also prevalent in biology. It is possible to categorise motor skills and physiological responses to stimuli as predictive or reactive. A review carried out by Bohm et al. highlighted the importance of how studying the ability of reactive (for example, the ability to catch a ball dropped into the hand while blindfolded) and predictive (the ability to catch a ball that can be seen being dropped before landing in hand) control methods is essential in designing intervention methods, such as targeting fall prevention (Bohm, 2015), where it was concluded that methods that aimed at training reactive and predictive stability control responses could be highly effective at reducing the risk of falling. Meanwhile, studying the differences in patients' reactive and predictive responses to similar tests could help identify conditions such as cerebellar degeneration, with specific patterns being consistent among those suffering from such problems and healthy patients (Nowak, 2004).

2.5.2 Control Systems in Prosthetics

Control systems are an essential factor in powered prosthetics, with electro-mechanical control of the articulations, such as the knee, ankle, elbow, wrist, and finger, essential in replicating a natural limb's performance as soon as possible.

An example is the proportional control of grip strength, demonstrated in Open Bionics' Hero Arm. Here, the magnitude of muscular contraction in the residual forearm, measured by electromyography (EMG) sensors, stimulates a proportional response from the actuation controlling the articulated fingers of the prosthesis: see Figure 11 (Bionics, 2018). Joint stability and speed monitoring ensure the successful adaptation of the prosthesis to the

continually changing environment.



Figure 11: the Hero Arm utilises a proportional actuator control based on the magnitude of muscle movement detected by EMG sensors (Bionics, 2018)

Geethanjali reviewed the different forms of control developed for the myoelectric control of prosthetic hands, with both reactive and predictive responses being studied. In this case, proportional control of a dc motor was linked to the magnitude of the electrical signal detected from the stimulated muscles, allowing a graded response. More complicated control systems, in the form of predictive and hybrid methods, have been used to estimate the required posture angle, particularly for hand and wrist articulation (Geethanjali, 2016). Predictive programming can be classified using algorithms, whereby a specific response (specific muscle group stimulation) can be used to derive a specific output response from the actuation system (a closed hand, for example). This is different from more hybrid systems, such as those that employ regression algorithms, which can interpret the input of several channels and continuously drive several responses (for example, open the hand while turning the wrist through x°) (Roche, 2017).

Despite this added complexity falling beyond the scope of the immediate project, it is worth understanding the potential for system development in any future iterations. While it is noted that it is currently challenging to mimic the number and effectiveness of a real limb's sensor and effector systems, as technology develops and external sensors get smaller, it will be

possible to reduce the performance gap, leading to a more biomimetic prosthesis. While upper limb prostheses have been more of a focus for development than lower limb equivalents, an increase in focus on the latter has been seen more recently. A much greater number of powered lower limb prostheses have become commercially available, with some, such as those with impact sensors in the heel, used to calculate the required torque at knee joints for the prosthesis to perform as desired (Tucker, 2015), becoming more common.

Although likely to be less complicated than knee stability, the desired system for the powered prosthetic socket suggested for the project is thought to require a similar system, one capable of detecting or predicting bone movement while filtering vibrations and other noise signals before quickly converting the data on the bone's position into a relevant response.

To be discussed more thoroughly in a later section, several key factors were identified as key influences in selecting a specific control system. With the novel device, the decision was made to limit the system's complexity. Considering it needs to be developed and tested within the limited timeframe of the study, it was thought that for initial research, a simple proportional style programme would suffice, with the overall control system designed to reactively respond to the changing feedback from the system with a mechanical response. This is in the form of linear or rotary actuators that respond well to the continuous nature of the input. As the concept was developed into secondary and tertiary versions, the control system and control manner would be enhanced and developed from the initial baseline design.

2.6. Technological Advances in Prosthetic Sockets

Outside of the more conventional developments in prosthetic design (such as PTB, TSB, prosthetic liners etc.), other methods for stress mitigation and residual limb volume change control are being conceptualised, tested, and made commercially available. With a notable

upswing over the last decade of research inter, the prosthesis interface is a focus (Safari, 2020). Two socket design ideas are presented here.

2.6.1 Stress Mitigation in Lower Limb Prosthetics

In recent years, techniques to reduce stress concentrations at the skin surface have been conceptualised and designed with the general purpose of reducing tissue stresses through a variety of different mechanisms. Despite the dangers of tissue flow about bony prominences causing increased stress on the internal cells of a residual limb, with increased stress leading to cell necrosis and DTI development, it has been common for many designs to be based on the reduction of stresses at the skin-socket boundary, customarily based on results produced from FEA models (Pirouzi, 2014), with the result often being an inaccurate representation of the load pressures at the skin-socket interface, while also not representing the key region of interest the bone tissue interface at the tibia end.

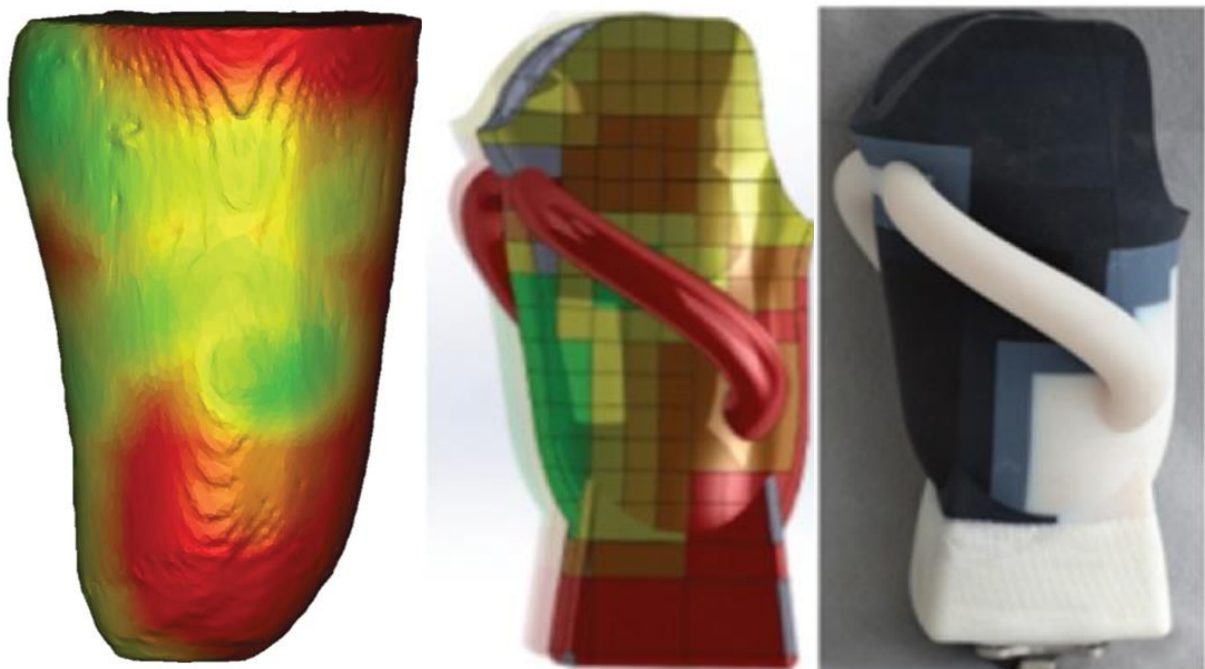


Figure 12: Step wise process to produce a variable impedance prosthetic socket based on tissue stiffness measurements at the skin's surface (D. M. Sengeh H. H., 2013)

A more accurate method for monitoring pressure at the interface was utilised by Sengeh, whereby the average loading of the residuum surface was measured by wrapping the entire

limb in pressure sensors, allowing a pressure map to be generated. This allowed a prosthetic socket to be produced from multiple, varying stiffness materials to support the loading in the most balanced manner (as indicated in Figure 12). The system passively reduced loads by approximately 8% at the tibia head region, highlighting the potential of the technology. However, it may be more beneficial if the pressure control was tailored to reduce stresses at the bone tissue interface, thus greatly reducing the risks of DTIs at their source.

2.6.2 Adjustable Sockets

As mentioned in section 2.2.3.1, one notable variable in below-knee prosthetic use is fluctuation in limb volume during day-to-day activities, let alone changes in limb dimension over longer periods. One such socket design was initially designed to act as a preparatory prosthesis, thereby reducing the need for several socket changes whilst the limb stabilised post-amputation (Wilson, 1987). An initial prototype was developed to accommodate limb volume change by an adjustable panel cut from the posterior of the socket, attached by adjustable clamps allowing for the overall socket volume to be increased or decreased as necessary during the full limb's stabilisation. With the added benefit of reducing the risk of shear loading of the limb during the donning of the socket, the panel allows greater freedom to insert the limb before tightening onto the limb. Traditional methods of controlling residual limb volume change include additional padding or inflatable bladders. However, they frequently need adjustment and considerable time investment from a prosthetist and the patients themselves (Nia, 2022). With adjustable sockets used for transtibial and transfemoral applications in certain cases, several case study examples show additional benefits to the technology. A study by Kahle et al. showed improvements in socket comfort, short walks with transitions, two-minute walk tests and a four-square step test. Improvements or parity with a standard socket with simulated volume loss, baseline, or volume gain (Kahle, 2016). Although the study held some limitations, regarding limited sample size and simulated volume change being difficult to achieve

accurately. However, the results for socket comfort were also mirrored by Nia et al. study into Varo's adjustable socket for a below-knee prosthesis. The device's comfort, which, although subjective, again scored considerably higher than standard socket types. This was noted to be key for the long-term benefit of the technology, with evidence indicating that, in general, rejection of new technology is predominantly down to user dissatisfaction from socket-related issues (Nia, 2022).

The presence of techniques to reduce stress concentrations and socket comfort is ever-increasing, with the desire to allow prosthetic users to return to day-to-day life unimpaired using a prosthesis. Although there is still no fixed solution to the numerous factors influencing prosthetic user well-being, further highlighting the need for greater research and testing of other solutions.

2.7. Hall Effect

As later sections will highlight, Hall effect sensing was selected as a novel method of potentially tracking tibial movement to allow for antagonistic loading of the lower limb. Due to this, further detail is provided on what and how the Hall effect has been used.

Discovered in the late 19th century by Edwin Hall (Leadstone, 1979), the principle of measuring the displacement and or speed of a magnet has been developed into highly effective sensors over the last century. Hall effect sensors are highly versatile solid-state sensors capable of highly accurate and repeatable velocity and displacement measurements, both linear and rotational. Whilst effectively filtering out the effects of undesirable vibrations in the system, making them suitable for several mechanical operations (Jezny, 2013). Capable of varying its output voltage in response to magnetic flux density, an array of sensors is an effective method to position a magnet in space accurately. Calculations from a microcontroller, such as an Arduino, allow for simple conversion of the measured voltage into a value for displacement

between the sensor surface and the magnets pole, with the sensors used to fill the failings of many optical and inductive sensors, whereby unwanted artefact interference and hysteresis are common problems, respectively.

Hall effect sensors deflect current flow through a semiconductor material when with zero magnetic influence, current flow maintains a constant directional flow of the charge carriers present in the semiconductor. However, when influenced by the magnetic field, where magnet orientation (north pole facing or south pole facing), the carriers can be manipulated to either the positive or negative pole of the hall effect sensors. Creating a potential difference across the sensor, which is measurable and repeatable, often makes them very applicable to many conditions. The main concern of using the hall effect is the range at which they work, a factor that is fully dependent on the size and strength of the magnet, requiring a level of tuning depending on the circumstance of the application.

2.7.1. Hall Effect in Prosthetics

The principle of utilising Hall Effect sensors and implanted magnets for prosthetic application is not new, with examples involving measuring the rotation of upper limb prosthetics being tested for potential future clinical trials (Li, 2008) in a study designed to test whether hall effect sensing of a magnet implanted in the distal end of the residual arm bone. In a similar concept as suggested for this study, Li et al. concluded that there was potential in measuring both direction and angle of rotation of the residual humerus possible by sensors positioned in the prosthetic socket. A theory was tested using computational modelling techniques to determine magnet displacement, alongside mathematical calculations using Maxwell's calculation to determine the corresponding flux density levels present at the hall sensor. Although limited, the evaluation was purely computational, with no measured data to support the simulated results; the study still suggests the concept's potential. Whilst also benefitting from the

evaluation of the magnetic shielding likely required to prevent external influences on the sensor, providing a starting point for future research into the area.

Similarly, although less relevant to the proposed study, hall effect sensors are becoming common in robotic and soft robotic applications. Demonstrating the capabilities when placed in mechanical systems such as prosthetic hands and other limbs, for example, demonstrated by Kyberd et al. in their integration of a Hall effect style device in the fingertips of the artificial device, proving feedback on force and slip allowing for highly sensitive and adaptable control of grip (Kyberd, 1993). A concept built upon to produce sensor feedback for robotic skins measuring forces, compressive and shear, for application in the soft robotic field. Test rigs evaluated single sensors and later larger sensor arrays to determine levels of hysteresis and temperature drift when using a silicon tissue simulant. Factors that were both present in the initial evaluation, therefore needing consideration in all studies of a similar type. However, the effects were possible to compensate for due to the repeatable nature of the errors. Therefore, calibration could reduce errors (Tomo, 2016). Again, the study showed how the technology could be implemented into soft tissue-like applications, with future studies being planned to understand how cross-talk between an array of sensors would be evaluated. Lending weight to the possibility of using Hall effect sensors and implanted magnets in prosthetic applications. Although, as is commonly the case, the testing range was performed over a small range and not a range like that of the distance between the tibia bone surface and the internal surface of the prosthetic socket.

2.7.2. Implantation

To effectively integrate Hall effect sensing into a lower limb prosthesis, it will be necessary, to achieve the best results, to implant a magnet in the tibia end of the amputee. A procedure that would likely occur upon limb amputation to limit the need for further wound healing later. A process that would be relatively simple for a surgeon to achieve during the amputation process.

It is necessary to understand how a magnet could affect processes such as bone healing while understanding how it is likely to degrade over time, furthermore, whether this would create issues regarding toxicity or possibly issues regarding fragments being dispersed around the body.

Although having been experimented with for several decades, accurate data regarding effects on bone healing had only recently been investigated in detail over the last decade. It has been found that static magnetic fields have positively impacted bone healing in vivo studies. Gujjalapudi et al. found a significant difference in the measured implant stability quotient (ISQ) between a nonmagnetic control and a neodymium boron iron magnet implanted in the mandible. The magnetic implants registered a score of 73.25 after 30 days, compared to 68.45 for the nonmagnetic implants. A result was replicated at 60 and 90 days, with the magnetic implant scoring 76.05 and 78.95, respectively, compared to 72.05 and 74.45 of the control implants (Gujjalapudi, 2016). A result has been mirrored by Kim et al. in their study of static magnetic fields in bone regeneration in rabbits, where it was concluded that the static magnetic fields that the results generated indicated a new and viable technique to improve bone healing in situations such as dental implants (Kim, 2017). These two modern studies indicate that in terms of bone healing, the implantation of a magnet in a tibia upon amputation may positively impact the rate of bone healing around the tibial end. An effect that, although secondary to the intended purpose of the implant, would be desirable, with the increased rate of healing being beneficial in facilitating the rehabilitation of the amputee post-operation. However, despite this, it is still necessary to understand how the body will interact with the magnetic implant over the amputee's lifetime. As many amputees suffer limb loss early or at the start of their lives, and to benefit the most, the implant would likely be fitted upon amputation or as soon as the bone stops growing.

With the larger pool of knowledge regarding the benefits of static magnetic fields, several clinically acceptable implants have been developed to begin utilising the method. One such implant developed to treat cancerous tumours in bone was constructed from a glass ceramic matrix infused with magnetic particles, designed to provide the magnetic field (that could be stimulated to heat up from outside of the body for cancer treatment) whilst being made of a bioactive matrix capable of cellular integration. In doing so, the pill could be implanted with no fear of the magnetic material coming in direct contact with tissues or cells of the body due to the insulation of the bioactive layer. This concept was reviewed by Cochis et al. (Cochis, 2017).

2.8. Conclusions

The process of identifying and reviewing key literature helped guide the aims of the research by highlighting to what extent work around socket stabilisation had been carried out in the past concerning identifying what mechanisms of interaction between the residual limb and below-knee prosthesis had been explored and the extent and the level of risk generated by DTI. The literature indicated that the perception of tissue injury about a residual limb was switching from the socket tissue interface to focus more on the interaction between the residual bone and tissue interfaces, particularly at the site of the tibial end. FEA had indicated that despite sites of high stress at the skin's surface, it was highly likely that the most significant stresses would be present at the locations immediately beneath the bony prominences. Such studies helped in understanding how stresses measured at and within the residual limb can be used to produce prosthetics sockets that help reduce the peak stresses. However, targeting internal stresses is not being attempted directly, primarily because of the difficulty in accurately measuring any changes in such stresses. This is a significant gap that has only been covered in FEAs of such complex issues; a limitation is the difficulty in accurately replicating the tissue make-up of a

residual limb, namely the composition of scar, muscle and fat tissue that varies significantly across individuals. This means only trends can be identified. With the literature for such a niche project being limited in the number of studies, it is possible to identify the main driving researchers for such topics, most notably Portnoy and Gefen, researchers that have published to a high standard in the most reputable journals. However, a small level of bias might be present in their conclusions due to the limited number of trials by alternative authors confirming their findings.

To progress the project further, it was necessary to define what aetiological factors would be targeted by the device to reduce the potential for DTIs in transtibial amputations. With a broad spectrum of known causes that are heavily intertwined in cause and effect. Because of this, the structure of the device design was furthered for the following reasons:

- Target mechanism, with the identification of larger shear stresses at the bone tissue interface and considerably lower dangers at the skin surface. The targeting of tissue strain within the residual limb was possible by applying antagonistic loading at the skin surface. Allowing the compression and therefore stiffening of the tissues surrounding the bony prominence, limiting the potential for dangerous cellular strains to occur during ambulation.
- Target measurement, it is thought that measuring the changes in lower limb stresses accurately and actively is difficult and easy to misrepresent. Therefore, by targeting known oscillations of the user's tibia relative to the socket wall, loading can occur appropriately depending on how the limb varies during the user's gait.
- The target sensor system, an effective method used in industry for small-scale displacement measurement, is through Hall effect sensing. Making it possible to track a magnet linearly through noninterfering mediums such as muscle and skin tissues. Although not feasible for a proof of concept, the intention would be to implant a magnet

in the tibia to allow consistent monitoring. However, for the project in question, interpreting gait stages was to be achieved by monitoring socket limb fragments with the magnet on the user's shank and the sensor at the socket wall.

The visualised concept was designed to build on pre-existing passive technologies, such as adjustable panels, providing an active and reactive element to help tailor performance to the variations likely to be seen throughout ambulation. Whilst also providing a potential starting point for future study in a topic (notably DTI reduction systems) with limited focus outside of more general technologies applied in the past.

Chapter 3 Initial Device Design and Manufacture

3.1 Introduction

The following section will provide information on the design and manufacturing method choices made to produce the initial prototype device and how a broad spectrum of factors relevant to the project influenced the selection of materials, components, and manufacturing methods. The chapter will describe the design process that was followed before defining the scope of the design process and evaluating the methods used to produce the initial concepts and prototypes.

3.2 Task Clarification

3.2.1 Problem Statement

With the oscillation of residual bone, most notably the tibia, in below-knee prosthetics having been identified as a mechanism that caused the generation of shear strains about the bony prominence of the residual tibia (and thus DTI), it was possible to propose a reactive device to be installed into a below-knee prosthetic socket capable of detecting residual bone movement and applying a proportional response to help stabilise it during gait. Being a proof of concept, the design requirements of the device were focused on the device's mechanical performance. Prioritising and parameterising the mechanical and electrical inputs and outputs with much more significance. Factors such as cost, environmental impact and the device's life span should all be considered but with less prioritisation, but not to the extent that the problem-solving ability of the device is compromised. Factors such as system performance and user comfort should be prioritised as they hold a more direct correlation to fulfilling the project's initial aims.

3.2.2 Research-Defined Requirements

Requirements for a device or product can be separated into demands and wishes (Pahl, 2013). Demands are requirements to be met under all circumstances, as they are essential functions needed to satisfy the underlying performance of the device. Conversely, wishes are requirements that should be considered whenever possible, being criteria that can benefit a product economically and environmentally but that are not directly linked to successfully fulfilling the aims and objectives of a project. If the device were marketed, such demands and wishes would be condensed into a product design specification (PDS) and described in the total design method (Pugh, 1991). However, as the project required a non-marketable device rather than a product, it was decided that a less specific PDS-style format was needed, mainly due to the trial nature of the machine making demands on the device's longevity, environmental impact and overall aesthetic of little relevance.

3.2.3 Device Demands

Understanding that the movement of the tibia was causing tissue deformation and hypothesising that control of this mechanism would reduce tissue-related injury, it was possible to draw up the following requirements:

- A stabilisation system capable of 25mm extension to match visualised tibial displacement away from its mid-stance position (Lilja, 1993), with the linear displacement being a measure to infer the effects of socket rotation about the residual limb.
- Tibial displacement should be focused on over-fibula influence, with estimated stresses at the bone tissue interface of the tibia being consistently five times greater than those at the fibula (Portnoy, 2008).

- External monitoring of the tibial position will be necessary for a reactive proportional feedback response.
- The sampling rate of bone displacement should be greater than two times the rate of gait (>2Hz) (Antonsson, 1985), but it would be more reasonable to sample at 150Hz, in line with previous studies of a similar nature (Convery, 1999).
- The stabilisation load should be large enough to significantly reduce the expected moments about the prosthesis of 0.3Nm/Kg at the anterior surface of the shank and 0.85Nm/Kg at the posterior (Kobayashi, 2016).
- Accurate displacement sensing to a range of at least 25mm through muscle tissue (Lilja, 1993).

3.2.4 Device Wishes

Thus, the project's priorities were established to investigate whether tibial stabilisation could be achieved, so minimising a contributing factor to DTI in prosthetic-using below-knee amputees. However, the project was devised to consider specific moral and ethical requirements that would not influence the overall outcome but could contribute to the overall success of the work. These considerations were as follows:

- The device should be manufactured on-site (University of Strathclyde) as much as possible, utilising the equipment and skills available to the Department of Biomedical Engineering.
- To maximise time and minimise costs, components with greater accessibility to buy will be prioritised over build-based solutions or components requiring larger learning curves.
- Proportional control of the stabilisation system would be beneficial for a tailored response to alterations in tibial positions, allowing for a minimal loading when the

device is used in less stress-inducing ambulation environments identified by Portnoy et al. (S. Portnoy J. v.-N., 2010). Allowing the device to provide peak performance at the largest tibial oscillations to increase the working life of the device.

- According to Pugh's method, consideration of several other factors is required; ergonomics, aesthetics, lifespan, size, and target cost (Pugh, 1991). The author deemed that although consideration of these factors is essential in device design, they were of lower priority at the current stage of development. The proof-of-concept nature requires a successful demonstration of the initial hypothesis to be deemed a success rather than the commercialisation of the technology.

3.2.5 Device Design Specification (Arranging and Checking of Requirements)

For the design of the device and to carry the demands and wishes in a structured and documented manner, a more precise script of requirements was established, which involved a thorough expansion on what was expected from the system regarding economic, social, and hardware and software requirements. Alternatively, at least guidelines and targets to be aimed for during the device's development should be established as the fluid nature of design requires certain adaptability in response to empirical evidence gathered during the process (Meißner, 2006).

3.3 Concept Components, Materials and Processes

For the progression of the device from a concept idea into a functional prototype system, a process of comparison and analysis was carried out for the components, materials, manufacturing methods and testing systems that would be required, using the device demands

and wishes as a balance of rigid and flexible guidelines to help guide the choices that were made.

For the methods comparison, the device was separated into its constituent parts: bone displacement sensor, microcontroller, effector actuator, structural componentry, and device

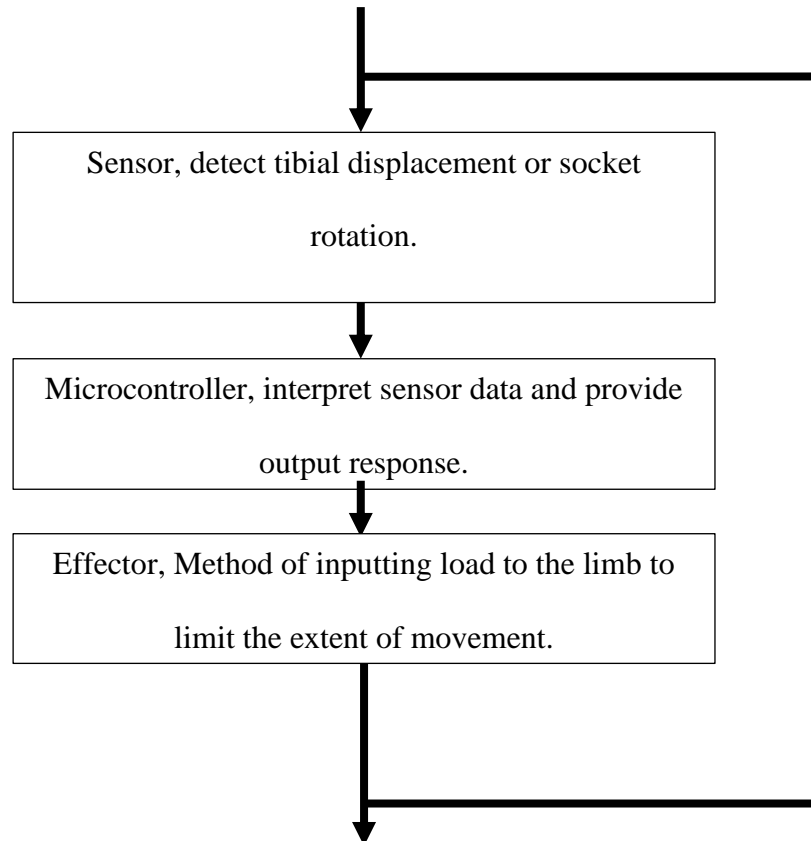


Figure 13: Basic block diagram illustrating how positional data from the limb will be responded to by an effector in a feedback loop.

testing mechanisms. Figure 13 shows a basic feedback loop of how the main components of the device will interact to generate the desired outcome.

3.3.1 Component Evaluation

As stated, a heuristic approach was established for selecting individual components and techniques, allowing certain subjective decisions to be made more quickly. Despite this, a weight rating method was employed for specific components that were similar in performance and overall preference. This technique allowed vital requirements to be used to evaluate individual components. Hence, each condition was assigned a range of importance, providing

the more significant conditions with greater weight based on their influence on the outcome (Roszkowska, 2013). Scores were generated against a datum concept that provided the scale at which other concepts were scored better (+), worse (-) or the same (S) against criteria developed around specific points indicated in the original device demands and wishes.

		Alternatives			
		Wt	Vendor 1	Vendor 3	Vendor 4
Criteria	Cost	.30	Datum	+	S
	Response time	.17		+	+
	Training time	.17		-	S
	Ease of use	.17		+	+
	Strong team	.10		-	-
	Team experience	.10		S	-
Pluses		1.0		3	2
Minuses				2	2
Overall total				+1	0
Weighted total				+.37	+.14

Figure 14: Pugh's matrix example (Ullman, 2006)

Figure 14 shows a representative example of the decision matrix used for comparisons. Ullman highlights some of the key benefits of such a method as its ability to provide “*relative importance*” so that priority can be enhanced as necessary. Providing a framework to compare all alternatives helps reduce the influence of biases when possible. The significant limitation of the method regards trade, where the deficiencies in one criterion might be evened out by the success of another (Ullman, 2006). Due to this, it may be necessary to justify decision-making

between concepts more heuristically, making decisions based more on the author's opinion rather than following rigidly the output of the comparison.

3.3.2 Displacement Sensor

It was hypothesised that prosthetic socket stabilisation could be controlled with a mechanical system responding to bone movement as the tibia is known to oscillate significant distances about its normal mid-stance position during gait, with a static study carried out by Lilja et al. identifying displacements of approximately 25mm and 10mm in the posterior and anterior directions, respectively (Lilja, 1993). To do this, five possible sensor types (Hall effect, light, pressure, ultrasound, tissue stiffness and electromyography) were assessed using a Pugh's weighted matrix with criteria drawn from the initial demands and wishes proposed, shown in section 3.4.2.7.

3.3.2.1 Hall Effect

The Hall Effect refers to the generation of a potential difference as a magnetic field moves into a conductor carrying a current (Figure 15), with the possible difference in voltage being proportional to the present and the flux density (Honeywell, 2013), meaning that with a magnet with a known magnetic field, it is possible to calculate the displacement between the magnet and the conductor, based on the measured voltage. The technology is currently being used in many applications, including those for tracking the orientation in spherical actuators, where a series of detectors surrounding the magnetic locator can triangulate the rotor's position from the various transducer set-ups (Yan 2014). Yan's article also highlights the benefit of Hall effect sensor systems having small non-bulky designs, meaning they can fit into components with minimal re-design or intrusion.

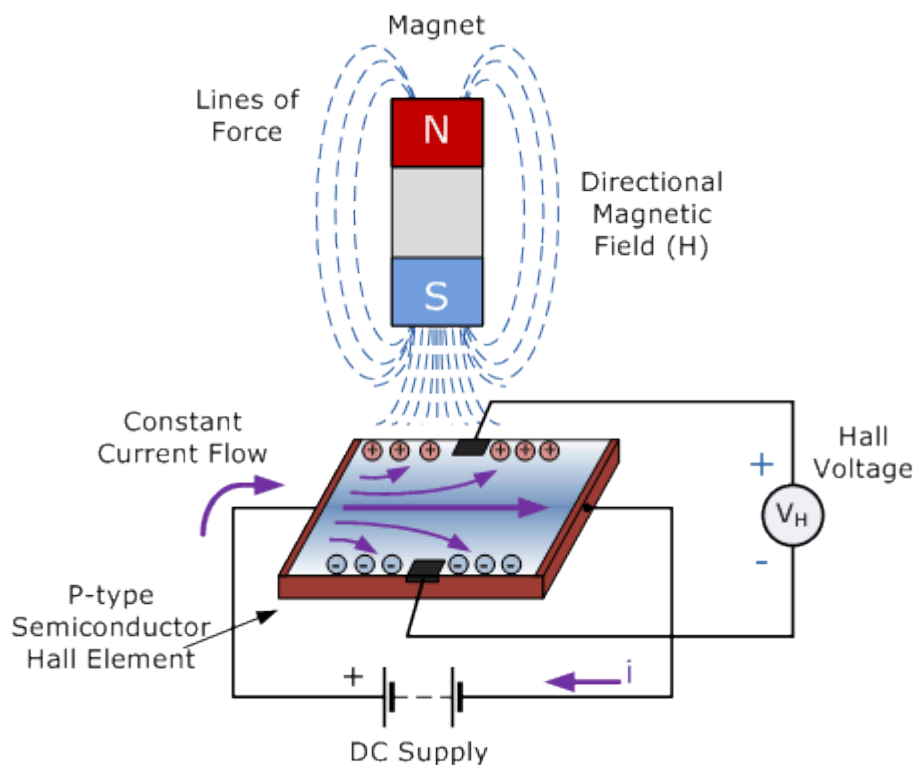


Figure 15: Signal generation using a Hall effect sensor (AspenCore, 2014)

The greatest concern with Hall effect sensing, with the application in mind, is the probable need for the implantation of a magnet, possible during the amputation process, for it to work

most effectively. This means a toxicology study would have to be carried out in advance to understand how the magnet could be successfully implanted with minimal effects over time. This has been explored recently in hearing implants, whereby a magnet is screwed directly into the skull to attach a hearing transducer (Reinfeldt, 2015). If it could be proven more advantageous and offer low risk to the patient, Hall effect sensors may prove a highly effective way of tracking bone movement.

3.3.2.2 Light

Another possible system assessed involved the emission and detection of reflected light to understand bone depth beneath the skin. Specific wavelengths of light are known to achieve greater depth penetration that would allow reflection spikes from the remaining bones (Ho, 2009). Using LED transducers would also be inexpensive and straightforward to set up, with minimal risks, and non-invasive. Likely, issues include light refraction and emitter-receiver positioning; however, calibration could overcome these issues. Furthermore, the technique would allow bone movement detection away from a familiar position for all planes, including pistoning detection. However, it would be challenging to detect rotation with light reflections. Furthermore, it was necessary to explore the best way to ensure the coupling of the sensor to the socket/skin interface, as coupling gel would be required, making implementation in a real device problematic.

3.3.2.3 Pressure

It was possible to pick up changes in bone displacement using a series of pressure sensors sitting on the surface of the residual limb. Monitoring the pressure changes between the skin and socket interface made it possible to detect pressure spikes formed by bone movement. If successful, it would be possible to enhance FEA studies to better understand stress levels within a residual limb during gait. Current studies, such as (Portnoy 2008), use MRI scans of a residual limb to build up 3D models of the limb (including tibia, fibula, muscle flap and socket wall) to

allow FEA programmes to carry out pressure analyses throughout the limb based on a rigid socket wall and the weight of the individual patient. Although the data is beneficial, it does not take into consideration the flow of the muscle flap within the socket or the movement of the bones of the limb, suggesting there may be errors in measured stresses at the different stages of gait, with the pressure distributions visualised potentially being inaccurate in terms of magnitude and location if tibial oscillation was to be adjusted for.

3.3.2.4 Ultrasound

Ultrasound waves are traditionally used as an imaging technique or a displacement measure based on time-of-flight measurement. However, it is also possible to accurately measure changes in displacement based on alterations in the Doppler effect of the waves. This technique is known as Doppler ultrasonography, and it is often used to measure blood flow through arteries or the motion of organs to diagnose diseases such as hypertension (Kim, 2015). The technique has been used in bone motion analysis to study joint motion under controlled conditions, such as knee analysis (Masum M. P., 2014). It can show accurate bone motion against an initial control frame. The difficulty with adapting this technique for the desired purpose of providing useable feedback will be in generating a suitable output indicative of bone position (potentially a voltage range) that can be measured, allowing a response to be generated by the system. A further issue is likely to be related to the coupling of the sensor for prolonged periods as ultrasound signals will not propagate through air successfully, meaning a coupling agent would be required, a concern for a device aimed at day-to-day use.

3.3.2.5 Tissue Stiffness

Tissue stiffness sensors are not commercial sensors but were hypothesised as a potential solution to the problem. Voice coils (more commonly known as speaker coils) are used to sense bone movement and the equivalent change in tissue stiffness at the tibial end landmark of the residual limb. The idea was based on the coils functioning as inductor coils when activated,

meaning that if a stinger (fixed to the centre of the speaker diaphragm) were to move, the displacement would be measurable based on the induced voltage in the system. Different displacements would be measured as different voltage peaks are recorded by the system over time, a number that could then be used continuously to provide counteractive loading from an external source, whether that be an electrical actuator or a similar mechanical system.

This concept holds advantages over light and sound-based transducer systems, as the influence of air gaps is far reduced with this more mechanical-based response; it relies only on a spring system to ensure the central stinger remains located on the tibial end landmark rather than the much more challenging use of gels that is required for the other sensors to function effectively. Furthermore, the system can be produced relatively inexpensively while being easily modifiable if specific characteristics are not deemed suitable, with larger coils providing more significant potential for depth measurement. The idea holds appeal in trials to better understand how the system could be implemented in scenarios outside this project.

Despite this, there were still concerns with the sensor, not just because it was untested, but whether the system would be capable of producing results at the same rate of bone movement with little to no lag time. How much hysteresis the sensor would produce and how influenced the system would be by artefacts such as bumps and jolts were also concerns, making the sensor a risky choice without much further experimentation.

3.3.2.6 Electromyography

Electromyography (EMG) sensors have been used in upper limb prostheses for over 30 years (Zhang, 2011). Here, electrical potentials are produced from muscular activity in the upper limb, with relatively small muscle movements particular to its corresponding limb movement. This factor makes it possible to replicate the same real-life movement based on the location and magnitude of these electrical potentials taken at the skin's surface while further having the

benefit of being non-intrusive but still highly sensitive and producing easy-to-manipulate feedback. Zhang et al. have researched the possibility of coupling accelerometers and EMG sensors to allow for accurate hand gesture recognition in virtual reality-style gaming systems, a popular area of research that is also driving the development of wearable electronics and smart textiles for both therapeutic and casual everyday use (Stoppa, 2014). However, although the initial sensing and feedback systems are very similar to those in existing upper limb prosthesis control, the question remains whether it is possible to replicate the movements of the upper limb with a lower limb prosthesis. One such study detailing some initial trials was carried out by Bai et al., in which EMG sensors were positioned on key muscles of the lower limb. At the same time, it was being unloaded and loaded (10lb sandbag attached) to simulate prosthetic walking. The results were variable in accurately identifying which muscles are stimulated and at what point during the gait process. As with several participants, significant data was produced for "*most*" of the muscles under scrutiny. However, for several muscle sets, on different volunteers, differences could not be classed as significant (Bai, 2017). This highlights the difficulty of achieving similar accuracy to equivalent upper limb studies and further indicates the difficulty of integrating EMG technology into lower limb prosthetics. Although not based on transtibial amputees, Hefferman et al. studied how trans-femoral prosthetic sockets performed against a list of comfort and performance criteria for four different EMG configurations, with a configuration of the suction socket and integrated surface EMG sensors performing best in terms of both comfort and in limiting large amplitude motion artefacts (Hefferman, 2015). However, no actual data on muscular output was collected, and it still needs to be determined how successful EMGs are at detecting muscular stimulation in lower residual limbs. Despite their use and application in an upper limb prosthesis, surface-mounted sensors are still far from perfect, having problems with measurements being influenced by non-targeted muscles, causing undesirable responses from the system, socket

rotation, causing electrode movement, and perspiration on the skin affecting the measured signal (Pasquina, 2015).

3.3.2.7 Pugh's Comparison

For the comparison matrix to be created, a list of criteria was drafted, taking into consideration the device demands and wishes developed at the onset alongside additional criteria covering other areas expected in Pugh's Total Design:

High Priority (Weighting 3)

- The accurate functional range should be as close to 25mm as possible; larger scores are more beneficial than lower scores providing accuracy is preserved.
- Sampling frequency should be maximised, as a higher sampling rate allows the system to be tuned as appropriate, whilst sampling frequency cannot be less than 5Hz.
- Safety and interaction with the body should be minimised as much as possible; the device should have as little impact on the user as possible in their day-to-day usage.
- Provide a suitable output for a proportional response.

Medium Priority (Weighting 2)

- Adaptability should be maximised; implementing and controlling the sensors in multiple different manners is beneficial if problems prevent the initial process from being carried out. Preventing a loss of time and money as the project is developed.
- Sensor availability and in-house knowledge should be maximised, as time for acquisition and configuration of the devices should be minimised.

Low Priority (Weighting 1)

- The cost of the sensor should be minimal as lower costs are better for the project's development moving forward.

- Size should be minimised, as smaller sensors have less impact on the final product size and reduce the interference with the device user.
- Weight should be minimised as lower weight again reduces the interference with the device user.
- Recyclability should be maximised; the device should be as recyclable as possible for environmental benefits.

However, upon an attempt at an initial comparison, it was found that an issue proved very difficult to overcome within the confines of the method. With the different sensors being relatively varied, some of the criteria being scored could not be described in the same manner, with factors such as functional range and displacement not suitably applicable to concepts such as EMGs and Pressure sensors. This meant that the author was forced to assess the concepts on their merits to establish a score, likely causing some bias in the comparison.

Table 1: Shows the initial Pugh's comparison to identify the most suitable sensor for the project, with Hall Effect set as a datum

Criteria	Weighting	Sensor					
		Hall Effect	Light	Pressure	Ultrasound	EMG	Tissue Compliance
25mm Functional Range	3	D	-	-	+	-	-
Body Interaction and Safety	3	D	+	+	-	+	S
Sampling Frequency (Hz)	3	D	+	+	+	+	S
Simple Output	3	D	-	-	-	S	S
Adaptability	2	D	-	-	-	-	-
Availability	2	D	-	S	S	S	-
Cost (£)	1	D	-	-	-	-	-
Size (mm x mm x mm)	1	D	-	+	-	-	-
Weight (g)	1	D	-	+	-	-	-
Recyclability/ Reuse	1	D	S	+	S	S	S
Score		D	-7	-1	-5	-2	-10

The initial comparison, shown in Table 1, produced a spread of scores by which to begin excluding initial concepts. Systems such as tissue compliance and light required more in-depth application knowledge than permitted within the project's timescales. Ultrasound holds potential benefits for proof-of-concept studies due to the range and available knowledge whilst losing out on design integration. Pressure and EMG scored relatively well against the Hall effect sensor and, as seen in several studies, show their benefits in terms of known usage, particularly for monitoring the skin's surface. However, they were assessed to be less suitable for accurate depth measurements of the shank/ tibia against a socket wall.

3.3.2.8 Conclusion

The nature of the proposed study allowed the research of a broad range of possible sensing systems to measure the tibial displacement of a below-knee amputee, with the initial research intended to identify solutions to a previously unstudied parameter. This meant concepts such as light transducers and tissue stiffness monitors were considered for the task; however, they were rejected for similar reasons: a lack of knowledge of their potential and, therefore, the requirement of a large time investment in their development and calibration. Systems such as ultrasound and pressure-based systems were also discounted. Despite the evidence of performance in other literature studies, they were thought to be limited in their prosthetic application, with the need for coupling gels and prolonged positioning within a socket likely to cause problems with feedback, particularly for design iterations that would be for more day-to-day use by a prosthetic wearer. While EMG systems have proven effective in detecting muscle stimulus, it was unclear whether measuring tibial displacement would be possible, making it a more complicated system to justify moving forward. With similar conclusions drawn from the matrix analysis, the process led to the selection of Hall effect sensing being the initially considered. Its simplicity and ease of configuration make it suitable for design integration. With the idea provisionally decided, a discussion was held to identify whether a magnet could be implanted in the tibia end to ensure the target user could use the technique robustly. This was discussed with surgical professionals and deemed feasible, allowing the inclusion of the Hall effect in the detailed design phase and triggering research into its range and integration with an appropriate control system.

3.3.3 Microcontroller

For small projects involving circuits capable of both sensing and inducing a response, it is necessary to include a microcontroller capable of understanding the received data and initiating an output appropriate to the continuously changing values. Differing from microprocessors,

microcontrollers usually contain input and output peripherals (IO), random-access memory, and read-only memory (ROM) in a fully integrated board for more complicated applications (Bannatyne, 1998).

For this study, a system capable of giving a rapid response to the continuously changing nature of gait, with events requiring full stroke from each actuator to be extended from a middling position in approximately 0.2s at HC before returning to its central position and continuing in the opposite direction to its TO position, within 0.4s (Kobayashi, 2016).

With a broad range of small-scale microcontrollers available on the market, the decision was made to maximise efficiency and select the Arduino platform. Being readily available and with easily available expertise for novice users, the device provided a good opportunity for trialling codes and communications with limited previous know-how.



Figure 16: Arduino UNO

The Arduino Uno, Figure 16, provides a high hardware level and simple software programming capabilities for small device design. Furthermore, within the Department of Biomedical Engineering at the University of Strathclyde, there was a high level of expertise in supporting programming and device configuration. At the same time, a sizeable online community hub also provided an excellent source of base code to build on. Arduino is also

versatile, with devices like the Mega providing higher processing power and hardware options if required (Arduino, 2020).

3.3.4 Actuator

The actuator system was critical in providing a stabilisation load for the residual limb to reduce tibial oscillation and tissue deformation. As mentioned in the device demands, the device was required to reach full extension in a 0.2s time frame to be able to respond in a fashion quick enough to balance the change in moment directions from the swing phase into heel contact, with large enough load potential to reduce the magnitude of tibial movement effectively. However, a relatively low loading magnitude was hypothesised to provide a suitable counterbalancing load if applied near the tibial end. Four standard actuator varieties were identified for comparison: hydraulic, pneumatic linear, and rotary electrical varieties. Each actuation method was evaluated for its positive and negative aspects in a simple comparison to identify which should be chosen for the initial prototype.

3.3.4.1 Hydraulic

Hydraulic actuators function by moving an internal piston, with the pressure created by an incompressible fluid and an external pump (Gonzalez, 2015), with the actuators able to return to their original position by altering the feed direction in a looped system or by a mechanical method. The systems are known for their high loading capabilities relative to their size, with excellent positional control. However, limitations include additional components and the potential for hydraulic fluid leakage.

3.3.4.2 Pneumatic

Pneumatic systems are similar or equivalent to hydraulic systems. However, the incompressible fluids are replaced by compressed gas (typically air) (Gonzalez, 2015). With similar componentry requirements, pneumatic systems tend to be lower powered than hydraulic

equivalents. However, they reduce the risk of environmental complications, with air leaks being more convenient than hydraulic fluid ones. Similarly, with the miniaturisation of technology, systems can be discretely installed in small-scale devices and hardware. Leaks and pressure losses cause the main issues with pneumatic systems, while contamination can lead to malfunctions.

3.3.4.3 Electrical Linear

Linear electrical actuators can take several forms. Torque-based varieties rely on driving a screw to drive the actuator to voice coil actuators (VCA), whereby the effects of Faraday's law of induction will drive the piston along its length, with various levels of control. Torque-based examples are highly accurate and controllable, with the limitations usually being a power-to-size ratio and the system's response time (Gonzalez, 2015). VCAs differ in that they can provide high loading quickly but with less controllable positioning and more complicated methods of returning the piston to its original position.

3.3.4.4 Electrical Rotary

Electrical rotary systems are similar to torque-based linear varieties; other than that, the rotation from the motor is not converted in a linear direction. Rather, it provides high levels of rotary torque that can be accessed with gearing and other structural components. The systems share the high precision of their linear counterparts, with a higher potential power-to-size relationship; however, the trade-off for this is difficulty in converting the rotary power to linear actuation.

3.3.4.5 Comparison

Market research into possible small-scale actuators revealed 11 potential candidates analysed against requirements developed in the device demands and wishes section. Each requirement

was given a weight between 1 and 3 (1 being of lesser importance, 3 of high importance), and each concept was scored against the performance and preferences of a selected concept device.

The devices included:

1. SMC Miniature Rod LEPY 6 Electric Actuator
2. Firgelli Linear Servo Actuator L12
3. Festo Single Acting Pneumatic Cylinder
4. Festo Double Acting Pneumatic Cylinder
5. AGI AGMS 1-2 Miniature Pneumatic Linear Actuator
6. Linear Actuator Conversion for RC Servo
7. Linear Electromagnet Solenoid
8. Interfluid Hydraulics' Hydraulic Cylinder
9. PICMA Piezoelectric Multilayer Ring Actuator
10. Moticont Linear Voice Coil Motors
11. Futaba S3306 Rotary Servos

Table 2: Comparison of small-size actuator concepts against specific device requirements

Criteria	Weighting	1	2	3	4	5	6	7	8	9	10	11
25mm Extension	2	S	+	S	S	D	S	-	+	-	S	S
Full Extension in 0.2s	2	S	-	S	S	D	S	S	S	+	S	+
Capable of 0.3Nm/Kg	2	-	-	+	S	D	S	-	S	+	-	S
Positional Control	3	S	-	S	S	D	S	-	-	-	S	S
Low Mass	2	-	+	-	-	D	-	-	-	-	+	S
Low Cost	1	-	+	+	+	D	+	+	+	+	S	-
Minimise Environmental Impact	1	+	+	S	S	D	+	+	-	+	+	+
Benefit from on-site expertise	1	S	S	S	S	D	-	S	-	S	+	+
Total		-4	0	1	-1	D	1	-7	-4	-1	2	4

Table 2 shows the weighted comparison study used to more easily differentiate between the available actuator devices on the market.

3.3.4.6 Conclusion

The comparison identified a clear contender for the device to be carried into further design stages. The Futaba S3306 Rotary Servos were electrical rotary servos that could be combined with a cam system to allow linear displacement to be generated via a piston configuration, with the advantages of size and ease of manufacture of the linear conversion system. Servos of this kind have a large community of experimentalists, providing detailed and varied information on how such systems can be developed and modified. Integrating and programming them to perform the desired function without a complicated troubleshooting process is relatively simple. The servos themselves are high performing in speed and force application while small, making them a desirable option for initial trials.

3.3.5 Socket Manufacture

3.3.5.1 Hands-On

Hands-on casting techniques have been the standard for prosthetic socket manufacture since the realisation that socket comfort and fit are directly linked to the socket's design and overall construction. This technique relies on a trained prosthetist manually overlaying material directly onto the limb or, more commonly, on top of a silicone liner placed over the residuum surface. This initial cast is used to recreate a model of the residual limb complex, typically in plaster, that the final socket will be cast over (Safari, 2013). The advantages and disadvantages of the hands-on technique have been widely discussed and are more commonly understood than the following alternative techniques. The socket's comfort and fit are highly dependent on the skill and preferences of the casting prosthetist, and it has been noted that sockets cast on the same amputee by different prosthetists are rarely exact. This makes it very difficult to achieve a suitable standard of socket production due to the presence of factors that are mostly impossible to control. However, despite this, with little in the way of a suitable replacement, hands-on casting is often the most suitable and accessible technique available to many patients

needing a prosthesis. Fortunately, there are many skilled prosthetists capable of producing practical and comfortable sockets, which is a positive, but one that is slowly coming under greater pressure with the increased number of amputations seen globally, a number growing at a far greater rate than new prosthetists can be trained. Despite this growing demand for trained prosthetists in general, this would not likely affect the project moving forward as, with only a low number of sockets being required, our demand is not significant and can probably be fulfilled privately, utilising trained university staff rather than prosthetist professionals. Prosthetist demand is also unlikely to cause a problem for the project. The university has its own Prosthetic & Orthotic Section with trained professionals available to perform the necessary casting with minimal delay or obstruction.

3.3.5.2 Hands-off

An alternative approach that has been developed in recent years is that of hands-off socket casting, which is a process that no longer relies on the skills of a trained professional to design and shape the socket as they see appropriate but relies instead on uniform pressure across the residuum's surface to form the cast. In this process, the amputee must stand with their residual limb placed in a machine that envelopes the surface up to the desired height of the socket before applying static pressure across the surface with water within the machine. This, effectively, forms the first stage of the socket uniformly across the surface of the skin in a process that has proved to be far more repeatable than its predecessor, with measurements of only a 1.4mm difference between casts compared to differences of between 2.4 - 5mm seen in the hands-on approach (Safari, 2013). Therefore, if the consistency of production is essential, this technique holds critical advantages over the hands-on approach.

The technique was initially conceptualised as reducing the need for skilled prosthetists, as the device could be shipped to countries lacking the required expertise to fit prosthetics. It also provides a source of prosthetic production for many people without increasing pressure on the

number of available prosthetists mentioned earlier. With other studies showing high patient satisfaction and device performance, the method is expected to become much more widely used and commercially available. However, as it is not considered the standard, its usefulness for clinical applications is limited if it were to be deemed unproven. Despite this, the university has a wealth of knowledge regarding the technique, and many pressure-casting devices have been developed in the biomedical department; therefore, access to the necessary skills and equipment is unlikely to cause problems.

3.3.5.3 3D Printing

The final concept that will be discussed is the most recent development in the field, relying on three-dimensional scans of the residuum, thus allowing for almost exactly fitting sockets to be constructed using 3D printing technology, these sockets being modelled to minute accuracies based on the scans (J. ten Kate, 2017), and making it possible to make accurate and repeatable sockets for an individual with excellent repeatability concerning the intended use case between subsequent sockets and reducing differences in performance between sockets that a prosthetic user is using at any one time. For example, it is common for prosthetic users to use several different prostheses depending on their activities, ranging from sports-specific to social wear prostheses, on top of their everyday limb, with hands-on and, to a lesser extent, hands-off techniques both providing some variability in socket dimensioning that could cause discomfort and limb damage when switching between different prosthesis. The balance of repeatability is offset by the cost required for scanning and manufacturing, both being expensive processes. At the same time, the option of multiple prostheses is unlikely to be available to many amputees, particularly those with low incomes or from poorer countries. This makes the technology applicable only to the wealthier on the potential client list, a factor that may not also be practical for clinical trials not explicitly looking at the 3D printing of prosthetic sockets.

Furthermore, although colleagues at the university have carried out research into scanning the residuum, the concept of socket shape is influenced heavily. However, other clinical considerations (residuum growth during ambulation) exceed the original shape. Despite this, the technique is developing but is not at the stage of full automation, creating added variables that may influence an already unrivalled approach.

3.3.5.4 Conclusions

Understanding the relatively limited possibilities available for socket production makes it a more straightforward process to plan the design steps as the project progresses. For the tests that will involve non-disabled volunteers, it will be necessary to utilise hands-on techniques as the technology for hands-off does not apply to a complete leg, and, on balance, scanning and 3D printing would not be used due to the negative aspects of the technique. Some other design alterations are likely needed for the able-bodied socket to effectively replicate the socket movement of an actual transtibial. For example, the bottom of the socket will probably need to be bell-shaped to allow natural oscillations of the participant's lower leg. In contrast, it is likely that for the below-knee amputee volunteers, a hands-off technique will be used because of its repeatability and because we have access to experienced professionals who are interested in testing and using the technique moving forward.

3.3.6 Structural Component Manufacture

3.3.6.1 Computer-Aided Design

Computer-aided design (CAD), a powerful tool in the design process, makes it possible to visualise parts in a three-dimensional space, allowing the troubleshooting of designs before the manufacturing process, saving time and money and minimising waste generated by unseen device fit problems. Functions like 3D printing and computer numerical control (CNC) routers go hand-in-hand with computer-aided manufacture (CAM). CAD also makes rapid prototyping viable and is a time-saving process.

Several programmes are available for the processing of 3D design, with the likes of SolidWorks, AutoCAD and PTC Creo providing design-based platforms. Additional features like FEA technology and rendering techniques offer mechanical strength assessment and final product visualisation. While each programme has strengths and weaknesses, less thought was required in selecting a suitable method for this project. With the simple opportunity that PTC Creo was licensed and available to the university's biomedical department, there was no need to purchase other packages for what was seen as a purely design-based exercise. Although less user-friendly, in the investigator's experience, than SolidWorks, the programme needed to be more adept at producing accurate parts and assemblies for component configuration. With the immediate circumstances requiring minimal cost and time input, PTC CREO was utilised opportunistically.

3.3.6.2 Additive Layer Manufacturing Techniques

Additive layer manufacture (ALM) is the process by which CAD models can be manufactured into physical components by building the design layer by layer. More commonly known as three-dimensional printing (3DP), ALM can be used with various materials, ranging from plastics to metals to ceramics. However, each requires different speciality equipment to afford effective production.

For producing an active and reactive prosthetic socket, a rotational servo system coupled with the Arduino and Hall effect systems would be suitable, the configuration requiring a frame and piston system to be designed and manufactured to support the necessary components. Due to the bespoke nature of the product and the likely need for quick design edits and re-manufacture, it was decided to use 3DP technology. This would reduce manufacturing and labouring time compared to the more traditional milling and lathing styles, which are also more likely to be affected by human error. It was also decided that lightweight material, such as plastic, would be a better solution than metal as it is relatively less expensive. At the same time, it still

possesses the required mechanical properties. For this reason, only 3DP methods that were polymer appropriate were investigated, while metal and ceramic-only techniques were ignored.

The remaining subdivisions of this section will give details concerning several available ALM techniques and a brief product design specification (PDS) to explain what criteria were being evaluated during the later decision-making process.

Fused Deposition Modelling

Fused Deposition Modelling (FDM) is one of the more straightforward and commercially available styles of 3D printing, relying on material extrusion through a heated nozzle to deposit material in the desired geometry. The solid material is supplied as a filament coil, fed through the nozzle and heated to the point that it becomes suitably pliable, can be moulded and deposited, and dries on impact in the desired position. The technique is often favoured for rapid prototyping processes as it is one of the fastest techniques available, producing a full-scale model in a brief period. It is also considerably cheaper than many of its alternatives. Despite this, it is limited by lower mechanical properties due to the porous nature of the deposition, creating less dense parts, often with poor resolution. However, this can be controlled by nozzle sizing to some extent.

Stereolithography

Stereolithography (SLA) uses photo-polymerisation, the process of resin being cured following exposure to ultraviolet (UV) light, to build up a model layer by layer in a vat of curable resin. The process involves incremental movements of a platform submerged in the vat of curable resin, the layers being cured before the platform submerges further, allowing the next layer to be cured on top of the previous. With the method capable of achieving very high-resolution parts at near-maximum material density, the process has apparent benefits in terms of mechanical strength and the level of detail that can be achieved. The drawbacks of the process

are that production rates are much slower and substantial cost increases, with SLA often being 8 – 10 times more expensive to use than FDM-type methods.

Methodology

Product Design Specification

A basic PDS was proposed to create a list of criteria for comparison of the selected manufacturing methods, highlighting details such as cost, recyclability and mechanical strength, as shown below:

1. Must have a high-resolution finish
2. The method should provide high material density when complete
3. Must be mechanically as strong as possible
4. The compatible material must be non-toxic
5. The compatible material must be as recyclable as possible
6. The process must use minimal scaffolding materials to reduce cost and environmental impact
7. Low cost is beneficial but not essential
8. The material should be resistant to wear
9. Low weight is desirable to minimise the impact on the device wearer's mobility
10. The aesthetic finish should be as appealing as possible to encourage participant use.

Method Selection

It was decided that for general expense, speed and adaptability purposes, the models would be manufactured using the on-site equipment at the University of Strathclyde. This significantly reduced the complexity of the selection process: only two processes, FDM and SLA, were available at the time of product manufacture. As suggested, it would have been possible to use the remaining two styles; however, this would have meant outsourcing production to a private

organisation, which would have increased production costs and time, factors that could limit the adaptability of the manufacturing process. This was important when considering the initial concept nature of the project and the probable need for design changes and alterations as development progressed. Therefore, it was decided to compare ALM's FDM and SLA styles using an adapted version of Pugh's total design method.

With only two concepts, it was decided to set the FDM concept as the datum and determine whether SLA was more effective after one comparison, with SLA scoring either a positive or negative result when compared to the datum. Scores were recorded as a + for better, - for worse and S for the same or equivalent scores. Each criterion was weighted between 1-3 regarding their overall importance to the project, with three being points that were key to the project, two being somewhat important, and one indicating less importance.

Table 3: Evaluation of SLA, with FDM set as the comparison datum

	Weighting	FDM	SLA
Resolution	3	D	+
Density	3	D	+
Mechanical Strength	3	D	+
Non-toxic	3	D	S
Recyclable	1	D	S
Minimal scaffolding	2	D	-
Low Cost	1	D	-
Wear-resistant	1	D	+
Low weight	2	D	-
Aesthetic	1	D	+
		Total	5

Table 3 shows the straightforward Pugh style comparison that was carried out to evaluate the differences in benefits that both SLA and FDM ALM would carry into the project if used. It was evident that SLA possessed the most beneficial mechanical strength and solidity characteristics. The process was deemed more desirable in device resolution, model density and material strength, all factors that were seen as being of vital importance to the product. As shown in Figure 17, the much greater resolution of the SLA style ALM significantly reduces

the surface roughness of parts, increasing model accuracy and density while minimising any post-processing of the printed components.

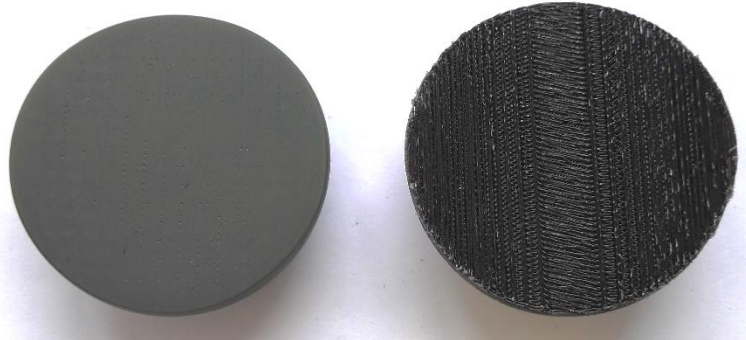


Figure 17: Left) SLA Resolution and surface finish, Right) FDM Resolution and surface finish.

Conclusion

Evaluating the most suitable additive layer manufacturing process available to the project was necessary to ensure time and effort were well-spent by developing and manufacturing inadequate and ineffective models. Several different ALM styles were researched that could have been used to produce models; however, the commercial sensitivity of the device meant it was necessary to build it in-house as much as possible. This meant that selective laser sintering and digital light processing were rejected, leaving fuse deposition modelling and stereolithography as the final two concepts to be evaluated. Using an adapted version of Pugh's method of total design, the simple comparison concluded that SLA was the best choice to manufacture the required components, providing the best mechanical properties, finish, and ease of post-processing.

Material Detail and Comparison

Having selected SLA as the method of manufacture, it was possible to evaluate the available materials for the method, where trade-offs between mechanical strength and cost needed to be understood when considering the viability of the production of the components. Two such materials were available for use in conjunction with the SLA machine: ABS-tuff (an

acrylonitrile butadiene styrene variant) and HTM140 (a high-temperature resistant photopolymer).

With the resolutions and surface finish being almost identical for both materials, it was necessary to compare them based on their mechanical properties and cost, as shown below in Table 4.

Table 4: Property comparison between two SLA-cured materials for 3D printing.

	ABS-tuff	HTM140
Tensile Strength (MPa)	75	56
Tensile Modulus (MPa)	1927	-
Elongation at Break	5.20%	3.50%
Flexural Strength (MPa)	125	115
Flexural Modulus (MPa)	3016	3350
Hardness	83	-
Resin Specific Gravity (g/cm ³)	1.11	1.10
Time per gram (h/g)	0.089	0.113
Cost per gram (£/g)	0.810	1.123
Cost per hour (£/h)	9.091	9.962

Here, the properties were split between material-based properties and factors influenced by the required printing machine, such as time and cost. Mechanical strength and flexibility were prioritised over overall cost; however, if there were large differences in cost between the materials with similar mechanical properties, the

lower-cost material would be considered. This factor proved to be negligible as it was found that ABS-tuff was more mechanically robust, with a tensile strength of 75MPa as opposed to the 56MPa of the HTM140. After initial trials, this material was found to be faster and more cost-effective because the production rate was faster and less expensive per gram of material. Therefore, it was relatively easy to select ABS-tuff as the chosen material for the final components.

3.3.7 Device Testing Methods

To monitor the overall performance of the device, evaluating the stabilisation element and the comfort, new and more standardised techniques were established. The Hall effect sensor data provided the baseline performance values, which the more reliable Motek CAREN supported. At the same time, a basic written feedback system was used to gauge the participant's perspectives and experiences.

3.3.7.1 Sensor Feedback

The microcontroller needed to calculate a numerical value for the magnitude of the magnetic field passing over the sensor's surface to employ the Hall effect sensor in a way it would act as the input data, whereby a proportional style control could be returned. As detailed further in this thesis, it was possible to track the displacement of the magnet accurately while providing a value that could be tracked in real-time to assess the device's performance during specific activities. However, displacement tracking was not considered the only method, but rather a system that could be validated in some way by a more industry-standard system to validate the novel displacement system.

3.3.7.2 Motek Computer-Assisted Rehabilitation Environment

Motek Medical Computer Assisted Rehabilitation Environment (CAREN) system uses body tracking cameras to record the movement of key body landmarks to aid patients' physical and mental rehabilitation. Patients may suffer from problems ranging from post-traumatic stress disorder (PTSD) to stroke (VICON, 2013), where the virtual environment and treadmill configuration is used for active rehabilitation in a safe and controlled environment. The system allows for the motion tracking of the body, with infrared markers reflecting the position of bony landmarks to the motion capture cameras. This makes it possible to computationally model a person's motion and provide data on joint mobility, muscle power, stride length and

the reaction forces of each foot (amongst others). Data that can be interpreted to identify inefficiencies in body function, gait defects and much more. Making it possible to design subject-specific rehabilitation programmes. Using a programme that includes the Motek CAREN, along with an inbuilt safety harness and treadmill, light rehabilitation work can be carried out at the patient's speed in total safety; the harness prevents any falls occurring if the patient were to trip, while the system is backed up with a mechanism that stops the treadmill if a trip were to occur. The virtual reality screens help encourage the training by providing an exciting and variable method where simple walking scenarios or games can gradually rehabilitate the patient, depending on their circumstances.

The motion capture is carried out by VICON Vero cameras, designed to emit and then receive reflected infrared light, a system of multiple cameras placed around the target space providing full three-dimensional tracking of the body as the patient enacts the required motion. Reflective markers placed on bony landmarks or clusters on limbs provide the feedback, with computer algorithms designed to estimate the bone positions based on the patient's height, weight and limb lengths.

3.4.7.2.1 CAREN and Prosthetics

The Motek system has advantages for rehabilitation, and the technology can also be utilised for lower limb prosthetic users. Providing an environment where patients, unaccustomed to their new prosthetic or amputation, can train and become acclimated without the risk of injury or any other psychological hindrance caused by more public training. Introducing visual cues increases the rate at which the patient can return to walking outside safely (Isaacson, 2013).

Marker-based tracking of transtibial amputees, measuring the oscillation between the residual limb and the socket during gait, has been carried out previously, with one such study concluding that marker-based systems could be utilised to evaluate suspension systems, despite

a source of error being caused by skin movement (Childers, 2016). As the errors were always of an order of magnitude lower than the level of angle change between the residual limb and the prosthesis, the system can analyse and compare suspension or stabilisation methods added to the limb.

It was decided that the Motek CAREN system would be used for the proof-of-concept experiments to validate the tibial stabilisation device. The first experiment, involving a non-disabled patient, would require the treadmill and harness system to analyse whether a mechanical system could balance a similar oscillation style to that seen in prosthetic-using transtibial amputees. If the stabilisation were successful, it would be possible to extend the device for use on participants who actively use a below-knee prosthesis. This situation would require an accurate system of determining anterior/posterior movement between the residual limb and the prosthetic test socket and where the data regarding displacement and change in angle could provide direct evidence of the stabilisation device's success when comparing results with the device engaged and disengaged.

3.4.7.2.2 Project Marker Selection

Requiring a configuration of infrared reflecting markers to be able to numerical data on the device influence, it was necessary to select a suitable marker system or model for use. Despite many marker models being well researched (such as plug-in-gait and even markerless systems), upon the advice of experts at the university, it was decided to progress with a simpler model capable of generating three distinct vectors to allow for angle comparison to being monitored. This involved using a fixed vector mounted to the orthotic device (see Chapter 4) and two varying vectors for posterior and anterior rotations of the shank. It was devised so that the angles marked in Figure 18 could be tracked with the device engaged versus disengaged to provide a more precise measure of the performance of the device overall during the participants' gait cycle.

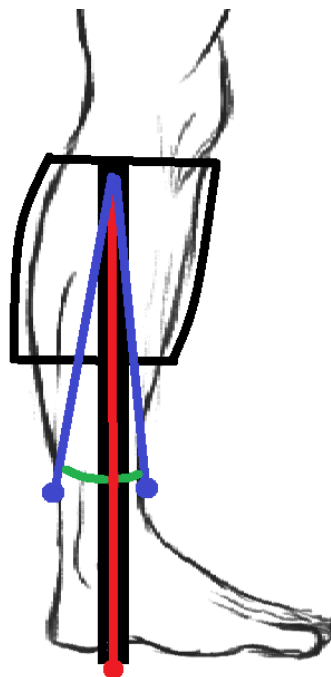


Figure 18: Vectors generated by a simplified marker configuration.

3.3.7.3 Participant Survey

Using a simple feedback format, the participants' views would be gathered after each study, making it possible to gauge subjective data on the system's comfort and overall feel.

Information that would be beneficial in a future redesign of the device architecture to increase comfort and use, as participant safety is paramount.

3.4 Discussion

To successfully structure the design process, the decision was taken to follow a heuristic approach, following a predefined but flexible format to ensure the project's progress towards the predefined goals. This also allowed for individual decisions which were not efficient in achieving the final targets but did allow for the development of the skills and interests of the investigator.

It was identified that the device would require three main components: sensor, microcontroller and actuator. The final method selections requiring configuration were manufacturing the prosthetic socket and the structural components and devising how the device could be tested for functionality. This process concluded that:

- A Hall effect sensor would be configured to provide displacement data based on the distance of the magnet.
- An Arduino Uno would be used as the microcontroller for sensor data collection and actuator control.
- Electrical rotary servos configured with a piston system would provide the linear actuation in conjunction with positioning, as signalled by the microcontroller.
- Prosthetic sockets for testing would be manufactured using hands-on casting techniques. However, hands-off techniques may be considered for comparative studies in future design iterations.
- Structural components would be designed using PTC Creo and 3D printed in ABS-tuff using stereolithography.

Device testing would be three-fold, incorporating the Hall effect feedback recorded via the Arduino IDE, the vector data calculated from the Motek CAREN feedback of the reflective markers and the participants' feedback.

Chapter 4 Detailed Design

4.1 Introduction

Following the decisions made for the appropriate methods and components, the following chapter describes the detailed design specifics for the required hardware and software. Building on identifying fundamental problems from previous chapters, an initial trial prototype was produced based on several solutions proposed to satisfy the demands and wishes of the device while identifying how the pre-selected components could be combined to achieve a completed device capable of performing to the expected level. Alternatively, at least to the level that device enhancements could be identified and carried forward, as the device was developed over subsequent design and trialling iterations.

4.2 Detailed Design

The following sections will explain how the various devices and structural components (socket, Hall effect sensor, microcontroller, actuator and assorted structural components) were developed and combined to form the initial device for testing.

4.2.1 Actuator System

It was decided that rotational servos (providing enough torque at a fast-enough rate) would provide the best compromise of power and comfort. It was found that a Futaba S3306 servo could provide 12.7 kg/cm torque, rotating 60° in 0.2s. Providing a response time within the expected rate of moment change of a normal gait cycle, whilst it was hypothesised that suitable stabilisation would be determinable with force applied by the servo. However, this factor was a relative unknown and would be assessed upon initial trialling. This would operate alongside a Hall effect sensing system that, after testing, indicated very accurate displacement measurements over an operating range of 70mm, with minimal hysteresis. This was considered

ideal for the expected displacements between the skin and socket wall or, more ideally, between the socket wall and the tibia end. This would make it necessary to implant a magnet in the tibia end during the amputation process to monitor the tibia position in situ and respond to it effectively. Hypothetically causing ethical problems for the initial trials. Therefore, only the skin-mounted magnet concept was explored, in which the anteroposterior movement of the magnet caused equal and opposite movement from the two servos present in the system.

A piston housing and servo housing were both produced, with the former being ergonomically designed to fit on both the front and back of a lower limb while matching the contours of the socket to maximise comfort to the wearer. Meanwhile, the stroke length was designed to incorporate both the large and small cam setups, only requiring a silicone spacer to be added when switching to the cam with a smaller stroke volume. The servo housing was designed to the dimensions of the Futaba servos while also being designed to integrate inside the piston housing, using an electromagnetic system to attach the two components and providing a quick release system, if required. Both the piston and the cams were produced in the same manner. A Creo parametric was used to build up and design the base components based on the servo dimensions and the expected size and shape of a below-knee prosthetic socket before later being converted into functional components using 3D printing technology. Stereolithography (SLS) was used, a process by which CAD models can be built up layer by layer using a curable resin when exposed to ultraviolet (UV) light.

With this completed, it was possible to create an initial representation of how the components would fit (and look) on a below-knee prosthesis - providing information on available space and an idea of how large the device would make the prosthetic - allowing for streamlining considerations to begin, as well as design enhancements to cover up the electronic equipment to produce a prototype that would be as close to marketable as possible.

4.2.2 Hall Effect Sensor Configuration

To be able to utilise a Hall effect sensor for lower limb prosthetic application, it was necessary to characterise its response to the changing magnetic flux caused by altering the distance between several different sized magnets and the sensor itself, with the direction of measurement taken inline/ parallel to the magnet axis.

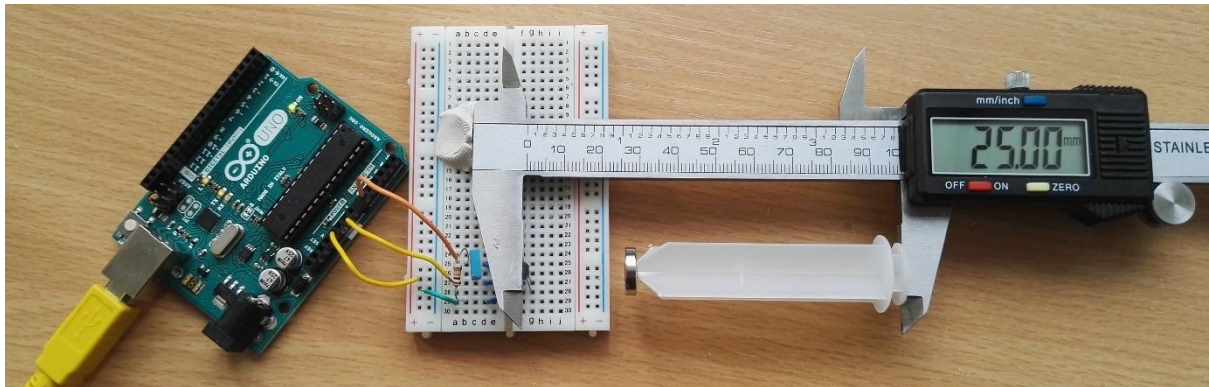


Figure 20: Experimental set-up, using digital callipers to measure the displacement between the Hall effect sensor and magnet.

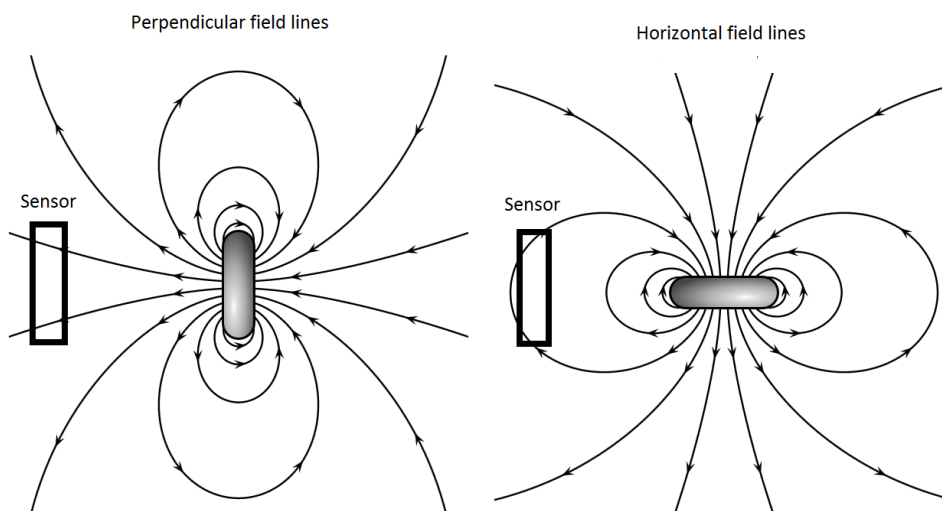


Figure 19: Magnetic field line orientations tested to establish which produced measurable changes in input over the largest range.

A basic experiment was designed to be an able test for this, with the output measurements of a Hall effect sensor being tracked by an Arduino microcontroller to generate an easy-to-read output. The displacement of the magnet was monitored using digital callipers, providing a system capable of 0.01mm precision changes, making displacements both fixable and easy to

repeat to ensure consistency. As shown in Figure 20, the experimental set-up offered quick measurement and repeated while being easy to adapt for the two different sizes of magnet used.

Data was generated for both magnets with the north pole facing the sensor, with results generated from both forwards and backwards movement to establish if any error was generated from hysteresis-like effects. Further, a singular comparison was conducted using the large magnet to establish whether a greater range could be achieved when the magnet was orientated so that the field lines cut the sensor horizontally or vertically, as shown in Figure 19.

The components required for the experiment included:

- 1 x Honeywell SS411A, Bipolar 3pin Hall effect sensor
- 1 x 10K Ω resistor
- 1 x 100nF polyester capacitor
- 1 x Arduino Uno
- 1 x digital callipers
- 1 x Neodymium magnet, 12.5mm diameter x 3mm
- 1 x Neodymium magnet 3mm diameter x 1.05mm
- 1 x Neodymium magnet 9.85mm diameter x 0.96mm
- Connecting wires

The code programmed into the Arduino was designed to measure the change in potential difference across the Hall effect sensor and convert the value to the magnetic flux (measured in Gauss) while averaging every ten readings to eliminate any random variation or wobble generated by variations in the atmosphere or vibrations.

4.2.2.1 Results

To establish the optimum magnet orientation (by which the best would refer to which orientation produced the most massive change in measured Gauss over the broadest range), two orientations of the same magnet were tested. The test successfully demonstrated that the orientation producing near perpendicular field lines relative to the sensor's face produced a much greater useful range, with useful data produced from 8 - 40mm, while the horizontal

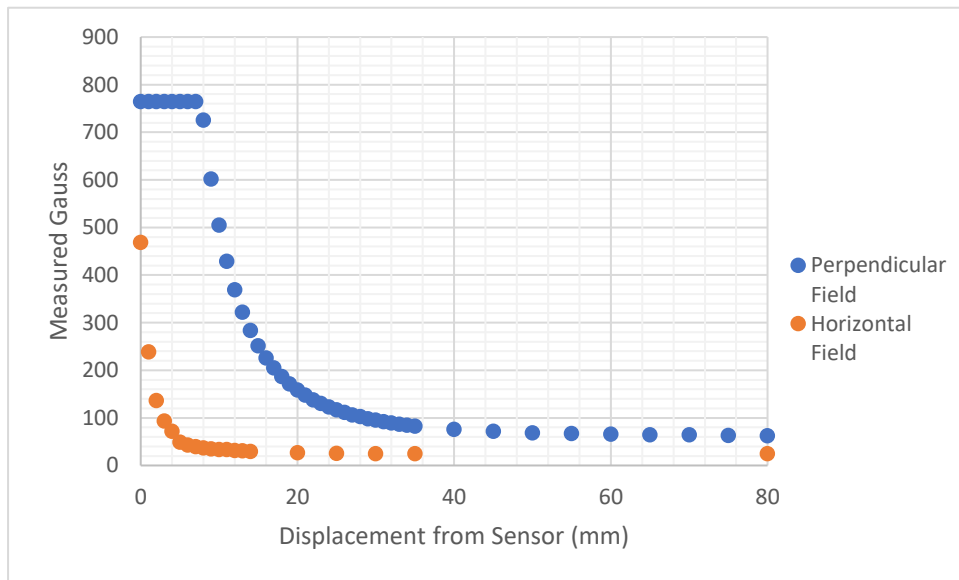


Figure 21: Graph showing the difference in sensor measurement for the same magnet depending on its orientation.

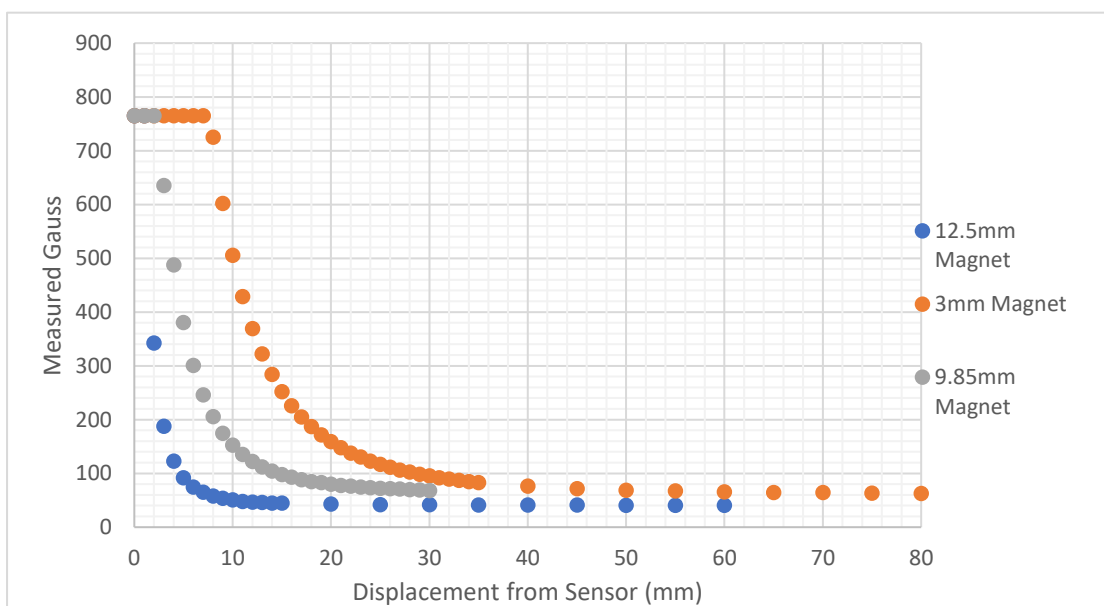


Figure 22: Graph showing the difference in sensor measurement for different magnet sizes

equivalent only produced useful data between 0 – 14mm and a reduced magnitude, as shown in Figure 21. Based on this, all the remaining tests used in the following comparisons were performed with the magnets aligned with the north pole and parallel to the sensor, producing near perpendicular field lines.

Similarly, the three different-sized magnets were compared to better understand how magnet size can affect the Hall effect sensor's ability to read the changes in magnetic field lines at different displacements.

As shown in Figure 22, and as you would expect, the usable range of a smaller, weaker magnet was again much reduced compared to the larger magnet at 0 – 18mm. However, at 0mm, the Gauss level measured was equivalent to the maximum recorded for the large magnet. However, this may have been generated by limitations in the coded programme, which may have enhanced the large magnet over short displacements (<7mm). It is worth remembering that the range that the magnet is likely to operate within the tibia of a transtibial amputee is between 5 – 50mm, making a similar style but slightly larger magnet acceptable for the application.

The 3mm magnet, with a similar diameter to that of the largest magnet tested, showed results that acted as a compromise between the two others, indicating that the diameter of the magnet

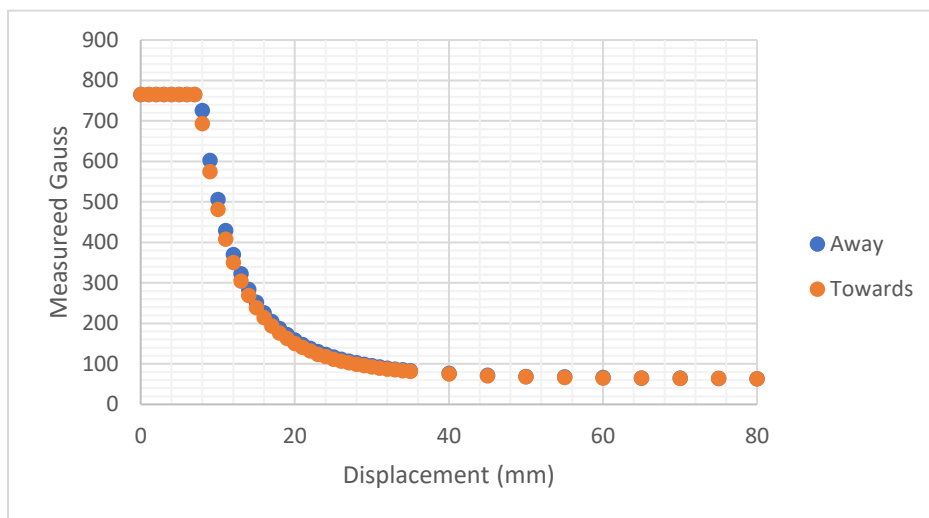


Figure 23: shows the difference in measured gauss depending on the direction of the magnet.

Controlled a large proportion of the strength of the magnetic field at the distances tested. This factor would prove crucial during the initial stages of product testing, during which the implanting of magnets was impossible. This meant that positioning a thin magnet on the skin's surface would be necessary to provide suitable data while minimising discomfort to the device's wearer. The data indicated that changes in measured flux could be identified for a working range between 2-15mm, large, and desirable.

The sensor's hysteresis was assessed by monitoring the Gauss measurement as the magnet moved away and back towards the sensor. An evaluation of each repeat experiment concluded that the maximum error between data points was 3% when comparing movement away. However, errors of this size were rare, with most error ranges being less than 2%. This result was like the forward data series. However, when comparing the average measured value moving away to the average measured value moving towards the sensor at the same displacement, some hysteresis was detected, with differences in values being a maximum of 5.7% different from one another, with the toward movement consistently generating lower values, as shown in Figure 23.

4.2.2.2 Conclusions

Hall effect sensors are used for various applications, popular in robotics and automation due to their high accuracy and lack of variation during repeated testing. They were most recently being integrated into soft robotic skins as a feedback system that would enable silicone-type skins to provide data on touch sensing and grip and slip applications. Similarly, the concept has been thought to be included in prosthetic applications, whereby the rotation of a residual arm could be sensed by the corresponding prosthesis and responded to appropriately. This scenario would require a magnet implanted in the residual bone end to provide a source of the magnetic field that the Hall effect sensor could detect. For this project, a similar idea was to be explored, except instead of upper limbs, it was considered for lower limb prosthetic application where

tibial oscillation could be detected and responded to. However, before this system could be developed, it was essential to determine what circuit, magnet and control system characteristics would be necessary to produce values suitable for the tuning of such a device.

With a circuit and microcontroller designed and programmed to measure the strength of a magnetic field, it was possible to compare magnet orientation and size to build a spectrum of ranges of displacement that could be detected effectively. The comparison proved that a neodymium magnet of 12.5mm diameter and 3mm thickness is adequate, producing a significant range of approximately 32mm between 8 – 40mm. This situation also proved to have very little error between forward and backward movement, indicating the potential of the Hall effect sensors for application. However, further work involving tissue simulant or biological tissue should be carried out to ensure effectiveness through such a medium, along with research into the shielding of the sensor from sources outside of the magnetic field, as it was found that specific materials could influence the output if kept within too close a proximity to the sensor's face.

Similarly, a thin magnet with a nearly equal diameter would likely prove useful if a skin-mounted magnet was ever required, as it was found to produce desirable output characteristics at an operating range similar to that of the distance between an outer socket wall and the surface of the skin of an amputee, Such a magnet was also thought to be thin enough that no significant discomfort or fit problems would occur if fixed on the skin's surface or embedded inside a socket liner.

4.2.3 Socket Manufacture

The initial trial was devised with a healthy participant to reduce the risk to the lower limb prosthetic user community. Thus, a modified socket was devised for use with a non-disabled

participant. A stilt-like orthotic was designed to simulate the residual limb socket complex, using an open-ended socket that the participant would wear, as shown in Figure 24.

The orthotic allowed moments of the shank to be generated like those expected from a below-knee prosthesis, as the stilt would contact the floor ahead of the participant's foot, with the lever arm rotating the socket around the shank.

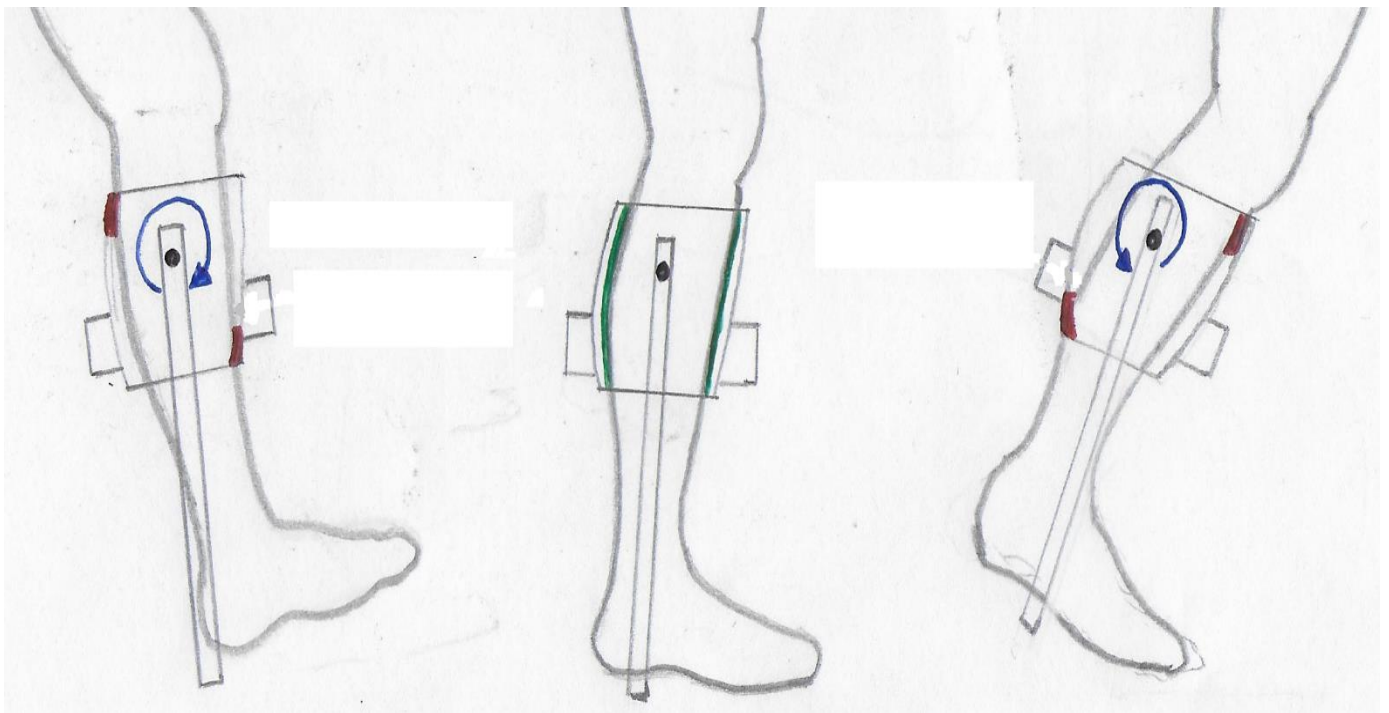


Figure 24: A diagram of the stilt like orthotic designed for able-bodied experimentation, complete with how the design would allow similar moments about the participants shank during gait

Using the skills and experience available at the University of Strathclyde's Departments of Biomedical Engineering and Prosthetics, a custom open-ended below-knee socket was cast on a volunteer participant, complete with a customised socket liner.

Figure 26 shows the initial socket cast taken before it was machined into the final shape. This was used to complete the final stilt orthotic used in subsequent trials. Similarly, Figure 25 shows the custom liner produced to maximise the orthotics' comfort and fit while enhancing the environment around the device.



Figure 26: Completed socket pre-machining



Figure 25: A custom socket liner for use with the open-ended socket to increase comfort and fit of the overall orthotic

The final socket was trimmed to allow it to fit around the shank of the participant, with holes cut to accommodate the additional actuator components while maintaining the volume and overall socket complex environment as best as possible, as shown in Figure 27.



Figure 27: Final, machined, open ended socket used to develop the initial prototype orthotic device for trials

4.2.4 Structural Components

The structural architecture was manufactured using CAD and CAM techniques. These techniques were employed to produce integrated CAD models using PTC Creo for spatial representation before producing final components from ABS-tuff material using SLA.

Furthermore, with the rotary electrical servo, it would be necessary to build suitable housing components with a cam piston system to transfer the torque from the actuator into linear actuation.

Final component list for 3D printing:

- 2 x cams capable of providing 25mm extension from the piston
- 2 x piston, easily attachable and replaceable to the cam
- 2 x piston cylinders

- 2 x actuator housing and fixing points

4.2.4.1 Computer-Aided Design

The following sections show the critical components designed using the CAD package PTC Creo, giving brief details on specific design features and their purpose for the functionality of the combined system.

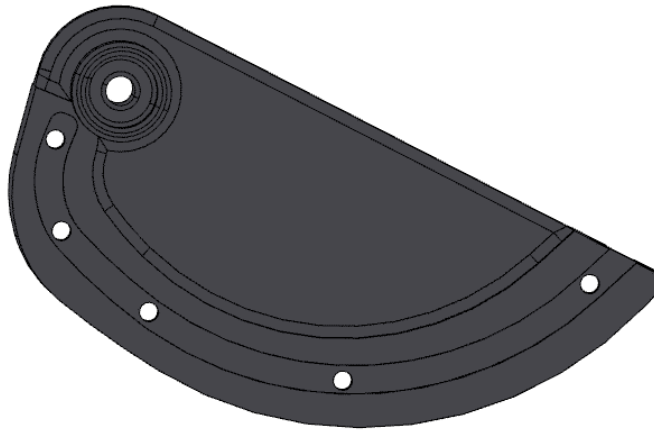


Figure 28: A cam designed to apply 25mm extension at full rotation.

Figure 28 shows the cam designed to achieve the initial requirements of a 25mm extension to the piston system, converting torque into linear actuation. The cams were designed to fit directly to the Futaba servos for ease of use, as shown in Figure 29, allowing the piston to be pushed and retracted via a rolling bearing fitted between the two components.

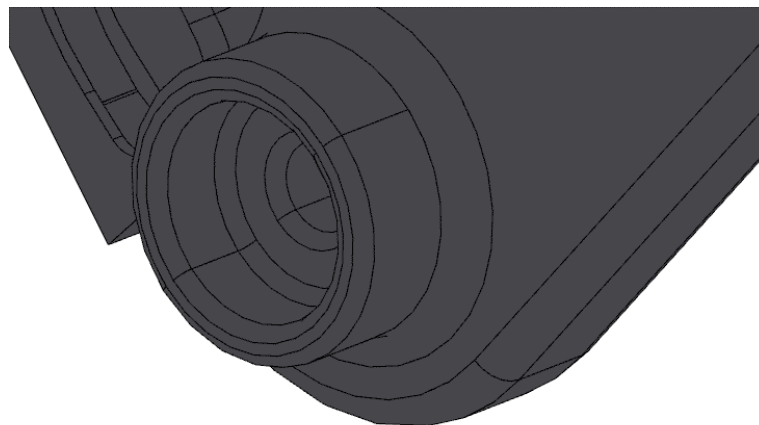


Figure 29: In-built collar to allow simple attachment to servo rotor.

A simple but effective manner of reducing the frictional losses caused by a plastic-on-plastic interaction between the cam and the piston was required. It was decided to use two small bearings per cam to help improve the device's efficiency, cutting down on jamming and reducing frictional losses. Figure 31 shows the simple housing designed in each cam to allow the bearings to run freely along the length of it without disengaging from the device.

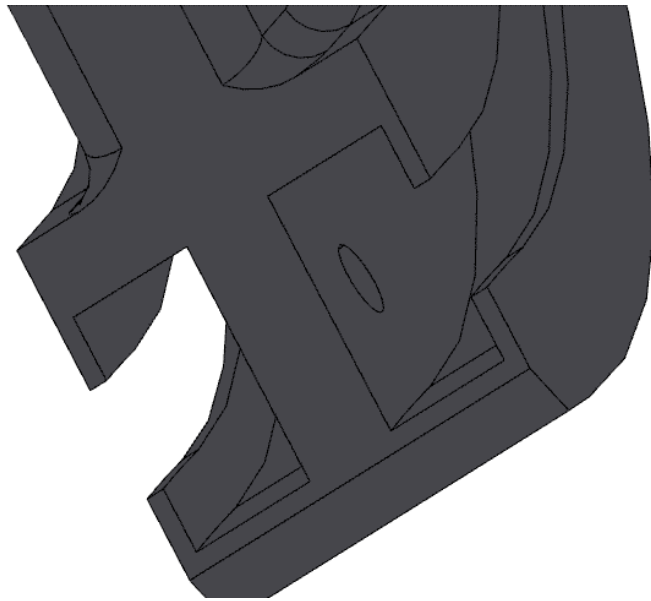


Figure 31: In-built bearing housing to allow low friction conversion of torque to linear motion.

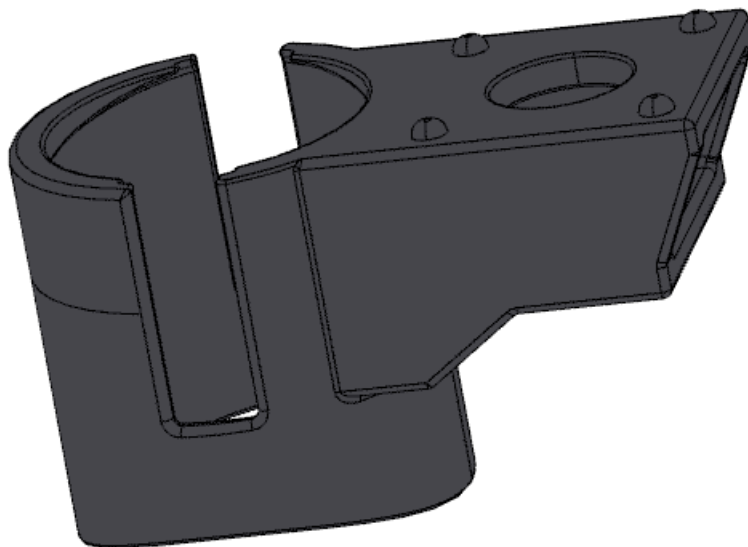


Figure 30: piston housing and servo housing mount

Figure 32 shows the custom piston used to apply loading directly to the participant's shank, incorporating tall fins to allow the full transition of the cam to a maximum extension without contact occurring to the piston surface. Similarly, the decision was made to curve the surface of the piston to allow a more comfortable application of load to the generally curved surface of the participant's shank.

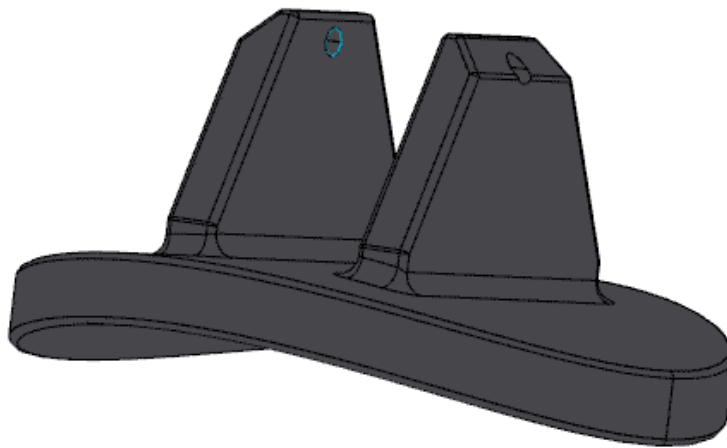


Figure 32: Piston complete with pin holes for bearing connectors to be fitted

Figure 30 shows that the main structural component devised for the system was the piston housing and the support mount for the servo housing. The piston housing contained a large slot (to the left) to allow the cam to travel across its full length. In contrast, the piston travelled across the length of the housing.

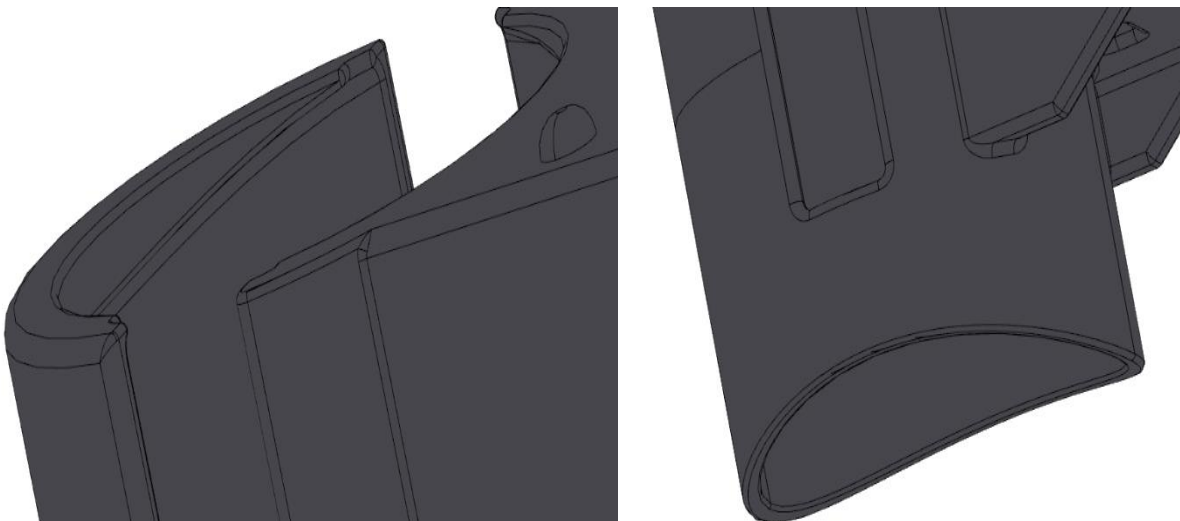


Figure 33: The piston housing was shaped to fit comfortably with the participant's shank, the socket, and the shape of the piston.

The housing shown in Figure 33 was designed to marry with the piston and the roundness of the shank and to cut down the risk of the piston jamming, while keeping a comfortable fit on the patient's shank.

To be able to mount the servo and servo housing in a manner that alignment would be consistent while allowing for detachability, the design incorporated four locator spigots that corresponded with four indentations on the housing itself, as shown in Figure 34, utilising the accuracy of CAD to ensure the spigots and indents matched together accurately under the tolerance of the stereolithography. Furthermore, a failsafe was incorporated for the detachment of the actuators, with the piston housing containing space for an electromagnet, with the intention being that the electromagnets would connect to a panel mounted in the servo housing that would separate if the participant pushed a quick release. They were designed as a safety feature if the loading became uncomfortable for the participant.

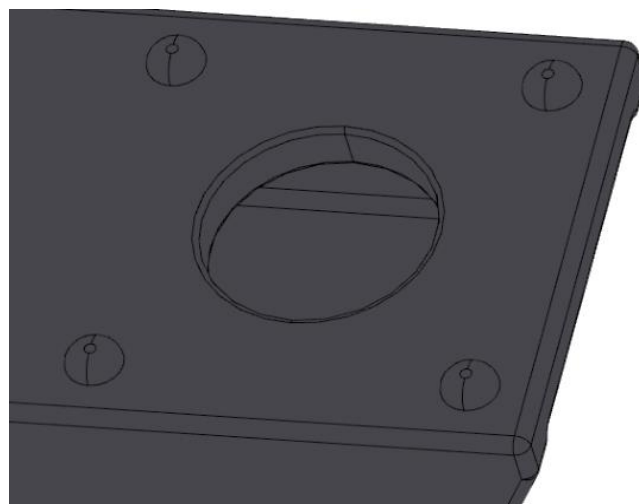


Figure 34: The piston housing was combined with the structure to carry the servo housing.

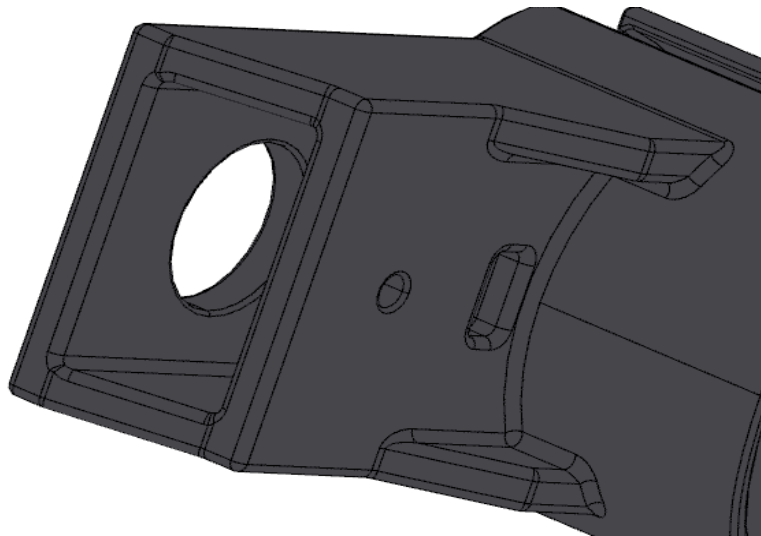


Figure 36: Underside of the servo housing mount, showing in more detail the space for the electromagnet attachment.

Showing the flipside of Figure 34, Figure 36 shows the structure designed to support the servo and servo housing while providing a fixture for the electromagnet to be bolted onto and a simple outlet for wires to pass, helping to reduce the presence of loose wires.

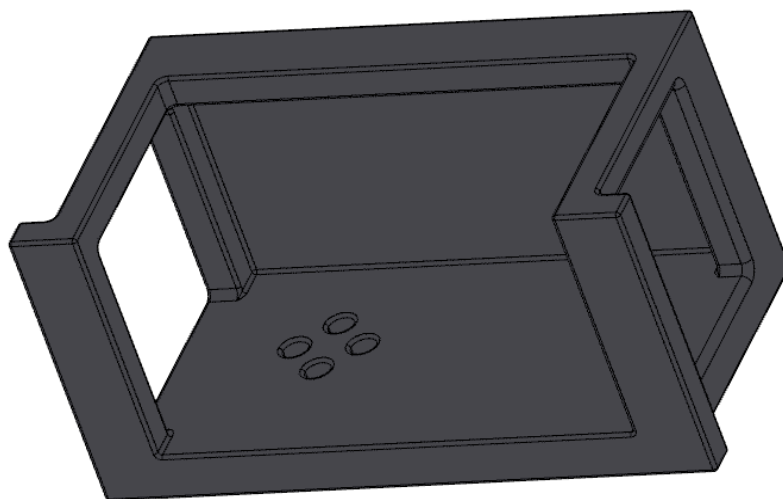


Figure 35: Detachable housing for the Futaba Servos

Custom designed to fit the Futaba servos, the servo housing was a simple structure to allow accurate alignment of the servos to the centre of the cam and the piston over the piston housing, with the additional lips, shown at the front of Figure 35, designed to allow for a suitable surface area for holes to be drilled. These would allow the servos to be bolted neatly to the housing when the best alignment was established. Also visible are four bolt holes for a metal plate to be attached to the electromagnet housed inside the piston housing component.

The underneath of the servo housing contains the corresponding indentations for the spigots present on the piston housing, making it possible to ensure consistent positioning of the piston

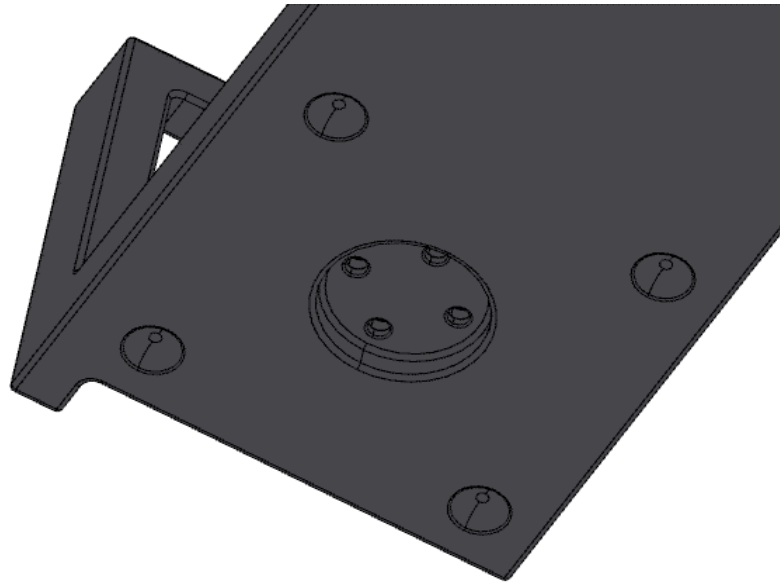


Figure 38: The underneath of the servo housing

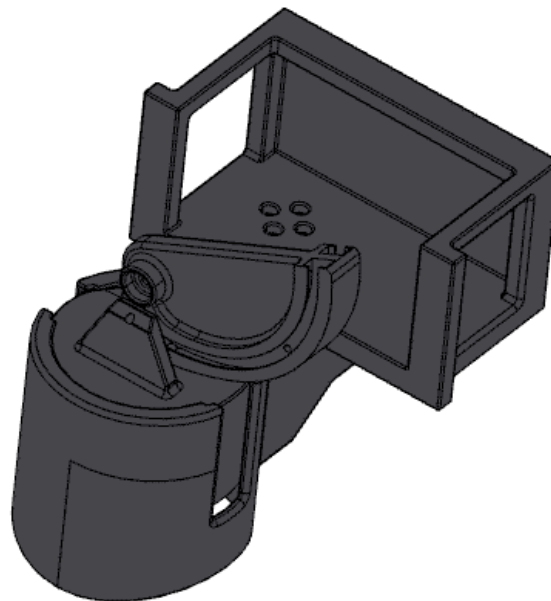


Figure 37: Assembly of the 3D printed components.

if the two structures were separated at any point and reducing the time spent re-centring the various components during testing processes. Shown in the centre of Figure 38 is a recess for a small metal plate to be inserted, with the plate providing the connection between the servo housing and the piston housing via a purchased electromagnet bolted in place. Utilising the

assembly function available to PTC Creo, combining the designed components as in Figure 37 and Figure 39 was a simple task and visualising better how the components would orientate in a three-dimensional space. Furthermore, the process made the troubleshooting a much simpler process, highlighting oversights in the design very quickly before the manufacture of the final piece was carried out. This process was further enhanced by the inclusion of models of bought components, such as the Futaba servo, which made the understanding of component alignment a much simpler task, with it possible to orientate components through their entire expected journey to identify if any obstructions would occur early in the design process, saving on time and expense from the modification or the scrapping of poorly designed pieces later on.

A basic CAD model was produced to establish the concept device's appearance, including a simplified below-knee prosthesis (**Error! Reference source not found.**). The process allowed the design to be evaluated, clearly establishing the possible device as too large and too

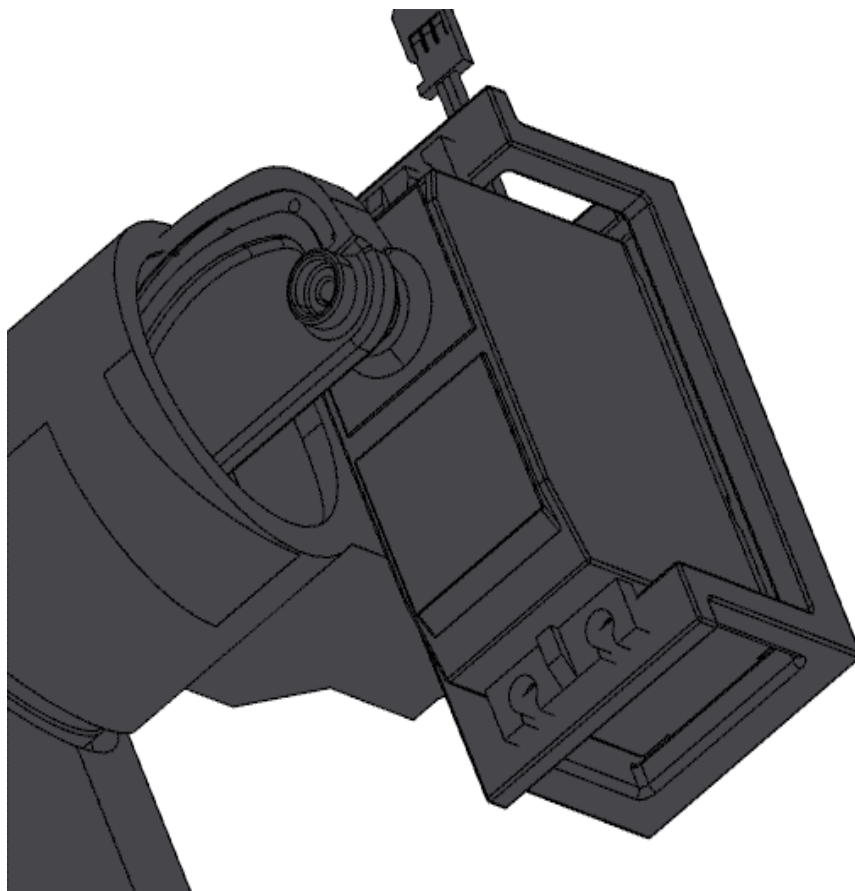


Figure 39: 3D-printed components assembled in conjunction with a Futaba servo.

aesthetically displeasing to be marketable. However, it identified the system as proof of a concept that could be developed, with new ideas and technologies likely to help streamline and reduce the device's size for more acceptable use.

4.2.4.2 Manufacture

Following the identification of components and design features, demonstrated in previous sections and chapters, it was possible to begin manufacturing and combine the various parts for pre-testing and checks.



Figure 41: Open-ended system components.

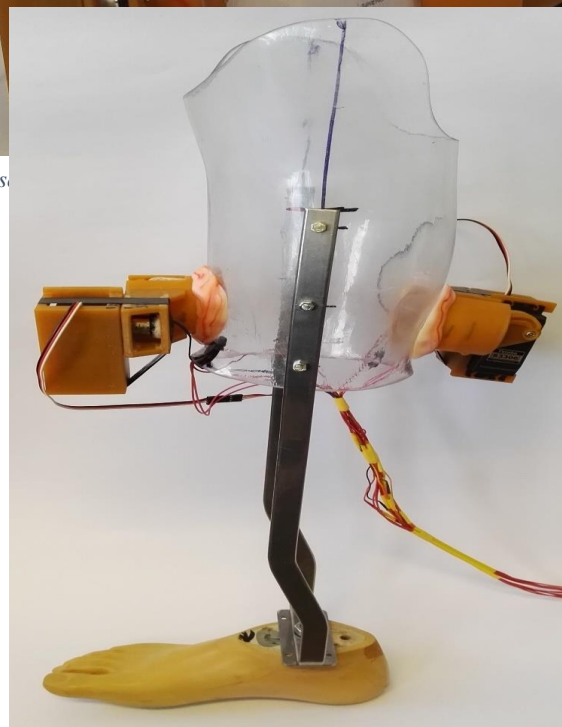


Figure 40: Completed orthotic device for initial able-bodied trials.

Shown in Figure 42, the various 3D printed components were combined and assembled into actuator systems, complete with a Futaba servo, with an identical unit placed at the anterior and posterior sides of the open-ended socket to control oscillations of the tibia. Alternatively, in this non-disabled participant, reduce the rotation of the orthotic in both directions. With the units fitting relatively well in the pre-drilled holes of the socket, it was sufficient to glue the servo housing to the socket with epoxy-based resin. This provided a suitably rigid and robust bond to hold the actuators in place.

With the servo units established in a manner deemed acceptable, it was necessary to complete the main structural components of the orthotic device. Namely, the fixing struts running down each side and the prosthetic foot used to complete the base. As shown in Figure 41, the struts were designed to be long enough to allow the participant's shank and foot to hang, suspended, above the prosthetic foot below. This helped accentuate the displacements created between the shank and socket wall during gait, thus simulating the tibial oscillation seen in other literature studies. The increase in displacements ensured the oscillation would be in line with what was expected if the sensor needed to be positioned on the socket wall and a magnet located on the participant's shank because of the apparent difficulties of implanting it. The author thought that if displacements of an equivalent magnitude could be generated, the system could be tested in, as near as possible, identical conditions to those present in a below-knee prosthetic.

The sensor and actuators were connected to the Arduino microcontroller and power supply systems in a backpack worn by the participant by a sizeable umbilical cord, designed to reduce the risk of entanglement. This also allowed easy access to the circuitry, if required. The circuitry was thought to be stored within the prosthetic to make a standalone and independent contained system.

The final manufacturing and component combining stage involved aligning the connecting bars fitted between the socket and the prosthetic foot. The process required an assessment of the participant's shank within the confines of the bars. The foot's position over the prosthetic foot was critical in providing a balanced system. In contrast, the medial-lateral position was critical in reducing obstruction of the shank from the bars, as shown in Figure 43.

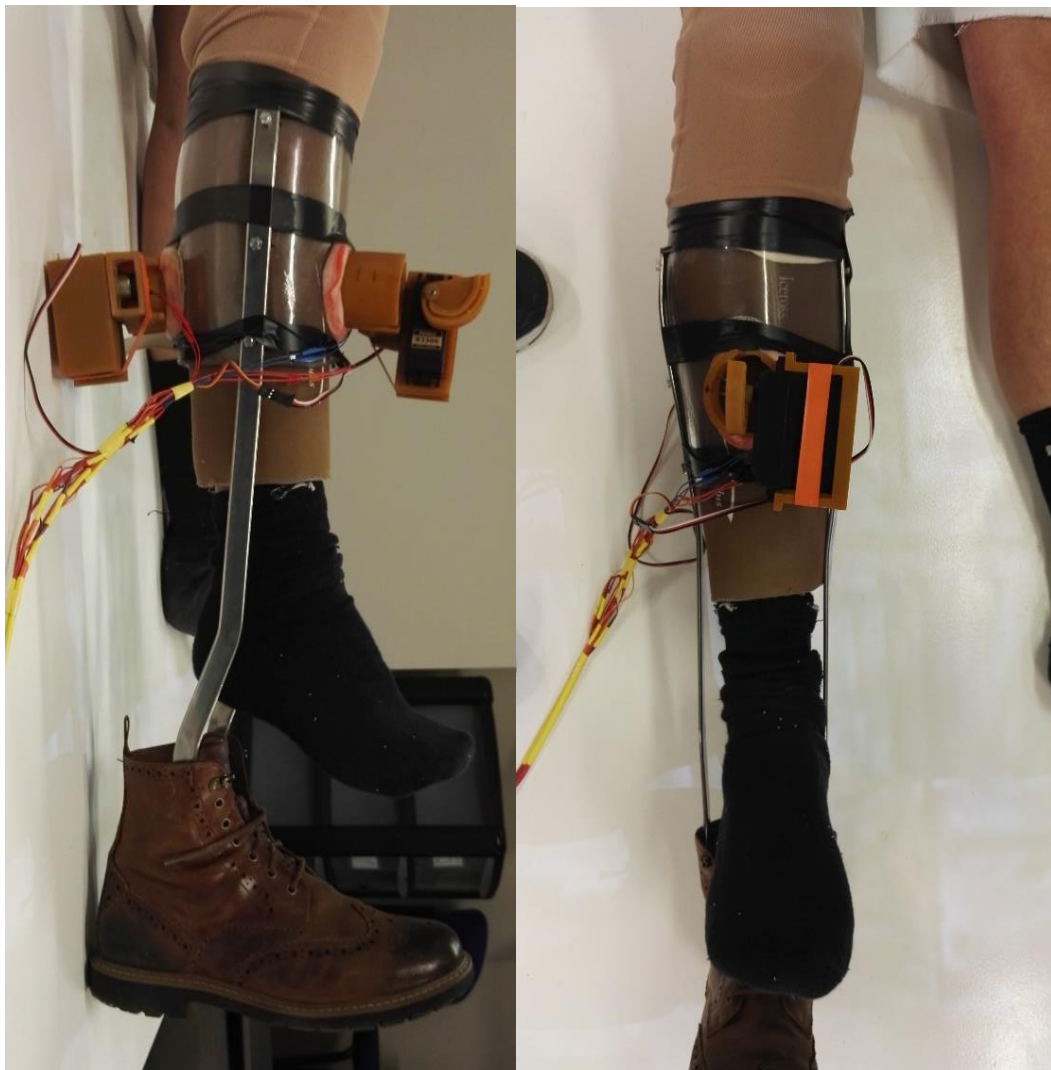


Figure 42: Alignment of the connecting bar was important in reducing obstruction of the shank.

4.2.5 Circuitry

The control of the two Futaba servos required a simple circuit in conjunction with an Arduino Uno microcontroller, where the servo library carries out the necessary work, predominantly within the Arduino's programming. The circuit can be enhanced to reduce phenomena affecting systems involving servos, such as noise and bounce, by using simple diodes to prevent cross-talk from the Arduino signals.

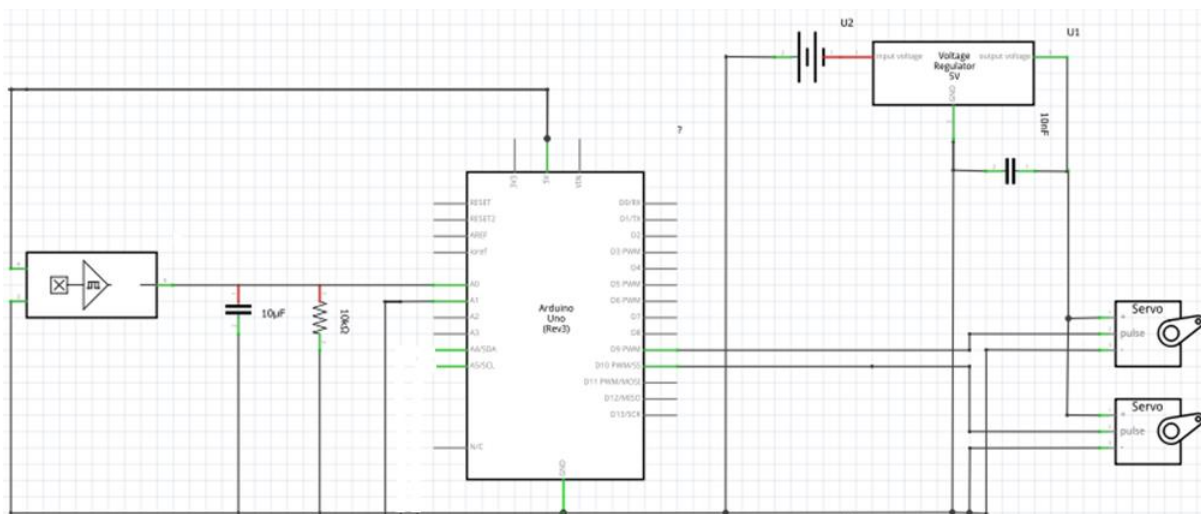


Figure 43: Circuit design, showing connections between the Hall effect sensing circuit, Arduino Uno and Futaba servos.

Figure 43 (full-page image available in Appendix 1) shows the basic schematic for the sensor and servo control circuit with the following components:

- 2 x Futaba S3306 servos
- 1 x Arduino Uno
- 1 x Hall effect sensor
- 1 x 9V to 5v Voltage regulator
- 1 x 9V battery
- 1 x 10µF capacitor
- 1 x 10nF capacitor
- 1 x 10KΩ resistor
- Various connecting wires

4.2.5.1 Required Servo Angle against Measured Magnetic Field Density

To drive the pistons to the correct angle and provide suitable antagonistic loading, two cams were designed, one large to provide more significant displacement and one small to provide greater loading if either was lacking during the initial trials. In doing so, it was possible to calculate the required servo output angle that corresponded with each cam's desired output displacement. A factor that was accounted for in separate Arduino codes:

- Large cam generating a stroke length of 45mm between 59.5 – 14.5mm of the cam centre, with a designed 30mm posterior and 15mm anterior movement, producing loading between 21 – 83N at varying stages of the cam rotation.
- Small cam generating a stroke length of 30mm between 44.5 – 14.5mm of the cam centre, with a designed 15mm posterior and 15mm anterior movement, producing loading between 28 – 83N across the cam's full rotation.

4.2.6 Coding and Control Systems

Control systems are an essential part of any transducer-based system, providing the vital link between the sensor and actuator that determines the final output performance of the system, with the desired result being made possible through the implementation of coding installed in the microcontroller. The microcontroller used was an Arduino Uno, providing a suitable balance in size, processing power and, with the presence of a large community HUB, an easily accessible technical support group. The microcontroller requires the necessary control system to be implemented to make it possible to track distal tibial movement in a lower limb amputee actively and (or socket oscillation away from the residual limbs mid-stance position) and cause an appropriate response from the systems effectors. With this in mind, it was decided to briefly look into the standard styles of control systems and evaluate them on their differences and their

subsequent advantages and disadvantages before providing reasons for selecting the type used and how it was implemented.

4.2.7 Control Systems

Although a wide variety of possible control systems could have been used, it was decided to use a relatively simple version for initial testing to provide a more straightforward troubleshooting process while acting as a learning curve for developing more complex systems in future iterations. Therefore, a simple proportional-style controller was chosen instead of producing a more complex proportional-integral-derivative (PID) controller. Although deficient in eradicating steady-state errors and inadequate responses, the risks could be mitigated carefully if overly broad gain values are used.

With the information gathered from previous Hall effect studies, the profile of measured Gauss was collected for all the magnets used in subsequent experiments. This, therefore, made it possible to map a suitable response that was required from the servos themselves, with the essence of the mapping function being based on a proportional controller and the desired output is a multiplication function of the input value. However, issues arose with the continuous nature of the balanced formula, as non-integer values could not be converted to discrete values to drive the servos to the correct rotation angle. Because of this, a slight modification to the coding would allow a step-based response from the servos where a discrete angle value would be driven for a range of Gauss measurements.

Programming the controller this way helped reduce the system's sensitivity, meaning the response was less likely to have an adverse change in gain that would cause large, dangerous, or incorrect responses from the servos. Similarly, with the stepping nature of the system, the proportional gain controller steady-state error could be accounted for, with its impact having less effect on some, but not all, the input values and calculations. Although the response is not

as continuous and elegant as would be possible with other control systems, the simple nature of the code made it possible to edit the results quickly, depending on whether variables (such as magnet size) were changed in the initial trialling and set-ups. Similarly, necessary testing, before final able-bodied experimentation, found that the system's response was suitable for what was initially desired, with both servo one and servo 2 (set to act equally but opposite to the position of servo 1) responding accurately and quickly enough, without much in the way of an unstable or excessively large amplification.

4.3 Conclusion

The detailed design process was essential in converting the initial concept ideas and design features into a functional first-iteration proof of concept. Building on the decisions made in the previous design chapters, the detailed design phase developed the corresponding hardware and software to test the initial hypothesis. While several key structural components required designing to facilitate their combination with the predetermined components, being able to develop the bespoke components in a CAD modelling software made it a simple task to facilitate the production without wasting time and expense on poorly designed components, allowing us to troubleshoot component fit in three dimensions without the need to make scale models.

As per the device's demands and wishes, the device successfully achieved/focused on the following:

- A stabilisation system was capable of 25mm extension in the form of a cam system coupled with gel inserts.
- Tibial displacement was the sole target mechanism; however, socket oscillation about the shank was the primary variable for the proof-of-concept trial.

- External monitoring of the tibial position will be necessary for a reactive proportional feedback response, achieved by developing a simple Hall effect sensor effector system.
- The sampling rate of bone displacement was desired to be at 150Hz, and the final device (for the Hall effect measurement) sampled at 500Hz, but the value was calculated as an average of 10 samples. Meaning an average value was taken at a frequency of 50Hz.
- Stabilisation actuators delivered approximately 1.2Nm, equating to approximately 0.015Nm/Kg. A number significantly down on the peak loads of 0.3Nm/Kg at the anterior surface of the shank and 0.85Nm/Kg at the posterior seen by Kobayashi et al. This was highlighted as a severe limitation of the device; however, it was desirable to understand how even low-level loading could influence the stabilisation regardless of the first iteration.
- Accurate displacement sensing to a range of at least 25mm was successfully achieved with a Hall effect sensor.
- The device was manufactured on-site (University of Strathclyde), with parts bought off the shelf as appropriate.
- Proportional control of the stabilisation system was programmed into the device as initially desired in the device's wishes.

Similarly, the detailed design stage made it possible to understand better the software requirements needed to understand incoming data and to affect a response. However, following the assessment of microcontrollers in previous sections and the selection of the Arduino, it was a simple task to begin learning and understanding how to write the necessary code by building on the knowledge available as part of the Arduino community hub, and its freely available database of resource data. With the most significant component, the open-ended socket, being a relatively simple component to produce, we could use the available expertise in the various

University of Strathclyde departments to efficiently produce and adjust the final orthotic to allow for trials to begin later.

Chapter 5: Experimentation with Participants

5.1 Introduction

Experimentation to recreate conditions that would, as closely as possible, match the conditions and mechanisms of motion present in the prosthetic socket complex of a below-knee amputee, a bespoke socket was required for use with a non-disabled participant. Having been conceptualised, designed, and manufactured following a heuristic method encompassing certain opportunistic concept choices, an initial working prototype incorporating Hall effect sensing and rotary actuation was manufactured to identify whether socket oscillation could be reduced during walking activities. This aimed to identify whether tibial oscillation during the gait of a below-knee amputee could be sensed and reacted to in a manner that stabilised the residuum complex, reducing undesirable tissue deformation. With unproven technology and a high-risk community, it was necessary to establish whether the idea was comfortable. Therefore, trials involving a non-disabled participant were devised, allowing the system to be validated for stabilising performance before the project progressed.

The following section gives a brief description of the system (given in greater detail in Chapter 4) and the general format and process of participant recruitment before presenting the results gathered from the Motek CAREN system, as well as the Hall effect sensor feedback, followed by a discussion of what the results indicated.

5.2 Methodology

5.2.1. Experimental Procedure

For a study with participants N=1.

The author applied and obtained ethical approval for the pilot study. With approval granted by the University Ethics Committee for “*Approval: UEC18/29: Buis/Giardini/Childs: Design and Development of a Prosthetic Socket Stabilisation Device: A Pilot Study on a participant*”.

The protocol involved two visits from the participant (organised at the participant's convenience).

The first visit involved:

- Five minutes to review the consent form and for participant questions.
- 10 minutes to review the investigation and its purpose, allowing for additional questions.
- Five minutes to explain what the visit will comprise.
- 30 minutes to cast an open-ended socket on the lower leg of the volunteer and take body-specific measurements to ensure the comfortable fit of the prototype for the following visit.
- 10 minutes explaining what will happen between visit one and visit two.

Second visit:

- Five minutes reviewing the procedure for a visit.
- 10 minutes for the attachment of the socket and device to the volunteer
- 10 minutes acclimation period of the device
- Five minutes to secure the participant into the CAREN device.
- Five minutes' data collection phase at 0° gradient with the device switched off.

- Five minutes' data collection phase at 0° gradient with the device switched on.
- (The process of walking with the device on and off was repeated three times in total)
- 10 minutes' rest for the participant was allowed between each trial.
- Between the first and second visits, the final open-ended lower limb socket was produced from the cast taken on the participant during the first visit, providing the main framework for all the attached components.
- Before the second visit, the completed prototype was tested under conditions as close as possible to the actual trial to ensure problems were mitigated before the second trial had commenced.
- Upon completion, the participant was asked to fill out a questionnaire to provide useful information on the device's performance and to help understand what may need to be changed for follow-up trials.
- Other results regarding the device's performance, generated by the microcontroller, were assessed in the follow-ups to the trial.

5.2.2 Data Acquisition and Feedback

Due to the untested nature of the system, it needed to be clarified on the trustworthiness of the Hall effect sensor data. This factor led to combining this data with that collected from the CAREN system to offer a more accurate data collection method. The results were generated twofold, firstly, utilising measured gauss taken from the Hall effect sensor to help validate the findings; the second method utilised the CAREN system to measure vector angle changes between the shank and the orthotic. The data produced by the Hall effect sensor was analysed to identify whether the range of displacement was being altered with the system engaged compared to when the stabilisation device was turned off. Further data was gathered by the CAREN system, whereby the infrared reflective markers made it possible to measure changes

in vector angle between the participant's lower limb and that of the orthotic device throughout the gait cycle. This data was recorded by placing two markers on the fixed metal strap of the device, one at the top (near the knee) and one at the base of the device.

Similarly, markers were placed on the anterior and posterior of the participant's shank. As shown in Figure 45, the angle between vector 1 (red) and vector 2 (blue) was monitored for changes, alongside changes in the angle between vector 1 (red) and vector 3 (blue). This made it possible to identify whether the stabilisation device was effective and confirm whether the Hall effect system was a reliable analysis method.

Data was gathered during walks with the system, both engaged and disengaged. Each block was broken down into individual gait cycles, whereby the limb of interest completed a cycle from heel contact through to toe-off and on through its swing phase.

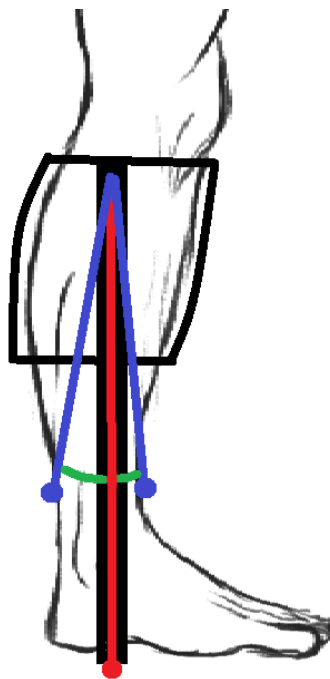


Figure 44: Diagram visualising the vector angles that were compared with the CAREN device.

Measuring the magnetic field at the Hall sensor position on the participant's shank was essential in programming the Arduino code to provide suitable output from the actuators. This way, a

series of initial walks were used to troubleshoot the system, identifying difficulties and failure modes and the intensity of the magnetic field that would be responded to. The first round of data collection was carried out with the actuators positioned in the central position. Direct loading to the limb was provided using a gel pad for comfort. Later iterations addressed modifications to the device and programming to compensate for deficiencies highlighted by the first set of trials.

5.2.2.1 Initial Magnetic Field Measurements (stabilisation disengaged)– Trial Troubleshooting

Two initial runs were carried out to investigate how the measurement system would respond with the magnet positioned close to the actuating surface, in its first position. The two initial walks are shown in Figure 45.

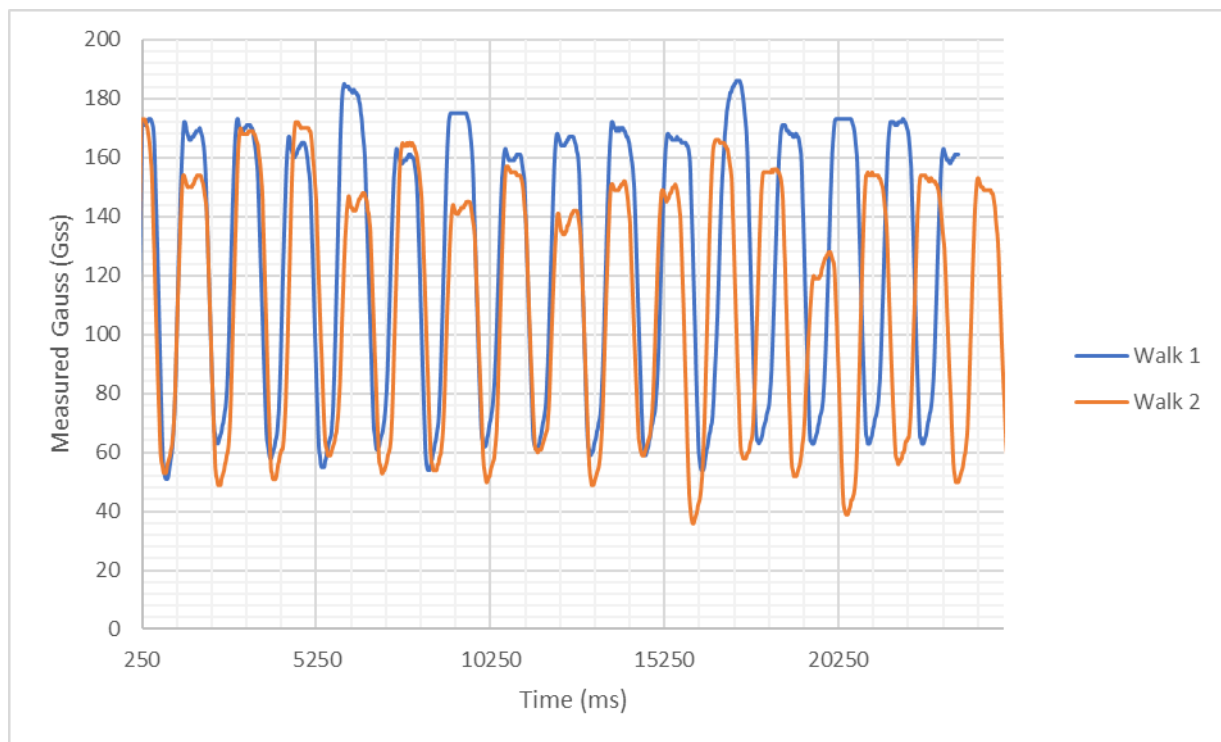


Figure 45: Initial magnetic field measurements taken by two initial walks for system characterisation and troubleshooting.

The test runs helped identify several factors regarding experimental procedures that would need to be mitigated and specific criteria that would need to be maintained:

- A discrepancy in the peak measurements between walks 1 and 2 can be seen, with the peaks slowly decaying towards the final steps of the second walk. This resulted from the magnets slipping out of position over time, reducing the magnetic field measurements. This could be expected because, as the magnet fell away from its original position, it also fell away from the Hall effect sensor. Consequently, the sensor was moved to the bottom edge of the socket, allowing more convenient access to the magnet for on-the-spot adjustments as well as reducing the influence of the magnet slipping on the magnetic field measurement as an increase in the distance between the magnet and sensor meant lower magnetic field measurements were detected.

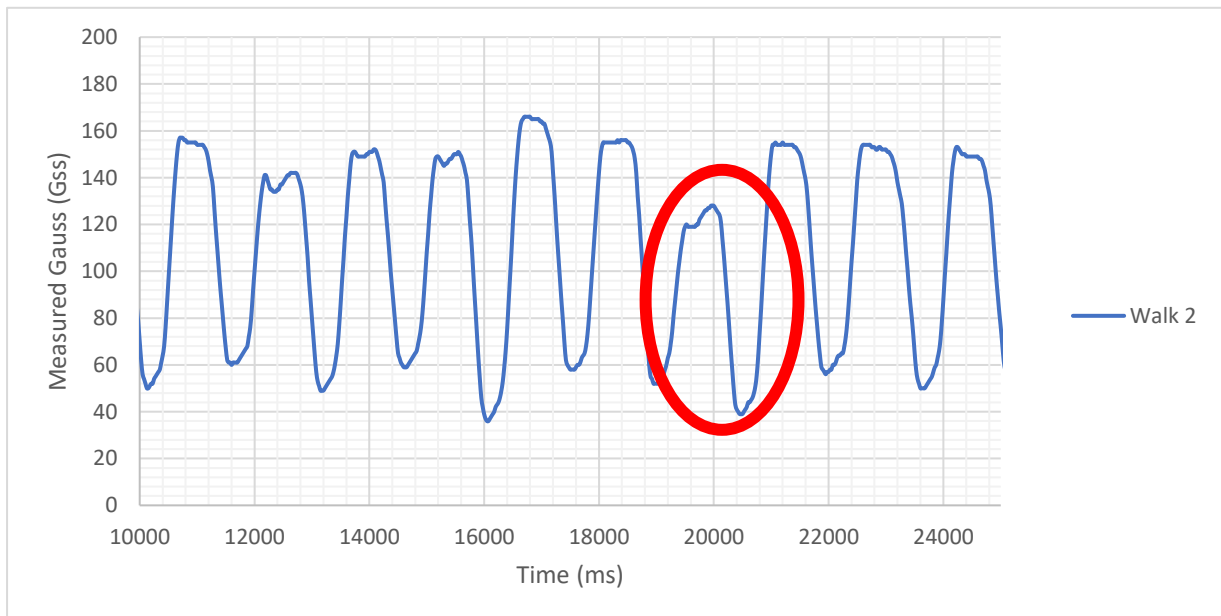


Figure 46: A misstep in the second walk, showing clear differences from the norm.

- The trials also showed the influence of missteps and stumbles in individual step cycles. Although they exhibited a significant difference from the judged normal variation in measurement characteristics, they had minimal influence on the trials other than making it apparent that data should be assessed on a cycle-by-cycle basis, with anomalies removed as appropriate, to prevent skewing.

- The repeatable nature of the measurements demonstrated that the system was detecting the movement of the shank as intended. This, in turn, meant that the system and experimental design could continue into the next phase.
- A final point concerns the feedback of the participant. During a short trial with the system engaged, it was noted that little input could be felt from the actuators themselves. Although this was ideal regarding participant comfort and safety, it also indicated that the servos might have a limited impact in controlling the moments of the shank. Because of this, it was decided to change the starting position of each cam so that when engaged, they would provide a more significant force than initially intended. More force was applied by rotating the cam so that the length of the lever was reduced, therefore applying a more significant load to the actuator earlier in the rotation of the servo.

5.2.2.2 Initial magnetic field Measurements (stabilisation engaged)– Trial Troubleshooting

To finalise the data collection, the servos were engaged to identify what form of response would be measured. The code was manipulated so that, with a smaller change in the magnetic field measured away from the normal mid-stance range, the servos would input a more significant load earlier in the cycle. The collection was carried out over three individual walks lasting approximately 30 seconds. The set-up was altered to allow better access to the Hall effect sensor and magnet as it was decided that for the final servo comparison, it would be more beneficial to assess vector data gathered from the CAREN system as this would provide more accurate data. The test was primarily about understanding the servos' response and feel while providing further troubleshooting runs to allow the development of mitigation methods for future trials.

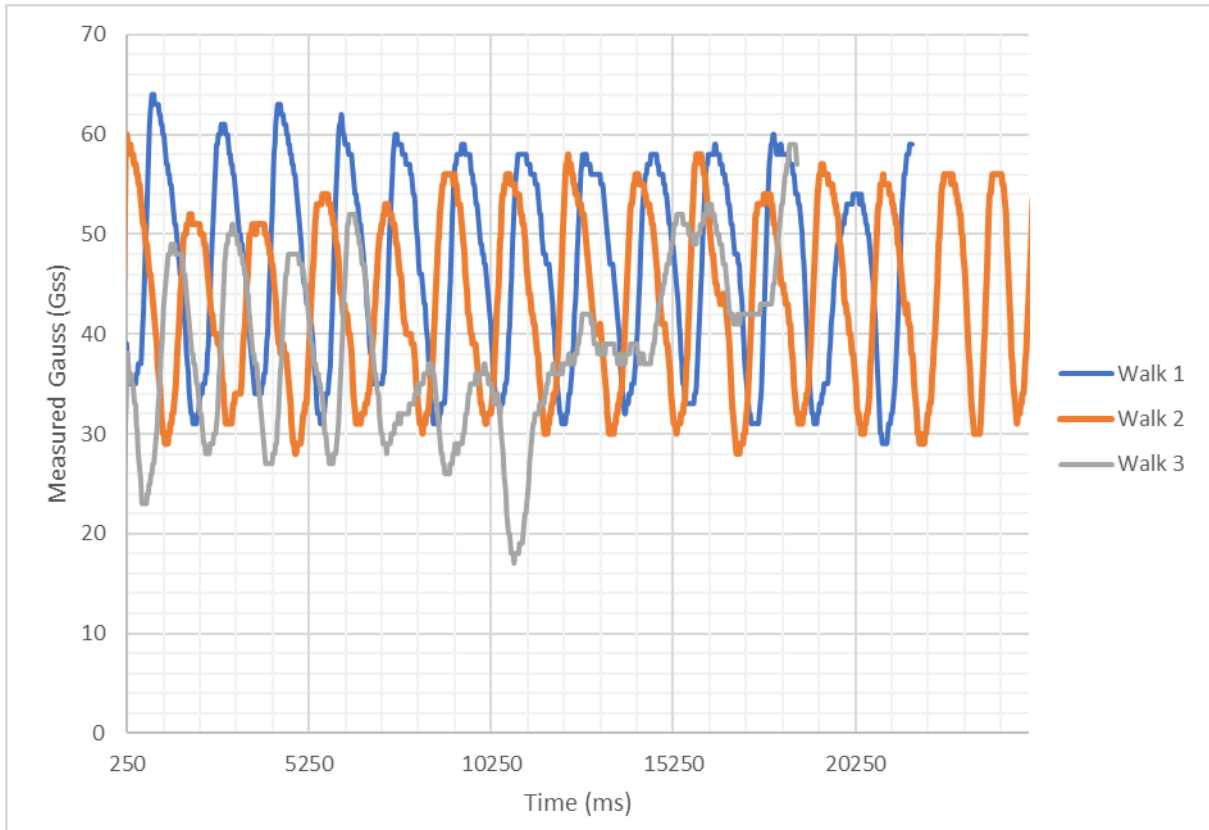


Figure 48: Magnetic field measurements taken during initial trials with the servos engaged.

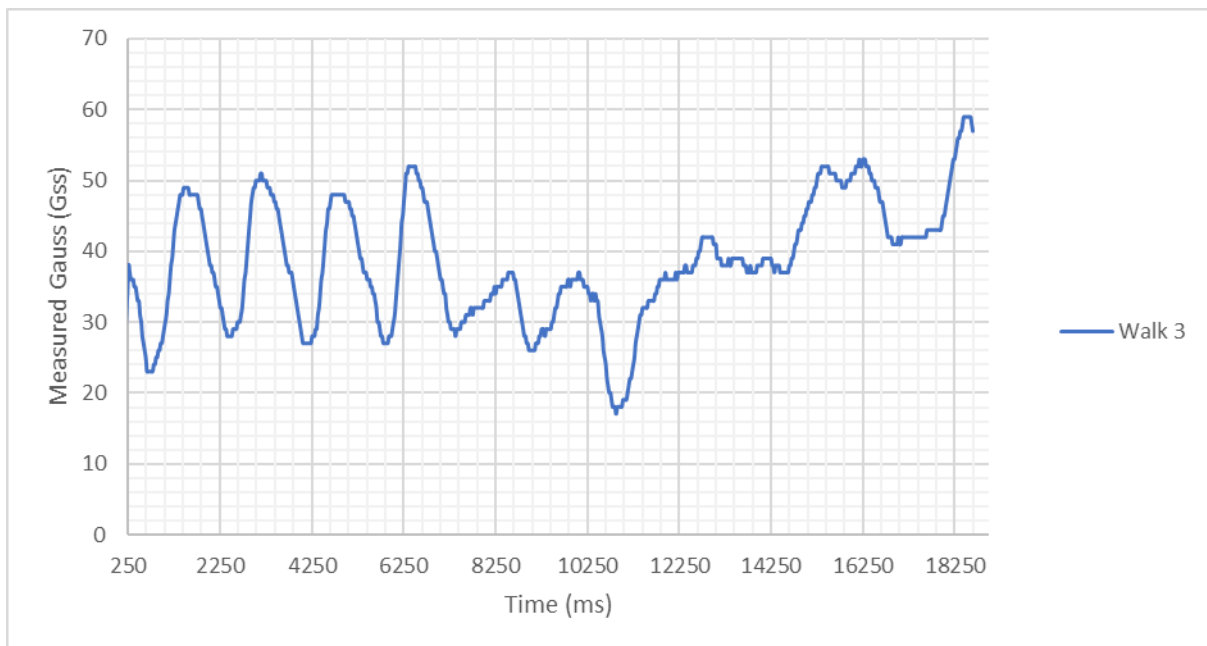


Figure 47: Walk 3 separated to better visualise the Hall effect measurement of a slip and the attempt at recovery made by the participant.

The results were varied, although not unexpected. It was interesting to see the range of values the system would need to operate in, with the first and second walks being similar but with key variations in maximum and minimum values during specific gait cycles. Similarly, considering

the nature of the orthotic, walk 3 (Figure 47) showed the effect stumbles could have, with the participant taking several gait cycles to return to the norm or, as was the case at times, aborting the walk early to minimise the risk to the participant.

Figure 47 shows the point after the fourth gait cycle at which the participant's walking pattern becomes irregular. Although unneeded, the data could be useful in determining which gait sets from future trials should be removed from the data collected by the CAREN system.

5.3 Results

After several walk iterations and the removal of poor step cycles generated by the starting and stopping of the CAREN system, over 60 individual cycles with the device disengaged and over 30 cycles with the device operating as intended were gathered for both the Hall effect and by the CAREN system.

5.3.1 Hall Effect Data Acquisition

5.3.1.1 Magnetic Field Measurements

This was done to increase the influence of the actuator, as proposed following the initial trials, with a series of trials running with the servos turned off and a series taken with the servos engaged. By breaking each trial into a series of individual gait cycles, it was possible to make more numerical comparisons between the data sets.

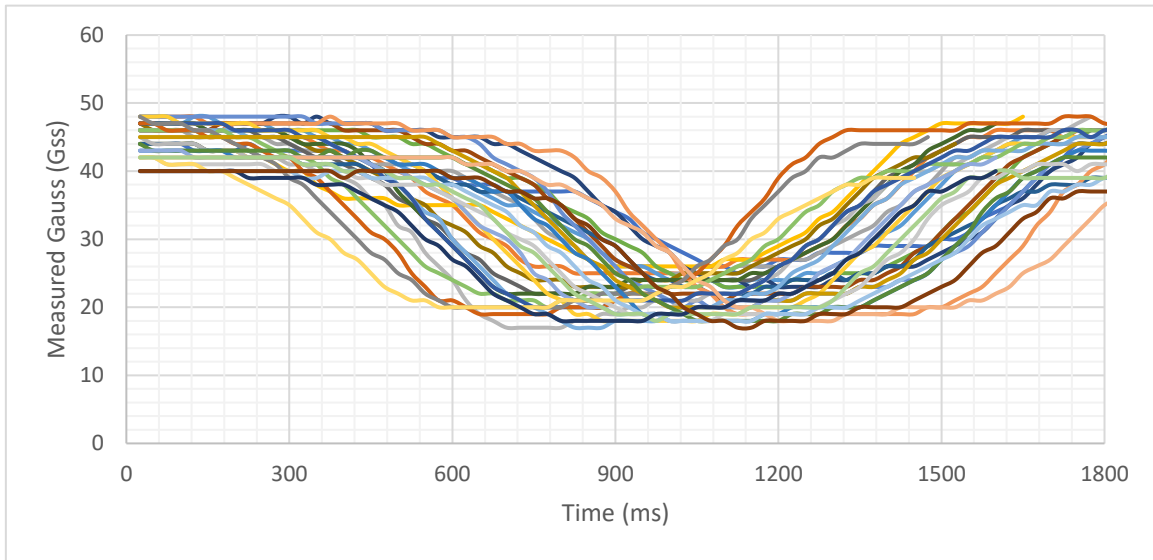


Figure 50: 32 individual gait cycles as measured by the Hall effect sensor.

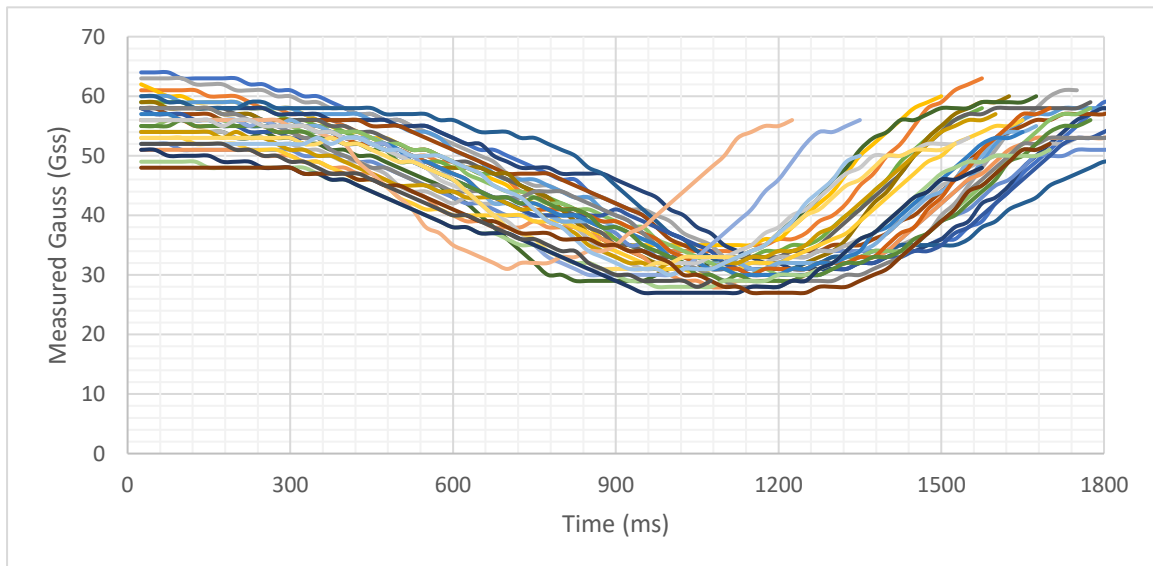


Figure 49: 33 suitable gait cycles as measured by the Hall effect sensor without servo engaged.

Figure 50 indicates the range and shape of the magnetic field measurement during each gait cycle, with the initial peak caused at HS followed by the trough caused as the leg progressed to TO. The socket caused the final upwards trend as it returned through its swing phase, its initial starting position. The process was repeated with the system engaged, providing a similar plot, as shown in Figure 49.

All gait cycle sets were corrected to span one full gait cycle to improve the ease of comparison. Allowing Gauss measurements to be compared at key locations of a gait cycle. Most notably

TO, Midstance, HC, Swing or as a full cycle. A representation of the correction shown in Figure 51.

An additional correction was to adjust the Gauss measurements to a more linear scale; however, due to the average displacement of the magnet during the trials being within a relatively linear proportion of the Gauss: displacement zone, limited change in the returned profiles was seen.

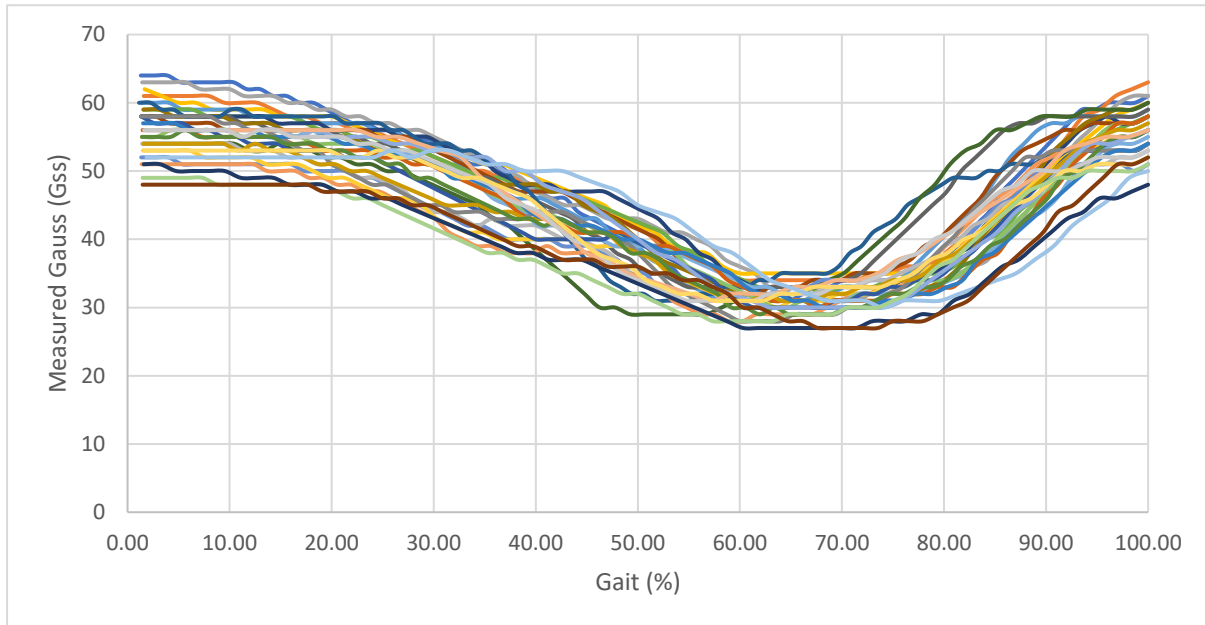


Figure 51: Representation of all off cycles corrected to ensure each walk was measured as a percentage of a full gait cycle.

To accurately average the data generated, each data set of hall effect and CAREN vector angles for each gait cycle were combined using the Vstack function within Excel before being interpolated for every 0.5% of gait. The average data for each set is shown in Figure 54.

The data was also compared and broken down into four phases for greater visual comparison. With data represented as box plots (Figures 53 -57) and a series of descriptive and statistical calculations shown in Tables 5 – 9. Whereby data was analysed for its overall range and variance whilst also comparing whether there was a significant difference between the data sets comparing when the system was engaged versus disengaged.

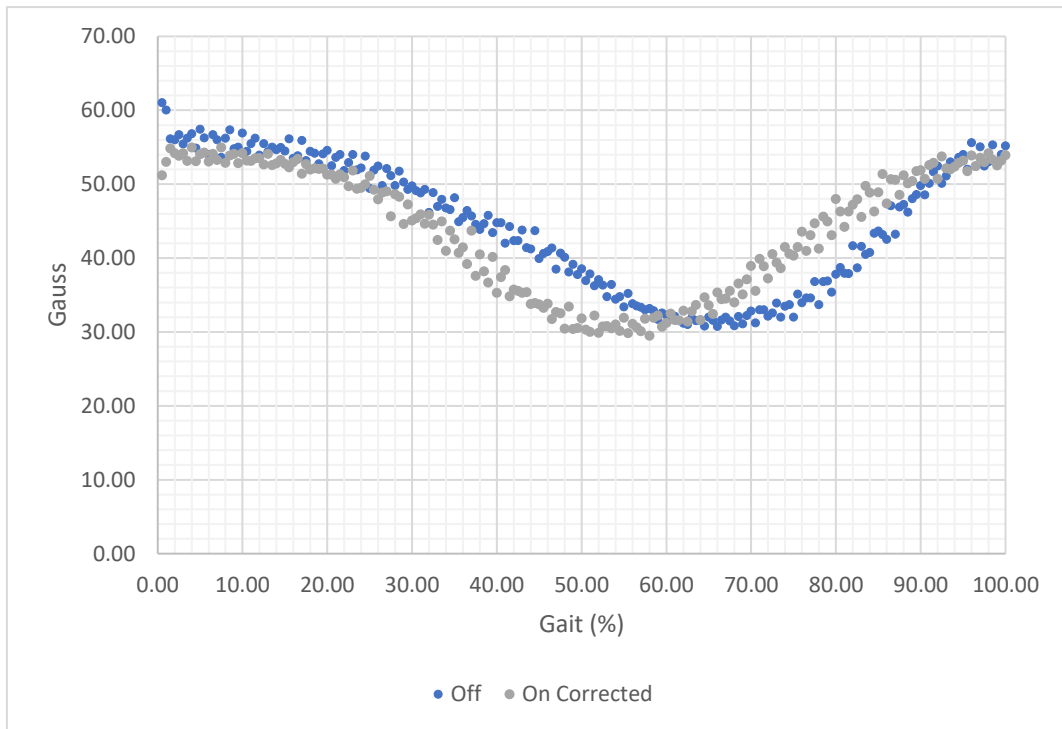


Figure 54: Average gauss measurements with the stabilisation device off versus on



Figure 53: Box plot showing the full spread of the Gauss measurement with the device disengaged versus engaged.

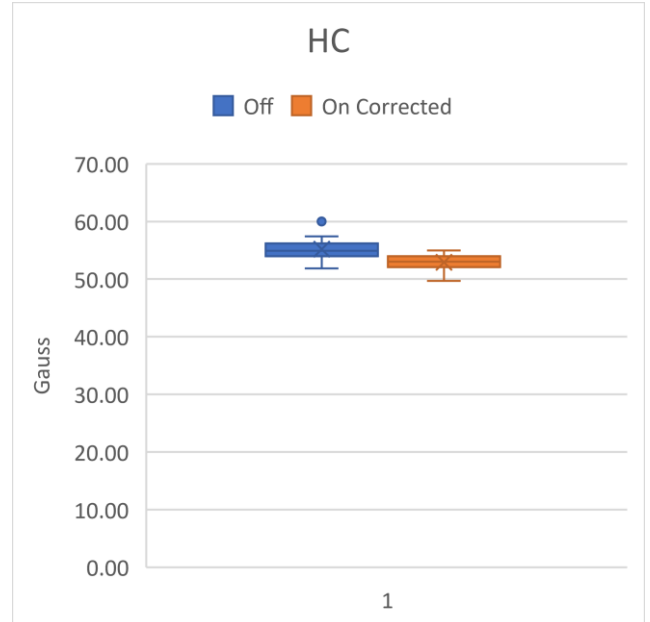


Figure 52: Box plot showing the Gauss measurement at HC with the device disengaged versus engaged.



Figure 57: Box plot showing the Gauss measurement at Midstance with the device disengaged versus engaged.

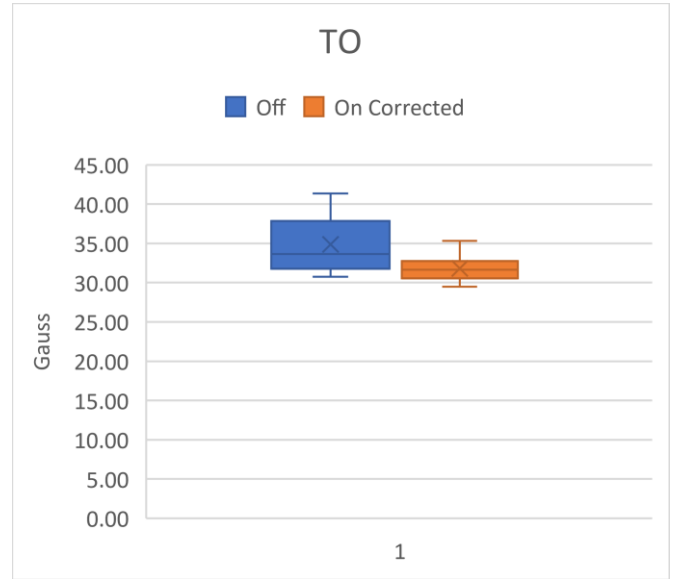


Figure 56: Box plot showing the Gauss measurement at TO with the device disengaged versus engaged.

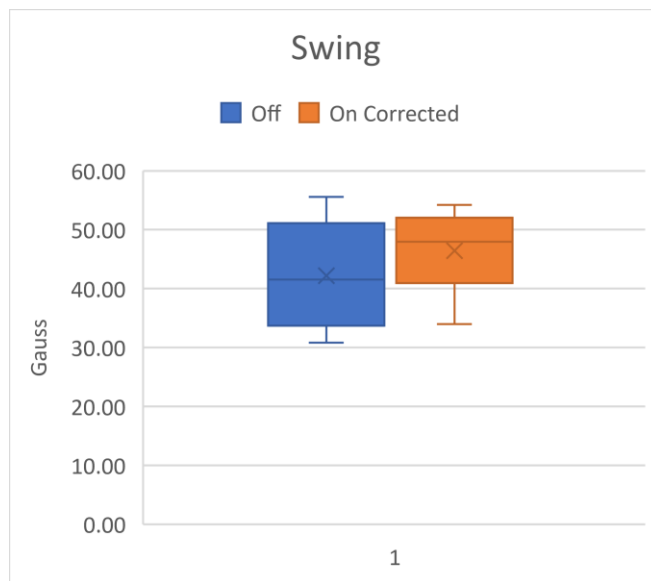


Figure 55: Box plot showing the Gauss measurement during Swing with the device disengaged versus engaged.

Table 5: Significance testing and descriptive stats for All Gauss Data

All		
	<i>Disengaged</i>	<i>Engaged</i>
Mean	44.642	43.857
Variance	79.446	72.658
P(T<=t) two-tail	0.369	
Standard Deviation	8.91	8.52
Range	30.25	25.47
Minimum	30.75	29.50
Maximum	61.00	54.97
IQR	17.01	16.81

Table 6: Significance testing and descriptive stats for Gauss at HC

HC		
	<i>Disengaged</i>	<i>Engaged</i>
Mean	55.191	52.920
Variance	3.142	1.436
P(T<=t) two-tail	0.000	
Standard Deviation	1.77	1.20
Range	9.17	5.28
Minimum	51.83	49.69
Maximum	61.00	54.97
IQR	2.19	1.75

Table 7: Significance testing and descriptive stats for Gauss at Midstance

Midstance		
	<i>Disengaged</i>	<i>Engaged</i>
Mean	47.345	42.744
Variance	12.596	28.726
P(T<=t) two-tail	0.000	
Standard Deviation	3.55	5.36
Range	12.80	18.05
Minimum	41.20	33.78
Maximum	54.00	51.83
IQR	5.19	9.37

Table 8: Significance testing and descriptive stats for Gauss at TO

TO		
	<i>Disengaged</i>	<i>Engaged</i>
Mean	34.866	31.791
Variance	11.112	2.082
P(T<=t) two-tail	0.000	
Standard Deviation	3.33	1.44
Range	10.58	5.84
Minimum	30.75	29.50
Maximum	41.33	35.33
IQR	5.97	2.14

Table 9: Significance testing and descriptive stats for Gauss at Swing

Swing		
	<i>Disengaged</i>	<i>Engaged</i>
Mean	42.201	46.426
Variance	71.502	37.461
P(T<=t) two-tail	0.001	
Standard Deviation	8.46	6.12
Range	24.75	20.22
Minimum	30.83	33.97
Maximum	55.58	54.19
IQR	16.80	10.85

5.3.2 Motek CAREN Vector Comparison

As in previous sections, data from the Motek CAREN system were arranged into individual gait cycles, with the data split between when the servos were engaged or disengaged.

The raw data was provided in the form of the XYZ coordinates of the markers positioned on the participant's shank and, therefore, required a degree of post-processing to return the desired vector angles as required. First, the vectors between the various points of the system had to be calculated. Then the angle between the corresponding vectors could be calculated for each time step in the programme. This made it possible to plot the angle progression over time, building a visual representation of how the angle changed throughout the gait cycle.

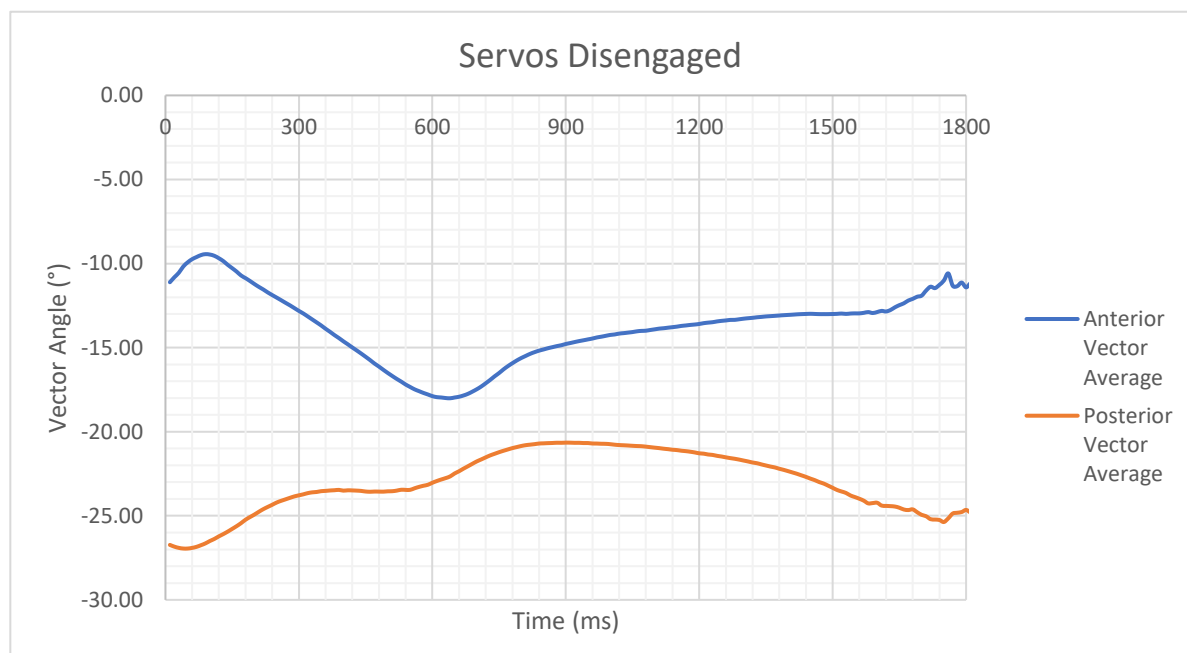


Figure 58: The general pattern of anterior and posterior angle with servos disengaged.

5.3.2.1 Anterior and Posterior Vector Angles – No Servo Engaged

Separating the walks into individual gait cycles, measured by the CAREN system, was a more straightforward process to remove irregular gait events, identifiable by a clear difference in the output vector angles/plot shape.

Sixty-one individual gait cycles were collected for the anterior vector with the system disengaged, alongside 62 complete gait cycles for the posterior angle. These presented a general shape, as seen in Figure 59, showing the expected relationship with the anterior angle peaking initially and the heel contact revealing the anti-clockwise moment of the socket. This pattern was almost inverted for the posterior vector angle, again, as was expected. Figure 60

shows the vector angles, calculated throughout each gait cycle, of the orthotic wearing leg, in both the anterior and posterior directions, without servo stabilisation.

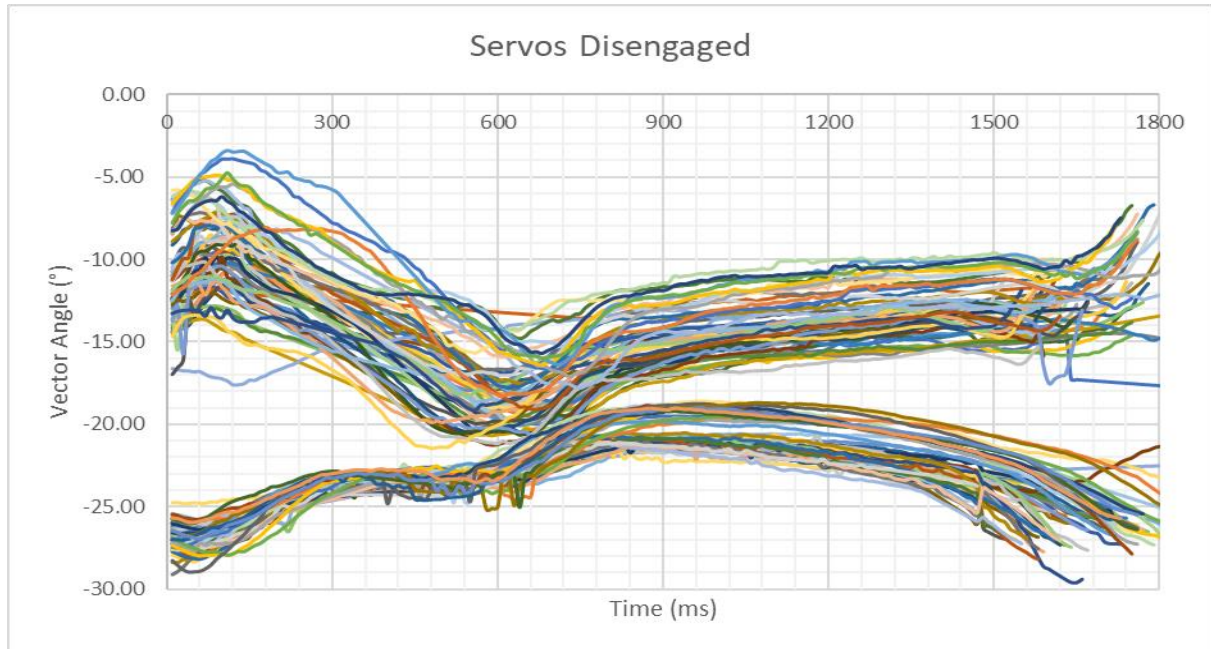


Figure 60: Shows the range of measured angle change of both the anterior (Top set) and posterior (Bottom set) vectors against the centre line of the orthotic.

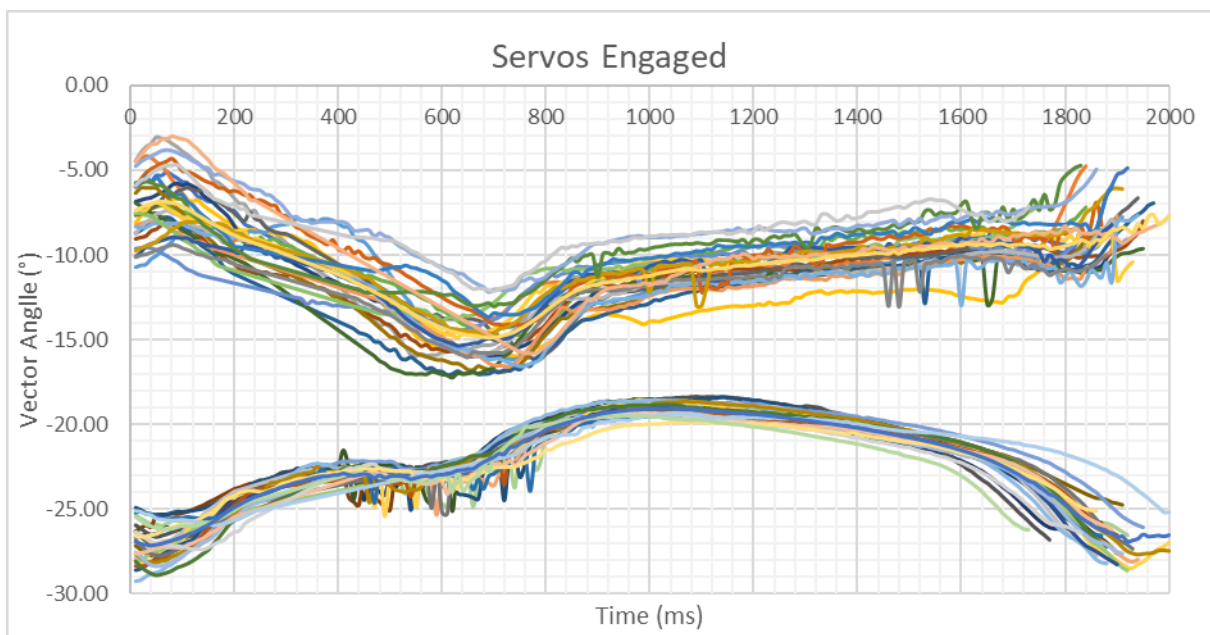


Figure 59: Shows the range of measured angle change of both the anterior (Top set) and posterior (Bottom set) vectors against the centre line of the orthotic

5.3.2.2 Anterior and Posterior Vector Angles – Servo Engaged

Due to system functionality, producing as many acceptable gait cycles as possible with the servos engaged was more challenging. Instead, 27 gait cycles were identified for the anterior angle and 25 for the posterior angle (Figure 59), with a general pattern as shown in Figure 61.



Figure 61: Anterior and Posterior vector angles calculated from data derived from the Motek CAREN system while the servos were engaged.

5.3.2.3 Data Correction for Comparison

For better data comparison, it was decided to reproduce the plots with each gait cycle plotted with the variable measured against the percentage of gait rather than as a timestep. This made it possible for data to be compared at key percentages of gait without short or long gaits imparting error upon the overall data population. Figure 63 shows the data sets corrected as a percentage for post-anterior and posterior vectors with the servos disengaged. To accurately average the data generated, each data set of hall effect and CAREN vector angles for each gait

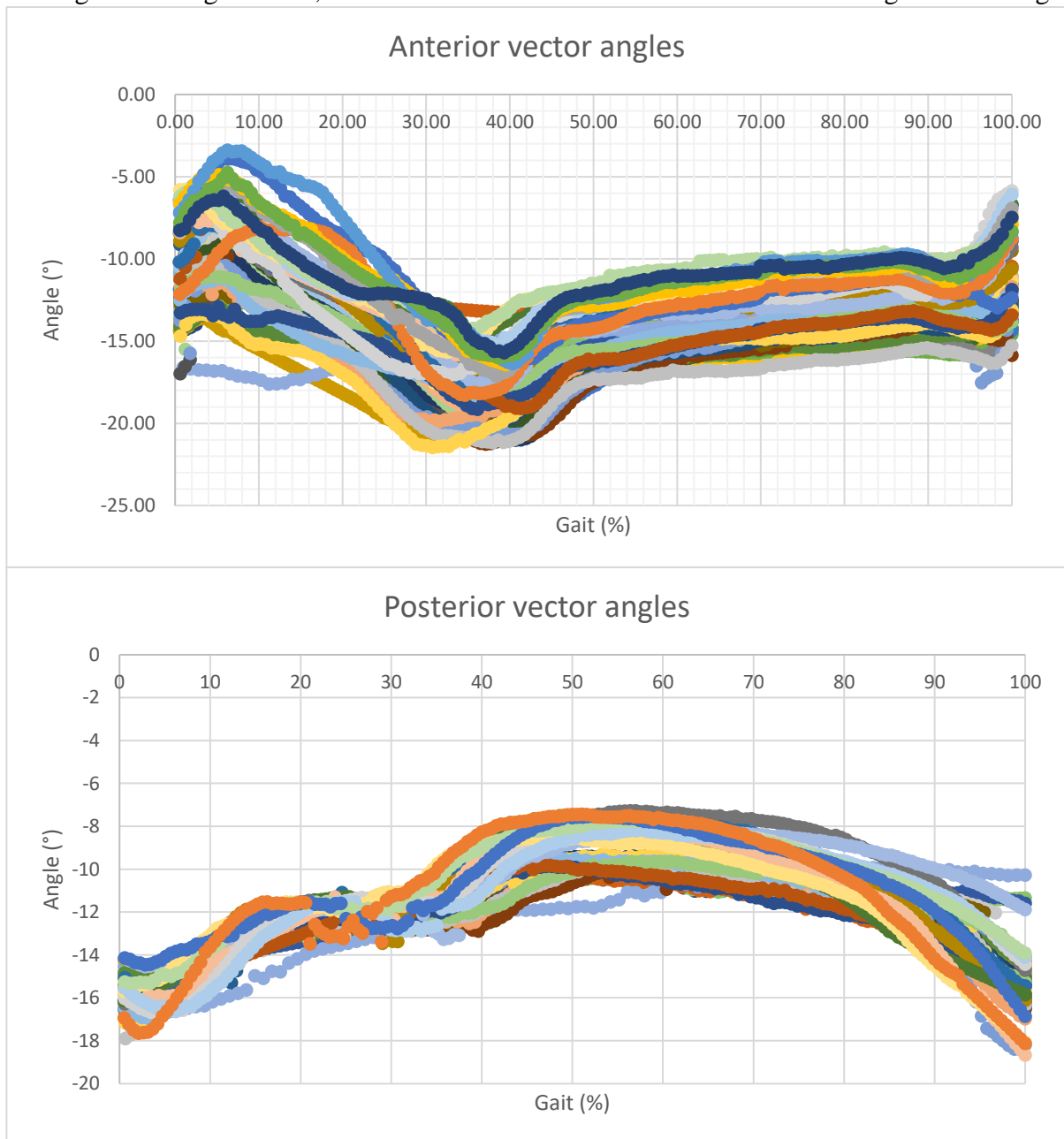


Figure 62:gait cycles compared as a gait percentage to allow greater comparison of gait stages.

cycle were combined using the Vstack function within Excel before being interpolated for every 0.5% of gait. The average data for each set is shown in Figure 63.

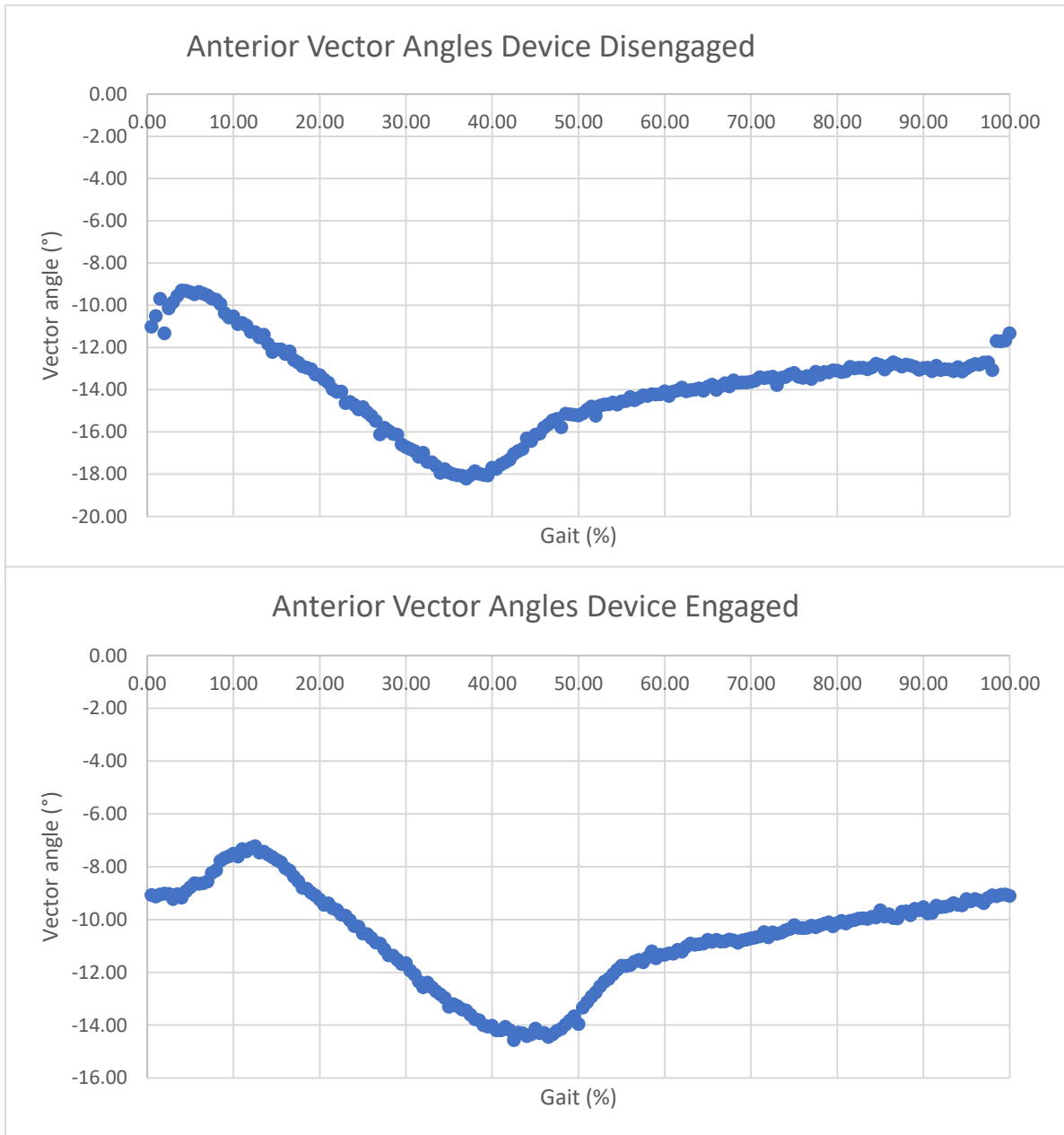


Figure 63: Average gait cycles vector angle for anterior CAREN data Top) device disengaged, Bottom) device engaged.

To determine how best to analyse each data set in the later stages, the normality of the data was also checked. The four plots of Figure 66, Figure 65, Figure 68 and Figure 68 show the data distribution of each data pool, with both anterior data sets showing smooth, uniformly distributed data sets showing high levels of normality. Anterior data differed in that only the data set with the servos disengaged showed a normal distribution but at a lower level, whilst the final data set of posterior angles with the servos engaged showed a skewed data set with little normality. Due to this, it was noted that anterior comparisons would be taken with higher

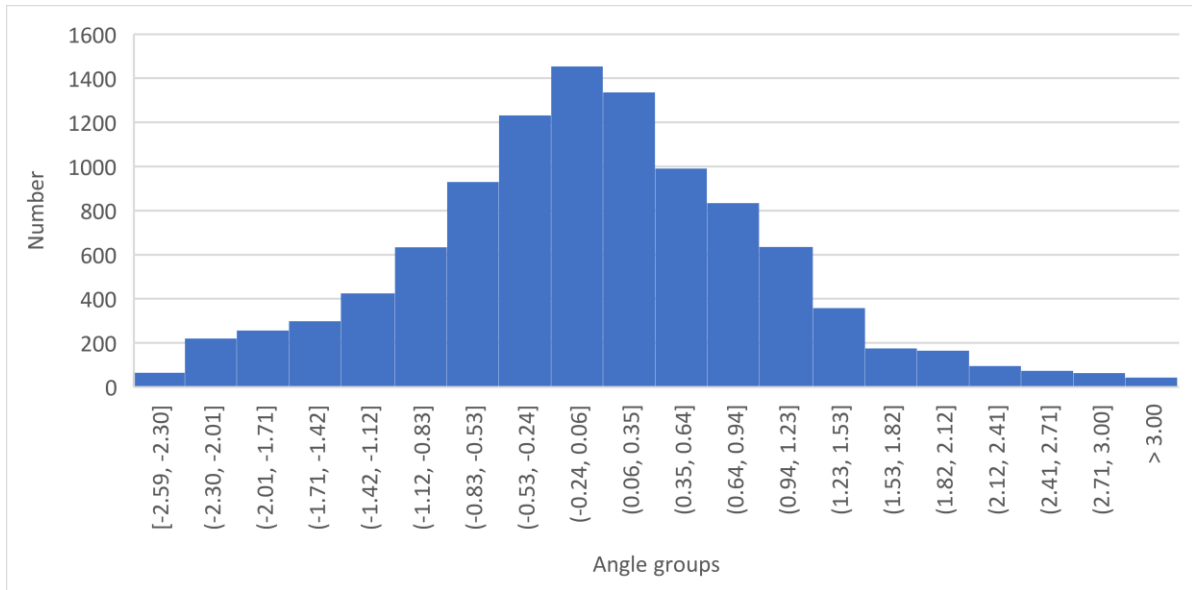


Figure 64: Distribution of Anterior Disengaged Data

confidence levels during further analysis. The posterior data would need to be further analysed using nonparametric methods.

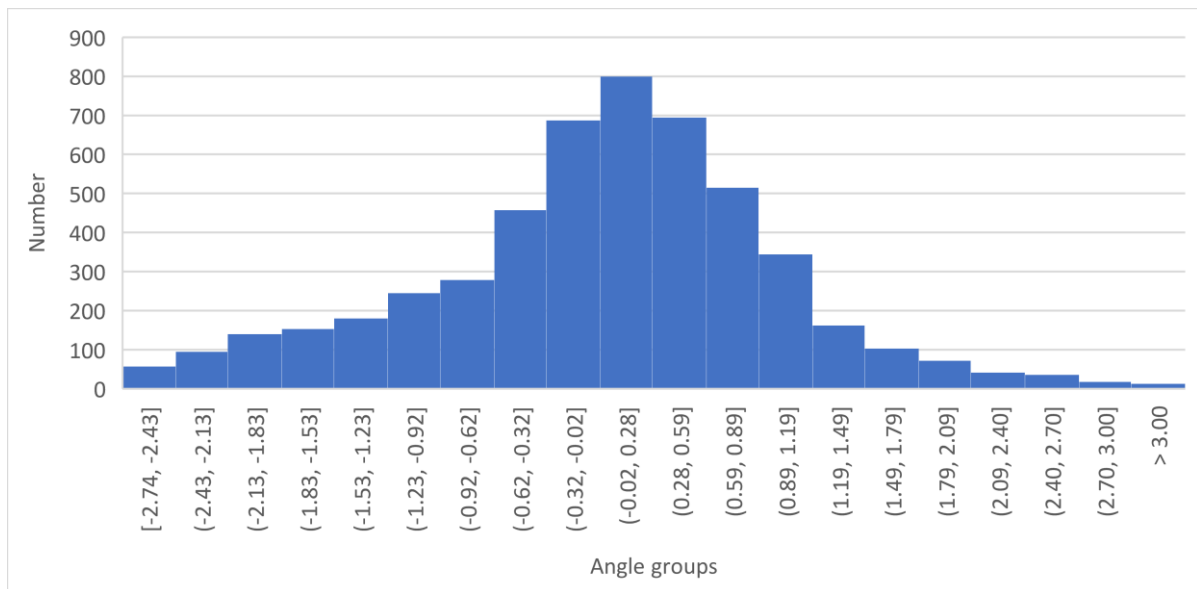


Figure 65: Distribution of Anterior Engaged Data

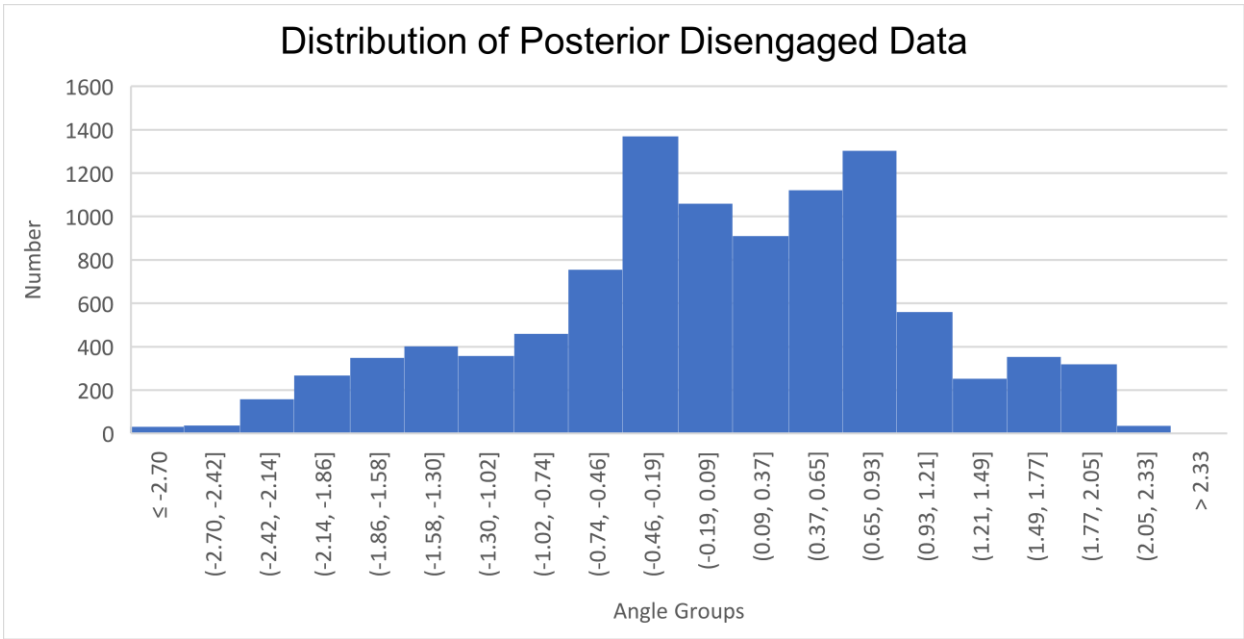


Figure 66: Distribution of Posterior Disengaged Data

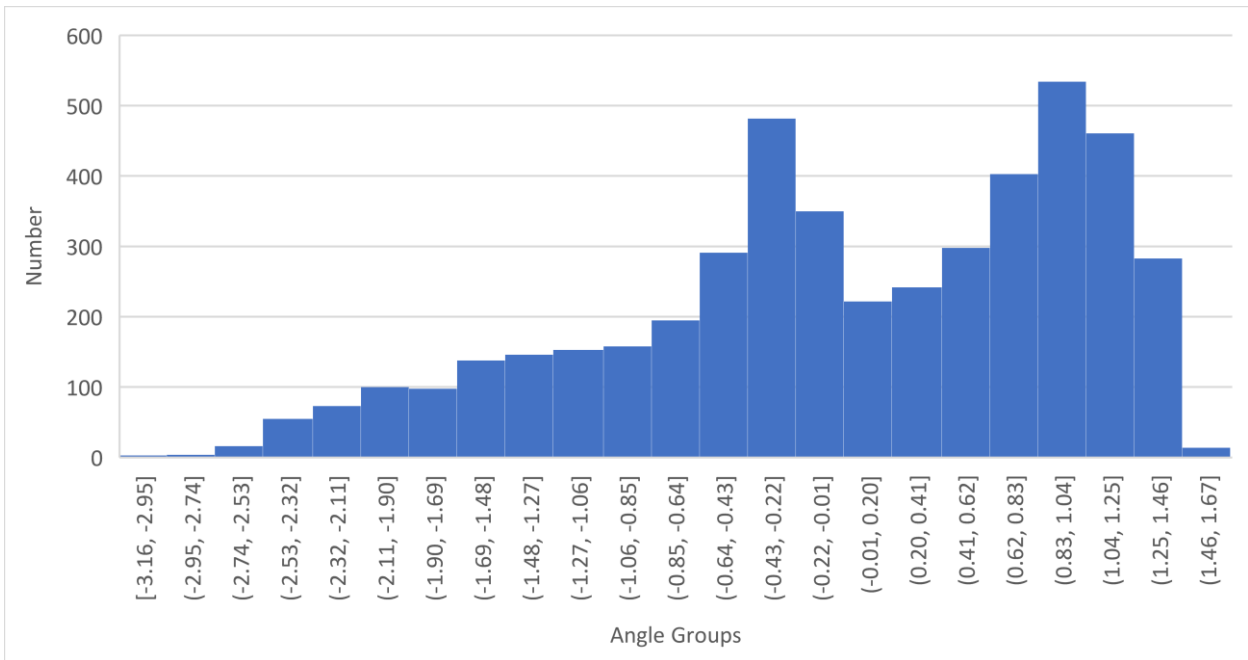


Figure 67: Distribution of Posterior Engaged Data

To better understand how the actuation influenced the oscillation of the shank, Figure 68 shows how the average angle progression altered throughout gait. It approximated that Heel contact was from 0 – 22.5%, Midstance was between 22.5 – 44.5%, Toe Off 44.5 – 66.5% and swing phase from 66.5- 100%. It was noted that there was a shift during the trial between engaged versus disengaged runs, potentially caused by marker/ magnet migration caused during the removal and re-application of the socket. The data was standardised about the median value of the disengaged run to show the data series overlayed with its corresponding device on/off

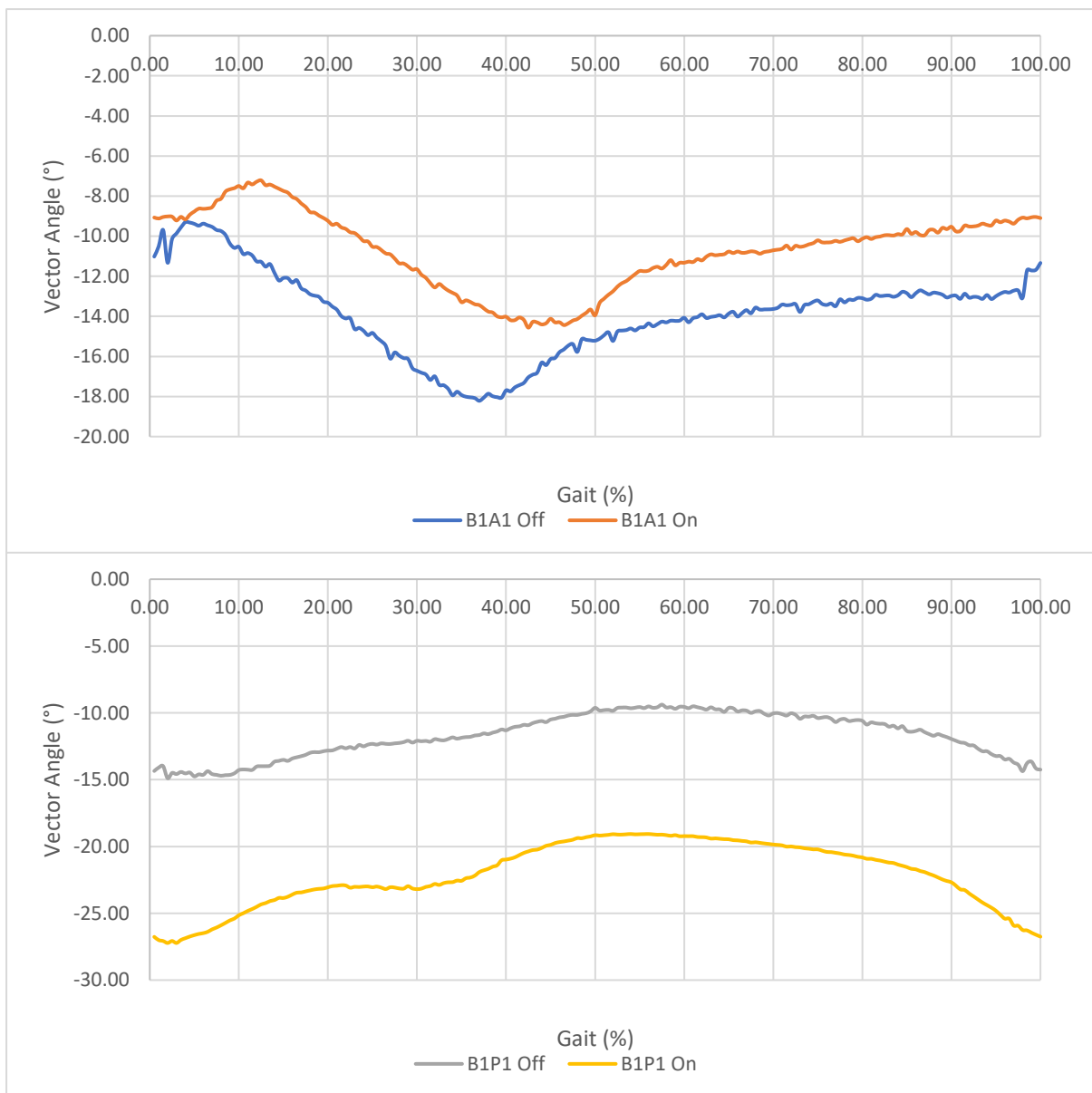


Figure 68: Top) Average anterior angles with servos engaged versus disengaged, Bottom) Average posterior angles.

measurement. This made it clearer to identify how the actuators altered the profile of the data sets, as shown in Figure 69.

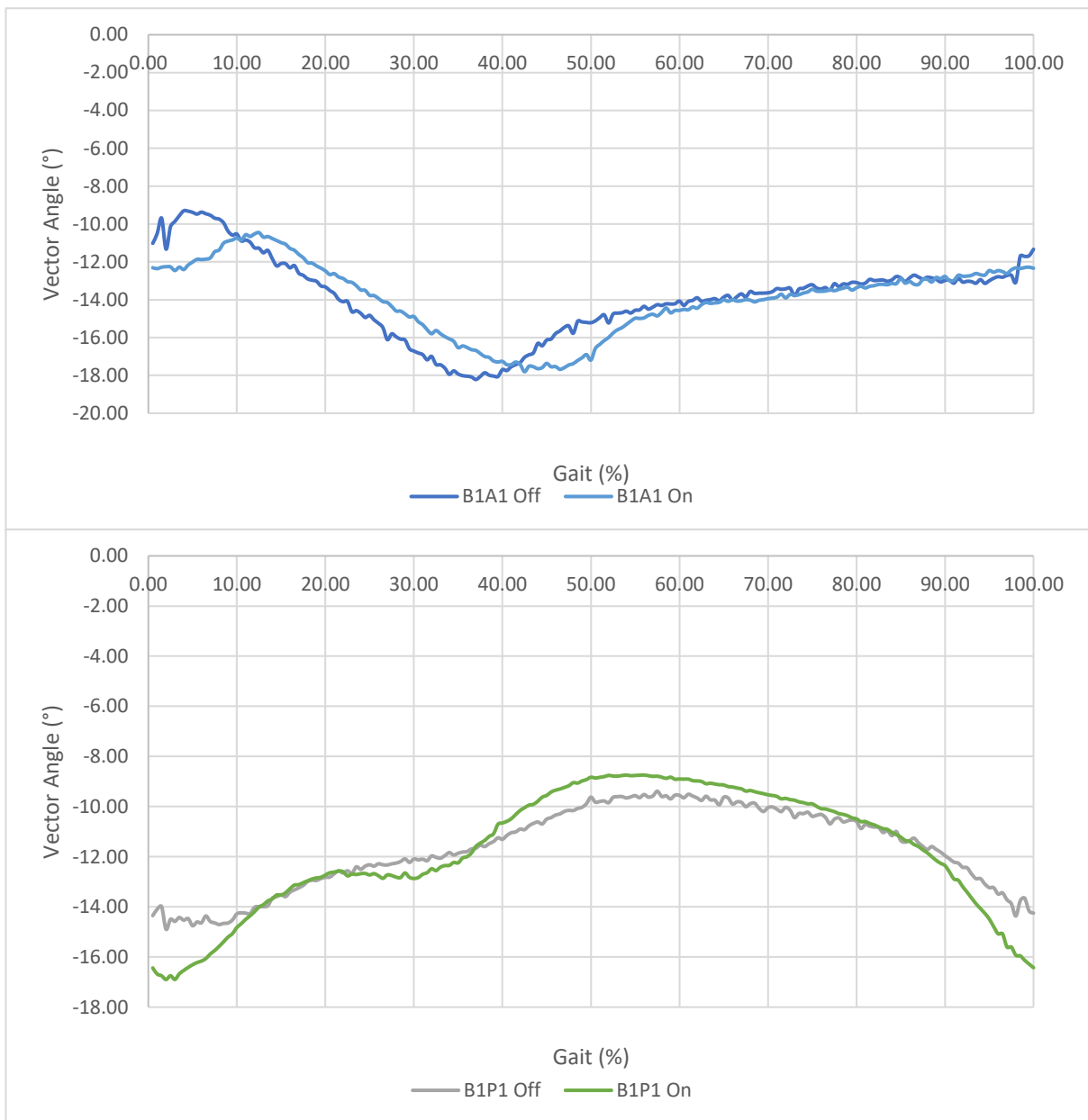


Figure 69: Vector angle averages corrected about the median values of each data set.

To quantify the influence of the system. It was decided to look at each scenario in terms of standard deviations and ranges, alongside how these values compared to their equivalent averages as a percentage, thus providing numerical data that could be quickly evaluated for performance. It should also be noted that with only half the number of cycles available to the engaged scenario, it is impossible to judge whether the maximum and minimum values

calculated accurately represent the true spread of data that could have been achieved with further cycles. However, with 27 cycles compared to the 61 available for the servo disengaged, a good representation would have been gathered. A significance test was also carried out alongside descriptive statistics to quantify whether the differences seen can be more confidently attributed to the device being engaged.

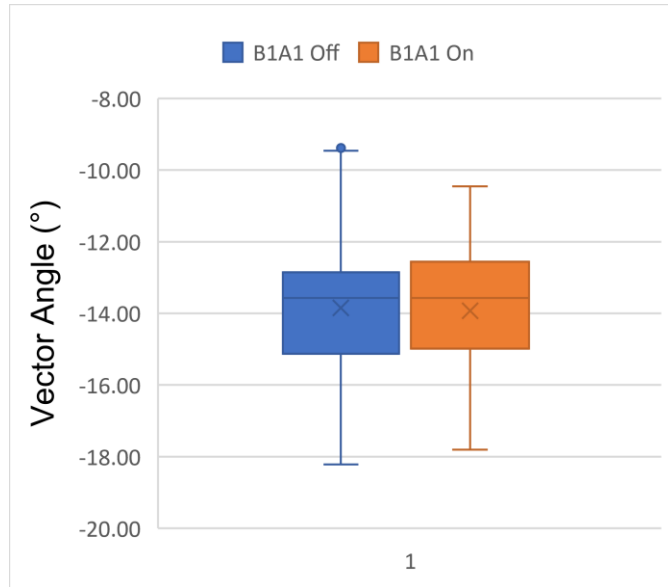


Figure 71: Box plot showing the full spread of the anterior vector angle measured with the device off versus on.

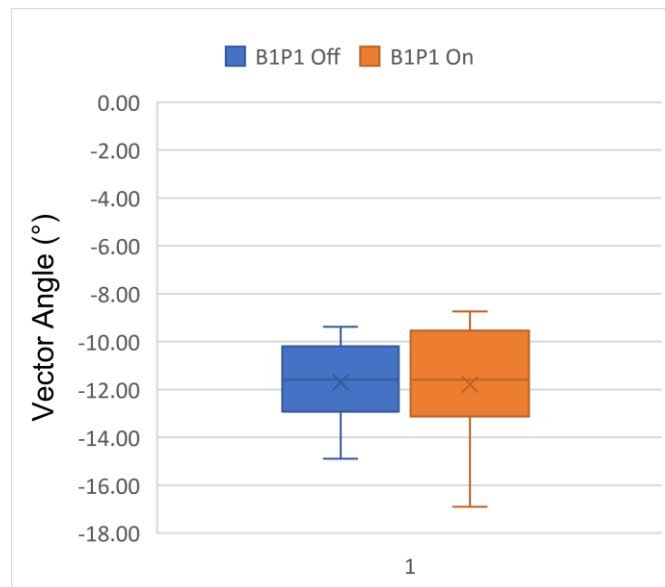


Figure 70: Box plot showing the full spread of the posterior vector angle measured with the device off versus on.

Box and whisker diagrams were produced for the data sets to visualise better the overall spread of data from the CAREN trial. Figure 71 and Figure 70 show the overview of the full data ranges for both anterior and posterior vector angles with the device off/disengaged versus on/engaged. Despite this, it was decided to break the gait cycle down to HC, Midstance, TO and swing phases and repeat the process to understand better how the device potentially influenced the vector angles seen about the orthotic device for the different stages of gait.

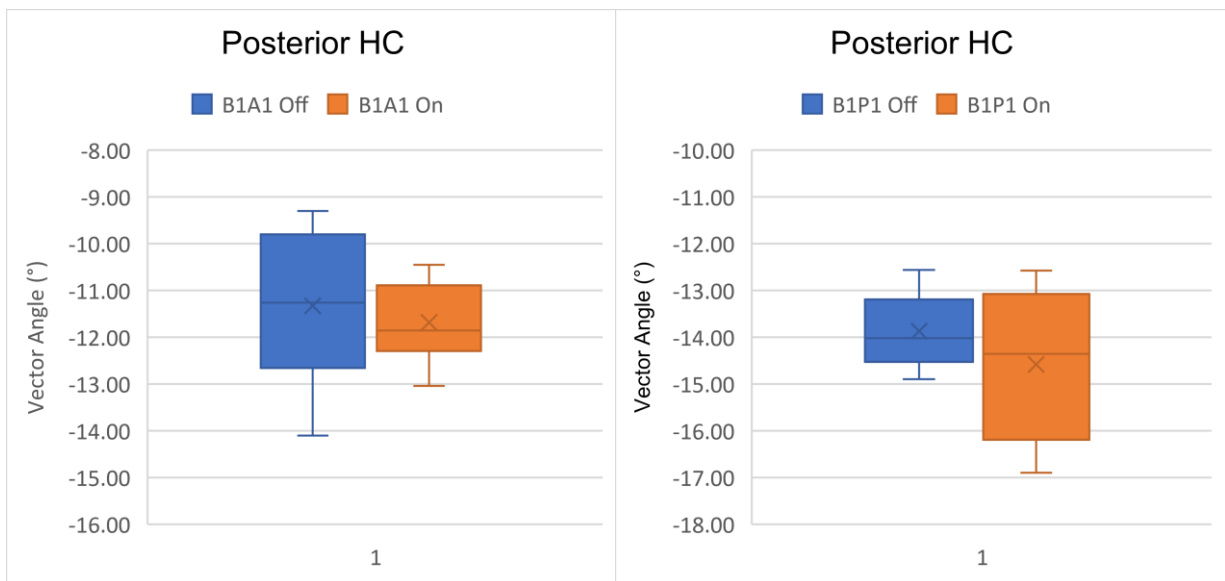


Figure 73: Left) Anterior vector angles at HC, Right) Posterior vector angles at HC

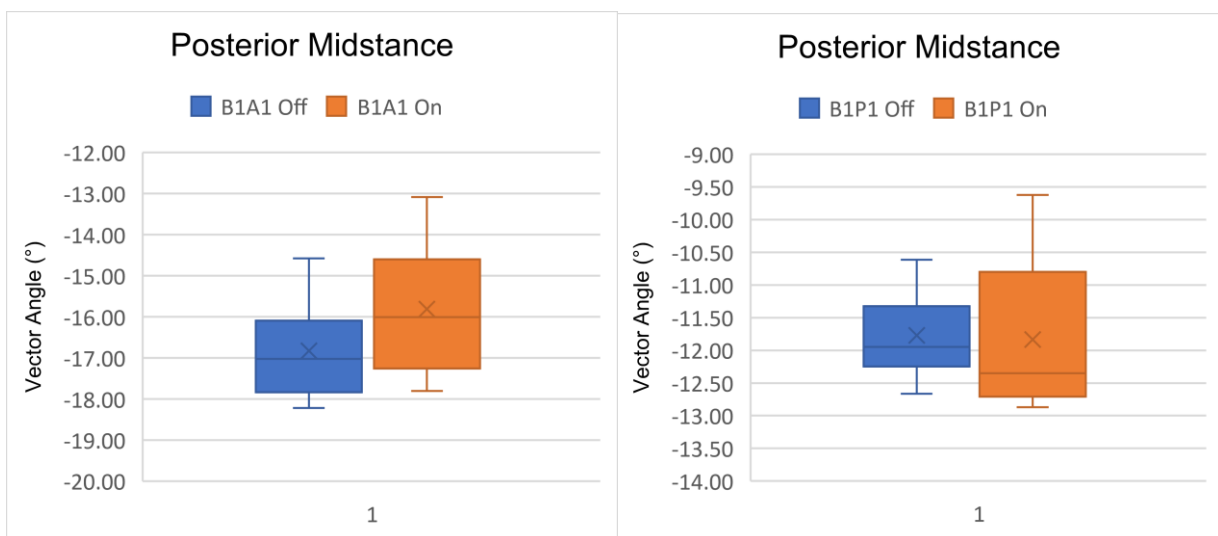


Figure 72: Left) Anterior vector angles at Mid-Stance, Right) Posterior vector angles at Mid-Stance

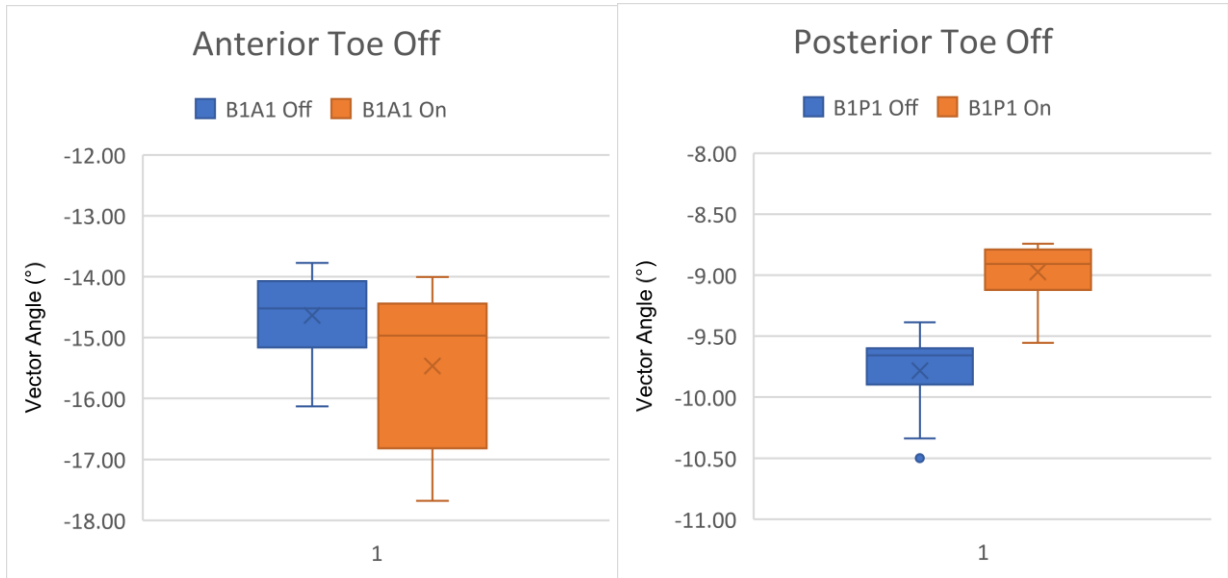


Figure 75: Left) Anterior vector angles at TO, Right) Posterior vector angles at TO

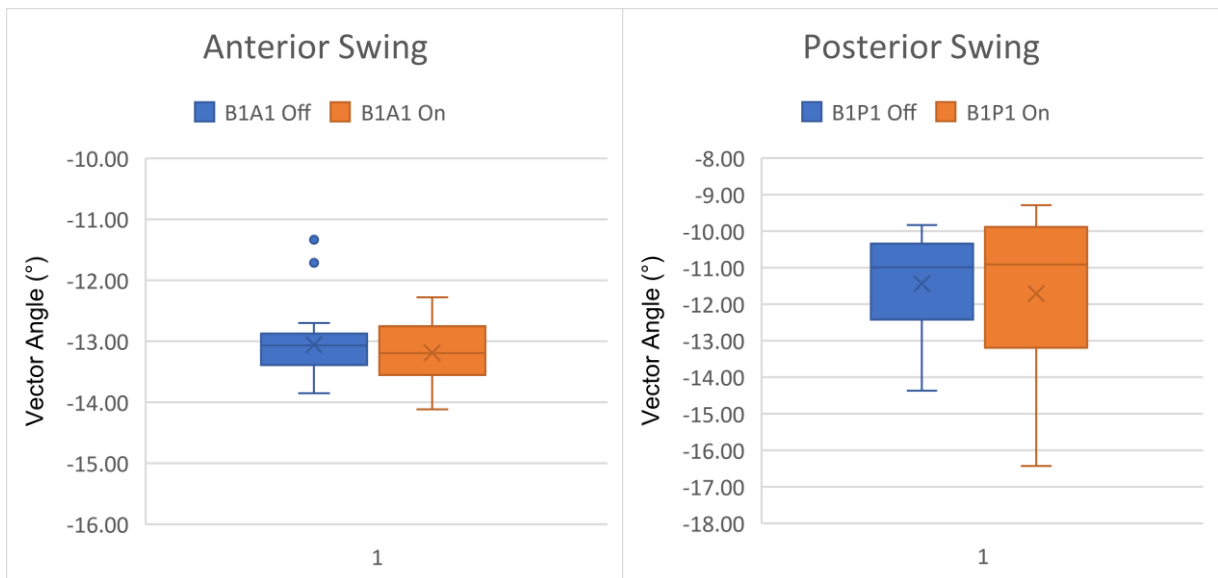


Figure 74: Left) Anterior vector angles at Swing, Right) Posterior vector angles at Swing.

Figures 73-74 show the variation in the spread for the data sets with the device disengaged versus engaged for both anterior and posterior vector angles across the various stages of gait. With the data separation allows for further descriptive statistics and significance testing to take place.

Using a two-tailed T-test, it was possible to identify whether there was any significant difference between the data sets (device engaged versus disengaged). The datasets were

compared before being broken down into the four stages of gait mentioned previously. Using an alpha value of 0.05, it was possible to question the hypothesis:

- Null hypothesis (H0): there is no difference in vector angle when the device is engaged versus disengaged.
- Alternative hypothesis (H1): there is a difference in vector angle when the device is engaged versus disengaged.

Table 10: Significance testing and descriptive stats for All Data

All Data					
	Anterior		Posterior		
	<i>Disengaged</i>	<i>Engaged</i>	<i>Disengaged</i>	<i>Engaged</i>	
Mean (°)	-13.85	-13.93	Mean (°)	-11.70	-11.78
Variance	4.69	3.65	Variance	2.68	5.82
P(T<=t) two-tail	0.69		P(T<=t) two-tail	0.68	
Standard Deviation	2.17	1.64	Standard Deviation	1.91	2.41
Range	8.91	5.51	Range	7.35	8.16
Minimum	-18.22	-14.89	Minimum	-17.80	-16.90
Maximum	-9.30	-9.39	Maximum	-10.45	-8.74
IQR	2.26	2.38	IQR	2.38	3.57

Table 11: Significance testing and descriptive stats for HC

HC					
	Anterior		Posterior		
	<i>Disengaged</i>	<i>Engaged</i>	<i>Disengaged</i>	<i>Engaged</i>	
Mean (°)	-11.33	-11.69	Mean (°)	-13.87	-14.58
Variance	2.31	0.57	Variance	0.53	2.35
P(T<=t) two-tail	0.17		P(T<=t) two-tail	0.01	
Standard Deviation	1.52	0.75	Standard Deviation	0.75	1.53
Range	4.80	2.59	Range	2.59	4.33
Minimum	-14.10	-9.80	Minimum	-13.04	-16.90
Maximum	-9.30	-7.22	Maximum	-10.45	-12.57
IQR	2.74	1.38	IQR	1.38	3.05

Table 12: Significance testing and descriptive stats for Mid-stance

Mid-Stance					
	Anterior		Posterior		
	<i>Disengaged</i>	<i>Engaged</i>	<i>Disengaged</i>	<i>Engaged</i>	
Mean (°)	-15.81	-16.83	Mean (°)	-11.77	-11.84
Variance	2.11	1.26	Variance	0.32	1.15
P(T<=t) two-tail	0.00		P(T<=t) two-tail	0.73	
Standard Deviation	1.12	1.45	Standard Deviation	1.45	1.07
Range	3.64	4.72	Range	4.72	3.25
Minimum	-18.22	-14.57	Minimum	-17.80	-12.87
Maximum	-14.58	-9.85	Maximum	-13.09	-9.62
IQR	1.68	2.64	IQR	2.64	1.71

Table 13: Significance testing and descriptive stats for TO

TO					
	Anterior		Posterior		
	<i>Disengaged</i>	<i>Engaged</i>	<i>Disengaged</i>	<i>Engaged</i>	
Mean (°)	-14.64	-15.47	Mean (°)	-9.78	-8.97
Variance	0.42	1.61	Variance	0.07	0.04
P(T<=t) two-tail	0.00		P(T<=t) two-tail	0.00	
Standard Deviation	0.65	1.27	Standard Deviation	1.27	0.21
Range	2.36	3.67	Range	3.67	0.81
Minimum	-16.13	-14.44	Minimum	-17.68	-9.56
Maximum	-13.77	-10.77	Maximum	-14.01	-8.74
IQR	1.07	2.21	IQR	2.21	0.31

Table 14: Significance testing and descriptive stats for Swing

Swing					
	Anterior		Posterior		
	<i>Disengaged</i>	<i>Engaged</i>	<i>Disengaged</i>	<i>Engaged</i>	
Mean (°)	-13.06	-13.19	Mean (°)	-11.44	-11.71
Variance	0.22	0.27	Variance	1.73	4.61
P(T<=t) two-tail	0.14		P(T<=t) two-tail	0.38	
Standard Deviation	0.47	0.52	Standard Deviation	0.52	2.15
Range	2.51	1.83	Range	1.83	7.14
Minimum	-13.85	-10.88	Minimum	-14.11	-16.43
Maximum	-11.34	-9.04	Maximum	-12.28	-9.29
IQR	0.50	0.80	IQR	0.80	3.12

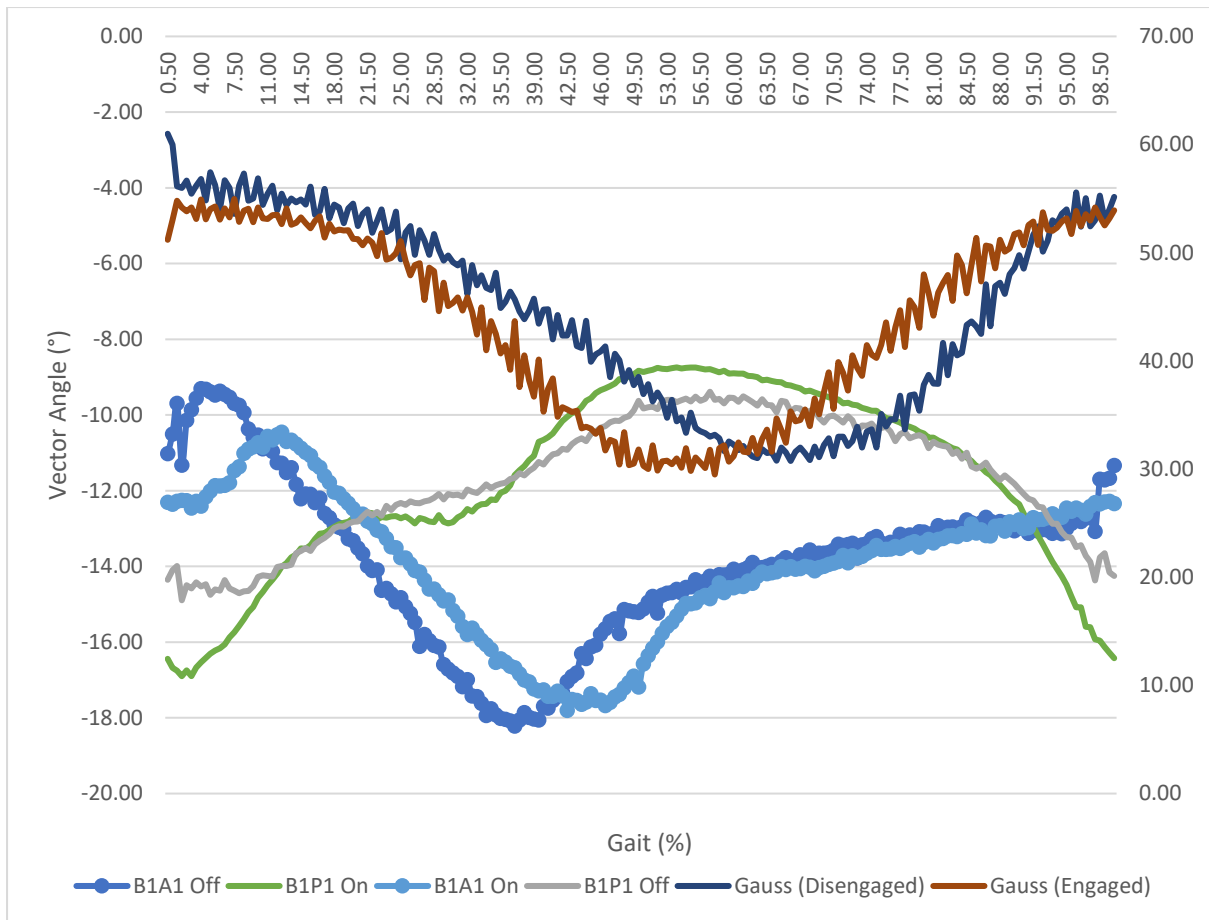


Figure 76: Hall Effect data superimposed with Caren Vector Angle for reference.

Tables 10 – 14 indicate how key descriptive varied for both scenarios. The columns are set up to include the full cycle and break down each stance and swing portion. This makes it easier to identify whether a greater influence was being found at certain stages of the gait in the same manner of analysis carried out with the Hall effect measurement. Figure 77 shows a superimposed plot of the hall effect data for both disengaged and engaged measurements alongside the data collected for the anterior and posterior data from the CAREN system.

5.4 Discussion

Monitoring the socket rotation of a below-knee amputee and reacting to it with counterbalancing load required evaluating a proposed solution on lower-risk participant groups. Following the design of a possible concept device, an orthotic device was designed and manufactured to replicate similar moments about a prosthetic user's residual limb but with the device designed to be attached to an able participant. Employing a Hall effect sensor positioned on the inner surface of the socket wall, the displacement of a magnet on the participant's shank was tracked, making it possible to detect the shank's position and respond with a counterbalancing load. This was supplied by two rotary servos fixed to the anterior and posterior faces of the limb, with the normal mid-stance magnet position stimulating no response from the servos and swing in either direction responded antagonistically. Feedback was split into two parts to assess the system's performance. Movement data was generated from the Hall effect sensor, and there may be a reduction in the range of data seen if the servos were able to stabilise the moments of the socket. Secondly, participant feedback was collected to identify whether the device significantly changed the participant's ability to walk or offered more overall comfort. The final feedback data was reported on the vector angles calculated from the infrared markers placed on the orthotic and the participant's shank. The Motek CAREN system tracked the markers in real-time, making it possible to assess whether the servos provided stabilisation. The assessments were based on vector angle changes during gait cycles, with the servos engaged compared to disengaged.

5.4.1 System Performance

The individual gait data derived from the magnetic field measurement provided by the Hall effect sensor proved successful in initialising a response from the servos, responding with a low lag time. Despite this, it was noted that the system did not provide loading forces significant

enough to provide the proportional control that was initially desired; instead, it seemed to be more suitable for an all-or-nothing response from the servos. In both scenarios, i.e., the servo engaged and disengaged, it was noted that during the magnet progression to its point of minimal separation, the measured magnetic field would level out. This was expected as the displacement would become fixed due to the sensor contacting the silicone liner at toe-off, resulting in a fixed thickness pad between the magnet and the sensor. This effect could be minimised with a re-arrangement of sensor locations without any significant influence on the magnitude of the recorded magnetic field. This effect was thought to have reduced the maximum output of the servos during attempts at proportional responses; however, as the trials were continued with an all-or-nothing response, this effect was negated.

In terms of stabilisation, the results can be analysed, assuming a reduction in the magnetic field measurement range would indicate the displacement being truncated and, therefore, more stable. Looking at the averages across the two data sets, the influence of the system on the stability of the lower limb is difficult to see. Despite this, in Figure 54, the data sets measured for the disengaged device versus engaged indicates an overall reduction in the values represented by larger Gauss measurements. The reduction in range at this extremity suggests greater influence was had during HC of and during the late stages of the swing. Whilst mean and IQR values remained very similar. Comparatively, only the upper quartile data saw a reduction. With a p-value of 0.369 suggesting a correlation between change in Gauss measurement device engagement cannot be made. However, by breaking the average gait cycle down into the four stages of gait, it is possible to see significant differences in data sets.

To better understand how the performance of the device influenced the overall data, the expected results for stabilisation are described next to what can be seen from the data and descriptive statistics.

- At HC, socket rotation would minimise the distance between the magnet and the sensor. Therefore, when engaged, the ideal would be a noticed reduction in the measured gauss, correlating to the servos counterbalancing the limb and increasing the displacement between the sensor and magnet.
 - This reduction can be seen in Figure 53 and Table 6; although the influence is small, a significant reduction during the HC phase is shown. Indicating that when the moments of the prosthesis are small, a level of stabilisation is achievable.
- Midstance, with the socket in its central position, it is to see no difference in data at this stage.
 - At midstance, an average reduction can still be seen for the data sets with the device engaged, Figure 58. and Table 7. This differs from what would have been preferred and indicates that the lag between the sensor and actuation was too large, and the actuators had an influence when one was not desired.
- TO, with moments of the prosthesis causing the displacement between the magnet and sensor to increase. The ideal would be to see an increase in the measured gauss representing stabilisation of the socket towards the central position.
 - Similarly to midstance, the device negatively impacts the transition to TO, Figure 57 and Table 8. Despite a reduced range of values indicating the rate of change of measurement was less, the overall positioning was maintained towards the lower Gauss values showing the higher positive moment was maintained. This effect is likely a culmination of lag between the sensor actuator system and poor influence of the anterior actuator during peak loading of the complex.

- With the limb passing through a reducing positive moment into a slightly negative moment, it would be desirable to see an increased Gauss measurement at the initial phase of the swing followed by a reduction towards the later stages.
 - Due to the moments swapping from positive to negative during the swing, it is more difficult to see improvement from Figure 56. and Table 9. However, the desirable effect can be seen visually in Figure 55. This further indicates that for low-loading situations, the device can provide desirable stabilisation in the data generated by the Hall effect system. However, performance tends to be limited or undesirable during high-loading situations.

The lack of servo influence was also noted in the user feedback, whereby subjectively, it was reported that the servos seemed to have little influence.

The overall detection of the magnet operated successfully at a displacement range of 10 - 15mm, with clearly identifiable gait phases. However, greater sensitivity was desirable, and variations in the magnet's size, shape and strength could be investigated.

5.4.2 Angle Change

The Motek CAREN system provided a more controlled method of measuring stabilisation, fulfilling the relatively simple task of calculating vectors and vector angles from reflective markers placed on the participant and providing highly accurate real-time feedback. The information was collated with the device engaged versus disengaged after the same data analysis process. The data was analysed descriptively as a whole and as phases of gait, with the significance testing helping to determine whether there was any notable difference between the two scenarios.

To increase the ease of comparison, the mean values of the data were overlaid, as shown in Figure 70, highlighting more clearly the effect of the actuator system when engaged for both anterior and posterior vectors.

When analysed for significance, the overall data comparison of the vector angles calculated from the CAREN system generated a p-value greater than 0.69, indicating that the null hypothesis (no significant change in vector angle is seen when the device is engaged) can be accepted. However, as per the Gauss measurements, significant differences can be seen in the four phases of gait.

Anterior Vector

- At HC, Figure 70 indicates that at HC, the anterior vector initially reduces before reversing in direction as a greater load is transferred to the orthotic. Therefore, when the device is engaged, the ideal would be the maintenance of a larger (more negative) angle than when the device was disengaged before transitioning to a comparatively smaller angle.
 - Despite the p-value in Table 10 being greater than 0.05 (0.17), it is clear from Figure 70 that the desired vector transition is achieved with the device engaged. Showing maintenance of the angle at first contact before controlling the overall angle at a lower magnitude as the transition to midstance progresses.
- Midstance, with the ideal socket in its central position, is to see no difference in data at this stage or a similar profile with equivalent magnitudes.
 - Table 12 and Figure 73 indicate a significant difference in data and an overall reduced vector angle when the device was engaged. The influence indicates that the device can still provide an influence; however, the actuators' input measures a greater overall range of data. This may be an artefact of the actuators

attempting to provide a stable influence but, in effect, causing the limb to oscillate irregularly under the increased loading.

- TO, with moments of the prosthesis causing the anterior vector angle to tend towards a lesser magnitude, stabilisation would be seen in maintaining a larger magnitude.
 - Table 13 indicates a larger overall mean value during the transition to TO as would be desired; however, as for midstance, larger values for range and IQR suggests the overall control of the angle manipulation is poor with the device engaged. This suggests that the control is not damped enough to allow timely control but in a non-oscillating manner.
- Swing, with the limb passing through a reducing positive moment; it would be desirable to see the maintenance of a larger magnitude of the angle between the vectors of the orthotic and limb of the participant.
 - The data shown in Table 14 indicates no significant difference with a p-value of 0.14. next to no influence from the actuators can be assumed. This indicates that the posterior actuator had minimal overall influence, as it should have been dominant for the range of motion, with a greater influence expected as the system was only loaded by the weight of the orthotic complex itself during the swing phase.

Posterior Vector

The CAREN data for the posterior vector measurements show variations between engaged and disengaged devices. Although, as before, little difference can be seen statistically, greater variation is apparent when broken down into gait stages. The overall variation from stage to stage appears undesirable, with greater overall ranges and IQR measurements for HC, midstance and swing, suggesting that external loading created a much larger oscillation of the limb than was expected. It theorised that the reverse would happen, and overall vector ranges

would be reduced across the gait cycle. The lack of control over the posterior angle further indicates that the posterior servo had less impact than desired, and the increase in external loading led to a noted increase in an overall variation in both anterior and posterior angles.

Further indicating that although influence can be seen, the control of the system was inappropriate for the task in mind. Overall requiring more loading potential and a more rapid response to Gauss measurement with greater damping of the overall output. Alternatively, create a more predictive feedback model to help reduce the lag seen.

5.4.3 Contribution to Knowledge

During the literature review (Chapter 2), it was found that the current state-of-the-art devices, such as the variable impedance socket produced by Sengeh, focused on the redistribution of surface loads to mitigate large pressures on the skin's surface of a residual limb (Sengeh, 2013). However, there is a correlation between researchers that indicate that not only stress magnitudes at the bone tissue interface far exceed those experienced at the skin's surface (Portnoy, 2008). However, also, stress generation is likely to be impacted further by factors such as terrain (Portnoy, 2010), resulting in increased loading during basic day-to-day walking than had been accounted for by the current mitigation devices. The device described in this thesis is designed to compensate for this by targeting the oscillation of the tibia during gait, a factor better visualised by X-ray (Lilja, 1993). The study's data indicates that the extent of rotation can be reduced by loading antagonistically to the natural direction of the moment. Whereby limiting this rotation would reduce the torque applied to the residual limb through the prosthesis and therefore reduce the magnitude of stress experienced. The proof-of-concept device targets contributing factors associated with DTI in a manner not yet explored, showing results that indicate that stabilisation in a prosthetic environment can be achieved for specific stages of the stance phase. Whilst further being an active solution, responding to changes in the user's gait is a factor that has only been tested sparingly by similar devices.

5.4.4 Mitigation Criteria for Future Design and Experimental Iterations

Several aspects of the experiment highlight areas of variability and overall weakness that should be improved upon in coming iterations of the design:

- **Bone sensing:** utilising a magnet was proven possible in the initial experimentation. However, without direct implantation into a participant's residual tibia, accurate monitoring of the movement of the tibia relative to a prosthetic wall is impossible. Due to this, developing a possible method of tracking bone movement in real time would be necessary. This could involve using real-time feedback from ultrasound scans to assess the tibia's displacement and provide a loading response.
- **Servo Influence:** with the apparent weakness of the system in stabilising the socket when the limb was subjected to higher loading, it was necessary to address how the servo system's power output could be increased. This could have taken many forms, including reducing the length of the piston arm to increase torque or possibly identifying a new loading system entirely. It was clear that to progress the concept for proper functionality in a prosthetic socket; it would need to be streamlined. This meant reducing its overall size and weight whilst increasing its output.

5.5 Conclusions

To be able to test and develop a new medical device concept, it is necessary to carry out several stages of testing to ensure that the device is safe and suitable for its intended purpose. For this proof-of-concept design, it was decided to investigate the suitability of the proposed technique in a study.

The study showed that the technique could stabilise a prosthetic's load during basic ambulation, particularly at HS. The Hall effect feedback system is being validated alongside vector data

gathered by CAREN. Data that allowed greater assessment of the device's performance when engaged, with a noted more positive angle in the anterior vector at HS. Indicating the system was counterbalancing the expected torque and reducing its impact on the would-be residual limb and, thus, DTI to an extent.

The trial provided a foundation by which future experimental and device iterations could be developed, highlighting critical areas in need of development and providing the initial data for the proof-of-concept experiment. However, the device was limited, particularly in the strength and influence of the actuators; the device only provided low-magnitude loading. An increased stabilisation (particularly at TO) likely influenced the system throughout the gait cycle; further, the device was coarse in its approach and design and required refinement. Factors that were to be considered for future iterations of the design.

Chapter 6 Discussion and Recommendations for Future Work

6.1 Introduction

This chapter provides a platform to theorise how the research findings and results could be utilised for future study and development. Offering insights into the thesis' significance and potential applications, highlighting limitations, and outlining potential future research directions.

6.2 Discussion

6.2.1 The Need

With an ageing population and an associated increase in the risk of chronic ulceration, with 3% of healthy over-60-year-olds and 5% of those over 80s experiencing the condition (Agale, 2013), it was possible to assume the presence of chronic ulceration in the form of DTI would similarly increase with time. Further to this, it had been identified in the literature that the prosthetic socket environment (particularly lower limb prosthetics) provided enhanced conditions for DTIs to occur. The skin flowing over the tibia end causes much greater stress magnitudes in the tissues surrounding the bone than had previously been measured at the skin's surface (Gefen, 2013). This was a thought mirrored by numbers seen by Meulenbelt et al. and Salawu et al., whereby separate investigations indicated that between 43 – 57% of below-knee amputees experienced stump problems relating to tissue damage (Meulenbelt, 2009), with at least 20% of the participants investigated in Salawu's study showing this was likely to be as a result of DTI (Salawu, 2006). Based on this, the indications were that a device capable of mitigating the development of such injury could greatly improve the day-to-day life of lower limb prosthetics users and reduce the potential for detrimental health developments.

6.2.2 The Design

A proof-of-concept device was designed to investigate the hypothesis to identify whether the new idea would be feasible and beneficial to its target user. To actively and reactively stiffen the residual tissue of a prosthetic-using below-knee amputee during gait. Made possible by sensing tibial oscillation about its mid-stance position and providing a tailored response from an external loading mechanism. Thus, limiting the conditions whereby dangerous levels of shear and compressive stresses would be generated.

The device itself would be a step in filling the gap in the medical device industry as limited technology currently exists that targets the same root cause variables, with the predominant focus being the reduction of stresses at the surface of the skin. The device comprised four major parts: a Hall effect sensor, an Arduino microcontroller, rotary servo actuators and the bespoke structural components required to combine the necessary hardware.

6.2.3 Hall Effect Sensing

The sensor was evaluated against several other potential candidates, with concepts such as electromyography and ultrasound considered in conjunction with the Hall effect sensor. However, the Hall effect sensor was selected due to its day-to-day practicality. Its simple installation and signal acquisition made it possible to produce a discreet sensor that was easily manageable with very few additional requirements. It was a point of concern that for the concept to be truly successful, it would require the implantation of a magnet in the tibial end of an amputee. However, it was thought that the technique was suitable to validate the device to move towards an implant for us with the target demographic.

6.2.4 Arduino Controlled Rotary Actuation

With a wide range of microcontrollers available on the market, covering various hardware and software options, it was decided to use again and opportunistic decision-making to select a

concept efficiently. The Arduino Uno was selected to provide a base of hardware options alongside a large community hub with a great deal of source coding for early-stage rewriting.

A similar search was conducted to select the actuation method; however, with more variability in the performance and connectivity constraints, a basic datum comparison provided more quantitative reasoning. The assessment was made based on the devices' characteristics, more so numerically than with too much author-related bias, although not entirely possible to remove with certain time and cost-saving opportunities available. The process highlighted rotary actuators as a suitably powerful and responsive mechanism. Questions regarding the size and practicality of the actuators were made related to the aesthetic and commercial viability. However, for the proof-of-concept nature of the study, it was deemed an acceptable compromise, particularly with the noted lack of ideal actuator candidates currently available on the market.

6.2.5 Structural Components

With structural components being essential to the combination and fixing of the other key components, it was necessary to understand how they could be designed and manufactured. Consideration had to be made regarding the stated device needs and demands related to its recyclability and the general environmental impact. These were held to be important in the original decision-making. Therefore, a CAD system was employed to combine and troubleshoot 3D models quickly and efficiently, making it possible to combine components in a digital space and troubleshoot them for their functionality. In conjunction with CAD, CAM-related processes benefit strongly from 3D modelling software, making it possible to use ALM and rapid prototyping methods to manufacture and model components from various materials quickly. For the project, and again utilising the skills and facilities available in the department, the significant bespoke structural components were manufactured with stereolithography of

ABS, with the material providing the best compromise of mechanical strength and surface finish to reduce post-processing.

6.2.6 The Design Process

The design process was kept as methodical as possible, while a heuristic approach benefitted the process by allowing the exploration of less optimal ideas. This allowed a broad spectrum of components and design configurations to be researched and analysed to understand whether they could be used to achieve the overall aims and objectives of the project. Similarly, detailed design development, testing and evaluation made it possible to establish an iterative process of design development whereby the subsequent planned experimentation was heavily influenced by the experience and knowledge gained from its predecessors.

Exploration of actuation and sensing methods, VCAs and coil induction, respectively, early in the design phase highlighted the limitations of certain concepts, with the trials showing that the only rate of change of displacement was measurable. Furthermore, the reliability and repeatability of these methods were proving too difficult to achieve. This resulted in focusing on calibrating a more industry-standard displacement sensor, a Hall effect sensor. When coupled with an Arduino microcontroller, it was possible to achieve smooth actuator control with simple coding, delivering driven positioning from the actuators in response to the displacement of the magnet from the sensor.

The initial Arduino coding was sourced and adapted in chunks from the Arduino community hub, with several authors supplying source codes for basic element control; however, a larger code was written to combine the Hall effect sensing and stabilisation alongside the correlated positioning of two antagonistic rotary servos. The code required several iterations following pre-trials, with the range and output of the Hall effect sensor needing to be calibrated on the non-disabled participant's shank, a process that highlighted the range and extent of expected

oscillation of the socket limb complex, meaning the proportional response from the servos needed to be matched to the expected gauss measurements. Initially, a step-based response to ranges of Gauss was used to drive the actuator response; however, in later trials, a simpler code involving a few steps was used to increase loading throughout the gait cycle, as input load was noted as an initial issue with the system.

6.2.6 Confidence in Scoring Matrix Methods

Scoring matrices are powerful tools in helping justify key design decisions, allowing initial discussion of conceptual designs to be embodied into a real form eventually. With Pugh's decision matrices forming a considerable part of the trial device's design process, a discussion regarding their benefits and limitations should be made.

Benefits

- Establishment of key comparison criteria to evaluate efficacy against essential parameters. The weighting of key criteria allows for objective concept evaluation by comparing independent factors.
 - Removal of designer bias with (when possible) data comparison rather than opinion.
 - Identifies areas in need of further investigation. The process draws attention to factors that could need greater understanding through additional trialling, for example, ensuring best practice design decisions are made despite a lack of prior knowledge.
 - Provides a source of justification through a systematic approach to concept evaluation.
- Overall clarifying the decision-making process in a relatively visual manner.

Limitations

- Subjectivity can remain in the form of arbitrary weighting to specific criteria. With a level of bias likely based on the opinions of the weighting setter, meaning differences could be present depending on who the lead designer is.

- Decision matrices comparing pre-defined criteria are limited in assessing less tangible factors. Certain concepts perform best on paper, but their implementation is impossible due to other external factors.
- Criteria independency overrides the consideration of criteria interaction.

Utilising the decision matrix as a tool is a challenging approach. As mentioned, several considerations must be made regarding the strengths and limitations that may impact the decision-making process. Due to this, a heuristic approach was also taken for certain decisions, with the option to justify opting against the perceivable best choice in exchange for alternatives that were known to be more achievable, particularly due to the proof-of-concept nature of the initial approach, where best practice for the progression of the study would differ significantly from any final marketable device.

6.2.7 Testing and Validation

To provide a more standardised data collection method, rather than solely the Hall effect feedback, a customised series of infrared markers was devised for the 2-dimensional assessment of socket stability in conjunction with the Motek CAREN system. This allowed for the calculation of an anterior and posterior shank vector to be compared against a fixed central socket vector, whereby the angles between vectors could be used to assess limb socket stability. The data was used to provide extra validity to the yet, unproven Hall effect measurement method, helping to provide more accurate and predictable data responses to the influence of the actuators.

The singular participant limited the testing process. With external factors limiting the time to conduct additional trials, the project would have been more conclusive with data gathered from participants of different gender and physical build. If the results proved similar, the project could be moved on to look at the potential for magnet implantation and how well the system

could perform with additional separation material between the magnet and sensor and increased detection range.

Despite the drawbacks, the testing and validation process was successful, with comparable data being produced and analysed side by side, with the repeatable nature of the Hall effect measurement ensuring that the desired response from the corresponding actuator system would be consistent.

6.2.8 Able-Bodied Trial

Culminating in an able-bodied trial, the initial device prototype was designed and manufactured to test the potential of the Hall effect sensors within an environment simulating a below-knee prosthetic. In this trial, an orthotic device, complete with a prosthetic socket and stabilising device, was worn by a non-disabled participant while they walked on a flat treadmill. The individual gait cycles were measured by both the Motek CAREN system and the Hall effect sensor and were evaluated with the stabilisation engaged versus disengaged.

The results of the process indicated that stabilisation of the shank was possible with a counterbalancing load; however, the current system loading conditions could only provide minimal reductions in measured vector angles, with an overall range reduction in the anterior vector angle of 8.24%, and 5.83% in the posterior vector angle and with a greater influence on the extreme stages of the stance and swing phases. The trial confirmed the potential for the technology to be used to satisfy the initial hypothesis of the project; however also highlighted the limitations of the device's functionality and indicated the difficulties in implementing the system with a below-knee amputee. It was noted that the bulk of the stabilising system was too large to be practical outside of laboratory conditions, and its output was limited. A system capable of larger loading would provide greater flexibility in terms of tailored output loads compared to the outputs developed by the system.

6.2.9 Design Enhancement Based on Trial Feedback

With the potential for stabilisation confirmed, it was necessary to enhance the system to build on the experiences of the initial trial while also planning for trialling with a participant with below-knee amputation. The key difficulty identified was how tibial oscillation could be monitored without a magnet, with implantation being the final aim of the trial process. However, it would be highly unethical to implant a magnet in the tibia end without evidence of the system's effectiveness at stiffening the tissues of a residual limb and stabilising tibial oscillation. To remedy this, a secondary sensing technique was devised involving the removal of the Hall effect system and the use of a real-time displacement measurement taken from an ultrasound image of the below-knee socket complex, combining OpenCV with a Raspberry Pi to calculate the displacement between like-for-like colour contours from an ultrasound image. Here, actuators would relay the real-time calculated distance between a prosthetic socket wall (first colour contour) and the tibia's front surface (second colour contour). The technology was programmed and set in place by the end of the project. Still, the ultrasound imagery and OpenCV compatibility testing were not performed due to the time limitations; thus, final testing on a target participant remained incomplete.

6.2.10 Device Implications

Although only in its infancy, the device showed evidence that the extremes of oscillation between a prosthetic socket and residuum could be reduced by introducing a stabilisation load. With a more expansive investigation, the overall benefits can be quantified; however, the targeted mechanisms identified from the literature evidence were influenced to a small degree. The overall vector angles measured by the CAREN show some reduction, indicating that the conditions generating the shear stress of the largest magnitude could be controlled. Therefore the device holds the potential to reduce DTI.

6.3 Future Work and Development

The device described and tested in the previous sections of the document was developed in a proof-of-concept scenario where the main aim was to design and test a system capable of sensing tibial oscillation and applying a load to counteract it. This is an effect that has been computationally confirmed to reduce stress (compressional stress but, more importantly, shear stress) developments at the bone tissue interface and is a factor that is contributing to the large numbers of transtibial amputees who experience pain, discomfort, and ulceration of the residual limb due to below-knee prosthetic use. Despite this, the project focused solely on designing and developing a method capable of achieving the desired results as effectively as possible. At the same time, practicality in terms of device shape and size was only considered to a lesser extent as they were deemed less important. However, for the project to be practically viable, the system would have to be developed so that the actuation system would be much more streamlined.

The remainder of this section will discuss techniques and technology that hold potential for use that could be developed into suitable systems or ideas that are currently undergoing development that, if developed to a useful extent, could be utilised in the future as some of the technology described holds potential but is currently at relatively early stages of its development and is still too unrefined to be used.

6.3.1 Electrostatic Materials

A material currently under development is an electrostatic gel which, when exposed to a voltage, will increase in volume and is, therefore, capable of imparting a load with a small increase in gel thickness. This is a concept that is considered to hold a great deal of potential for several reasons, particularly as it is expected that loading the residual limb at key locations will be enough to stiffen the tissues of the limb so that tibial stabilisation occurs without the

need for large displacements from the actuating device. In an experiment by Ogawa et al., several layered gel stacks simulated an artificial muscle whereby PVC gels were tested under strong electrical impulses, resulting in a rapid response to 7Hz, while outputting approximately 3Kpa of pressure (N. Ogawa, 2009). This indicates a relatively powerful loading mechanism over short displacements (1.3mm); however, the study showed that to achieve such results, very high voltage ranges were required, at over 1000V, making them impractical to implement near the human body. To have such high voltages near human biology, no matter how well shielded, would be a very risky undertaking, meaning that the technology requires refining and development to achieve similar results and working with much lower voltage levels to make it feasible for application. Despite this concern, some walking-assist wear has been developed and tested to aid basic human walking. Here, the electrode-based PVC gel pads are positioned on the leg in an orientation that amplifies the effect of the affiliated muscles of the leg, with initial testing showing a 10% increase in walking speed when the system is active compared to when the system is deactivated (Y. Li, 2016). However, a large mechanical backpack must have the necessary components. Further, a driving voltage of 400V is still considered risky to use with a system where the insulation has the potential to degrade over time.

6.3.2 Shear Stress Measurement

To truly assess the levels of stress development, particularly shear stress development, it would also be very beneficial to design and carry out a dynamic study of a transtibial amputee as they walk normally. This would provide the grounds to accurately identify levels of tibial displacement and how this affects the stress development within the residual limb. It would also make it possible to understand the level of difference between the true stress development and what has been estimated using more traditional computational and otherwise static experimental approaches. Using elastography techniques and the associated ultrasound technology, accurate mechanical properties of the tissue and displacements could be measured

respectively, making it possible to calculate the stress levels present in the limb as the loading values on its surface would be known. This would make it possible to produce a very accurate computational model of the limb throughout gait for an easier visual representation of a complex and difficult-to-understand biological assembly. Similarly, with a larger, more well-defined model, it would be a simpler process to calculate where and with what magnitude it is best to apply loads from the stabilising systems, making it possible to produce the most efficient system enhancing both the device's performance and the comfort and fit of the user's prosthesis. This solution would ultimately be extended to all the amputees requiring new prostheses, meaning fully customised adaptive and reactive sockets could be built for each prosthetic user. Although the time taken for the scan and the computational modelling may be extensive.

6.3.3 Magnet Implantation

Alongside the testing required to commercialise the product, it would also be worth further testing how magnetic implantation could influence bone healing. To achieve this, several key factors would have to be considered and effectively controlled, particularly body matching and monitoring all the recovery-based variables for amputees without the magnetic implant and those with the magnet implanted in preparation for the prosthetic application. It would be essential to match body size and shape as much as possible, along with the available rehabilitation and diet, to mitigate other factors influencing bone healing. The results would probably take the form of bone images recorded by X-ray at set times post-amputation (0, 4, 8, 16 and 32 weeks), with simple crack size measurements and visual assessments of bone growth being the mechanisms used to evaluate the results.

6.3.4 Embodiment for Productisation

As a proof-of-concept device, the design has clear limitations that would prevent it from becoming commercially viable. It is well known that prosthetic device uptake is much more successful for discrete, low-maintenance and comfortable systems. With the route to the market being complex and detailed, particularly for medical devices, the full productisation process would likely include the following:

- Further device design and development to encapsulate initial trial findings and embody the needs and wants of the customer.
- Investigation of alternative routes of control. Building on the knowledge gained to allow for potential machine learning opportunities for alternative sensor setups.
- Clinical implementation to allow for time-relevant data collection on a broader spectrum of candidate patient groups. To greater validate the efficacy of the system.
- With the next steps, including the progression towards commercialisation. Ensuring the device receives suitable regulatory approval, the design of the device can be developed to allow for efficient design for manufacture (DFM) and subsequent manufacture and distribution.
- With post-market monitoring allows for design enhancement and corrective actions to take place over time.

Although full commercialisation of the product is the goal for the medical device described in the study, a full assessment of the route to market is not practical at this stage of development; however, with an eye to future work, a perceived vision for how the device might progress to the clinical implementation is described below.

Further Device Development

To be discrete, the device would need a drastic redesign. A significant difference is how antagonistic loading could be applied actively and ideally maintained within or close to the socket. Allowing for greater ability to cover the device as would normally be possible. However, some compromise would be expected as adding new technology at the socket interface would increase the average size and weight of the complex. With the results indicating a low level of force required, the potential for technology such as electrostatic materials is particularly interesting. Despite the technology not being practical in its current level of development, ability to provide the load with low dimensional requirements whilst providing additional levels of comfort. Another clear change would be to ensure all the necessary componentry was maintained and housed within the prosthesis.

Alternative routes of control

An interesting method that could dramatically improve the overall control of the stabilisation device described is the inclusion of machine learning (ML) methodologies. ML refers to using computer algorithms that can develop based on experience, whereby the experience method can be split between supervised and unsupervised learning (S. Nayak, 2020). The key difference is that unsupervised methods effectively identify clusters and trajectories in a data structure without a response variable. However, supervised methodologies aim to predict a specific outcome variable based on previous data collected (T. Jiang, 2020).

Supervised/ predictive methodology is a very interesting concept for tibial stabilisation. Building on the individual hall effect measurement allows far greater detail to be obtained from a full network of sensors. In theory, the technology could help combine the hall effect (for tibial displacement) and a skin surface pressure sensor array across the residuum to help predict at what stage of the user's gait. The predictive nature of the technique allows for a corresponding loading response to be applied. The complexity of the predictive algorithm could be built to

include normal walking and the differences seen when walking on variable terrains, as seen by Portnoy et al. Currently, active lower limb prosthetics utilise similar ML methodologies to help power the response from driven knee and ankle joints to help provide the necessary energy to replicate the required biomechanics of a complete limb (A. Dillen, 2022). Although the methodology has yet to be applied to a tibial/socket stabilisation scenario, it still holds potential, although a rigorous and detailed clinical trial would be necessary. Not only to verify the technique but to build the algorithm suitably to prevent a lower level of error generation. It is likely necessary to provide different solutions to different populations of prosthetic users, differentiated by factors such as age, activity levels and cause of amputation. With iterations of design and trialling making, it is possible to establish the sensor data trends that would be appropriate to target. Whilst also making it to streamline the system, reducing the componentry makes the device easy to manufacture at a reduced cost. It maintains low dimension and mass to maintain user comfort and acceptance.

Clinical Implementation

Moving forward, another core concept of the project would involve any device's progression towards clinical implementation. The process to do this still needs to be fixed, but the Medicines & Healthcare Products Regulatory Agency (MHRA) has identified several points. These points can be elaborated on to explain how the clinical implementation process would look for the prosthetic device (MHRA, 2021). Although some variation is expected for prototype devices, any future design changes likely require further evaluation and acceptance by the governing bodies if made post-initial clinical study.

- Device compliance

A CE mark will be necessary for any medical devices being designed for retail. However, for specific medical devices produced in-house for patients with no objective to place on the

market, the MHRA does not need to notify (Research and Governance Integrity Team, 2021). It would be possible to limit the need for full MHRA acceptance as long as the device was in its secondary testing stage under the umbrella of a research group. However, when considering upscaling to a marketable device, full CE marking and compliance registration would need to be obtained. The data gathered from the study formed the start of the evidence base to evaluate the device's efficacy, safety, and potential benefits for patients.

- Clinical Investigation

The MHRA states, “*Thus a clinical investigation of a non-UKCA/CE UKNI/CE marked device must be designed to establish that the performance claimed by the manufacturer can be adequately demonstrated and that the device is judged to be safe to use on patients taking into account any risks associated with the use of the device when weighed against the expected benefits.*” Not only does it highlight the need for data detailing the intended purpose realised, but it is also used safely with the target audience. Identifying the targeted patient groups is likely to be achieved through collaboration with healthcare providers, researcher groups, and specialists to define specific criteria for patient selection. With the intent to define and identify which patients would see high benefits or would require exclusion due to high risk. Whilst assessing factors such as demographics, medical history, and amputation cause. Working alongside the National Centre of Prosthetic and Orthotics, it would be possible to gain access to candidate patients and the wider prosthetic community associated with the centre, such as WestMARC rehabilitation. Making it possible to reach a large pool of candidates and screen those most fitting to the agreed-upon selection criteria.

Working in collaboration with such healthcare professionals and rehabilitation centres makes the implementation process a multi-stakeholder process. Helping to ensure best practices and

results for the prosthetic user. With workflows designed to include patient identification, assessment, device implementation, and follow-up care and review.

- Device Registration

Although only speculative to consider the device progressing to a marketable stage, it is possible to identify the key works needed to achieve market registration and compliance. Information on the workflows needed for review to assess that the device would be fit for purpose and issues would be addressed. Such information packages might include:

- Training needs patient device use
- Evidence-based guidelines and protocols following clinical assessment.
- Post-implementation monitoring,
- Response protocol potential adverse events
- Strategies for recalibration or readjustment
- Communication strategies to show the benefits and risks to patients.

Designed to establish effective use of the device whilst facilitating further data gathering and evaluation to encourage future redesign for delivering an improved system, achieving the desired aims more accurately.

Chapter 7 Conclusions

7.1 Introduction

With stress concentrations experienced by the residual limb of transtibial amputees being identified as a significant factor in the cause of DTI, a project involving the active and reactive response to the changing conditions experienced by prosthetic users was devised. Building on the knowledge of cellular strain localisation at mitigation devices at the skin's surface (Sengeh, 2013) and the inference that internal strains (particularly at the bone tissue interface of the tibia) are far greater in magnitude (Portnoy,2008). It was hypothesised that with the known tibial oscillation during gait (up to 25mm away from its mid-stance position (Lilja,1993), reducing the high-strain levels within the residual limb would be possible if suitable stabilisation. A proof-of-concept device was developed to test this theory to impart a proportional load to the anterior and posterior shank surfaces.

7.3 Conclusions

This thesis hypothesised that tibial stabilisation by an external device could reduce the risk of tissue migration of transtibial amputees and the risk of associated injuries. Deep tissue injury generated by using below-knee prosthetics is becoming a more prevalent risk, with ambulation on various terrains showing evidence of large shear strains being exerted on the tissue of the residual limb. Significant strains have been identified at the bone tissue interface, with peak strains identified to correlate with tibial oscillations at their largest magnitudes. Tibial oscillation was identified as a controllable variable to help reduce strain induction. However, there needs to be more available technology designed specifically for the purpose. To target tibial stabilisation, a proof-of-concept device was designed to lay the groundwork for future development, investigating Hall effect sensors coupled with linear actuators for loading.

The device was one of the first to target tibial oscillation as the main contributing factor to residual limb injury rather than focusing on skin-socket level interaction. A custom orthotic device was produced to simulate a prosthetic socket environment on a less vulnerable participant, allowing the system to be tested to assess its performance. The device needed to be more precise in its approach, with the author's inexperience and the project time restraints identified as key limitations in the process. However, walking trials were carried out with the system disengaged to form a baseline and with the device engaged to assess the effectiveness of the stabilisation. With data tracked through Hall Effect measurement and validated with CAREN data, the latter showing stabilisation was observed particularly at the heel strike phase of gait but less so at Toe Off. In addition, further thought was put into how best to trial the device on the target demographic, whereby a visual technique was developed for use with ultrasound scanning technology coupled with OpenCV motion tracking to test the device without invasive surgery. However, further trials were not started due to the time restrictions of the project.

Despite initial evidence showing promise, the thesis has limitations in the extent to which the device was tested. The project would have benefitted from later studies exploring the extent of stabilisation in more detail, particularly on the targeted demographic. It is yet to be determined whether the device would reduce the risk of tissue migration-related injuries as was intended at the offset. Future studies would explore this problem, not only by trialling the device on below-knee prosthetic users. But also streamlining the device and the associated technology makes it more suitable for satisfying the targeted user's basic needs.

Bibliography

- A. Buis, J. Bagwell. 2019. Ethics Application Form. Ethics Application, Univeristy of Strathclyde.
- A. Buis, M. Kamyab, S. Hillman, K. Murray and A. McGarry. 2017. "A Preliminary Evaluation of a Hydro-cast Trans-femoral Socket, a Proof of Concept." *Prosthetics and Orthotics Open Journal* 1 - 7.
- A. Cochis, M. Miola, O. Bretcanu, L. Rimondini, E.Verne. 2017. "Magnetic BioactiveGlass Ceramics for Bone Healing and hyperthermic Treatment of Solid Tumors." In *Advanced Magnetic and Optical Materials*, by P. K. Iyer, V. Kumar, H. Swart A. Tiwari, 81 - 103. United States of America: Scrivener.
- A. Dillen, E. Lathouwers, A. Miladinovic, U. Marusic, F. Ghaffari, O. Romain, R. Meeusen, K. Pauw. 2022. "A data-driven machine learning approach for brain-computer interfaces targeting lower limb neuroprosthetics." *Frontiers in Human Neuroscience*.
- A. Gefen, B. van Nierop, D. L. Bader, C. W. Oomens. 2008. "Strain-time cell-death threshold for skeletal muscle in a tissue-engineered model system for deep tissue injury." *Journal of Biomechanics* 2003 - 2012.
- A. Gefen, K. J. Farid, I. Shaywitz. 2013. "A Review of Deep Tissue Injury Development, Detection, and Prevention: Shear Savvy." *Ostomy Wound Management* 26 - 35.
- A. Kemper, C. McNally, E. Kennedy, S. Manoogian, S. Duma. 2008. "The Material Properties of Human Tibia Cortical Bone in Tension and Compression: Implications for the Tibia index." *Journal of Biomedical Science (Virginia Tech)* 419 - 427.

- A. Masum, M. Pickering, A. Lambert, J. Scarvell, P. Smith. 2014. "Accuracy assessment of Tri-plane B-mode ultrasound for non-invasive 3D Kinematics analysis of knee joints." *BioMedical Engineering OnLine* 1-16.
- A. Nia, G. Toetschinger, T. Kubinec, S. Domayer. 2022. "Evaluation of the new, patient-adjustable socket system Varos in the early phase of prosthetic rehabilitation: a pilot study." *European Journal of Physical and Rehabilitation Medicine* 462 - 469.
- A. Pachi, T. Ji. 2005. "Frequency and velocity of people walking." *The Structural Engineer* 36 - 40.
- A. Roche, H. Rehbaum, D. Farina & O. Aszmann. 2017. "Prosthetic Myoelectric Control Strategies: A Clinical Perspective." *Current Surgery Reports* 1 - 11.
- A. Rowlands, F. A. Duck, J. L. Cunningham. 2008. "Bone vibration measurement using ultrasound: Application to detection of the hip prosthesis loosening." *Medical Engineering & Physics* 30 278-284.
- A. S. Dickinson, J. W. Steer, P. R. Worsley. 2017. "Finite element analysis of the amputated lower limb: A systematic review and recommendations." *Medical Engineering and Physics* 1 - 18.
- A. Salawu, C. Middleton, A. Gilbertson, K. Kodavali, V. Neuman. 2006. "Stump ulcers and continued prosthetic limb use." *Prosthetics and Orthotics International* 279 - 285.
- A. Shkel, R. Horowitz, A. A. Seshia, S. Park, R. T. Howe. 1999. "Dynamics and control of Micromachined Gyroscopes." *Proceedings of the American Control Conference*. San Diego: Berkeley Sensor & Actuator Center. 2119- 2124.
- A. Taggart, C. Benson, D. Kane. 2011. "Ultrasound in rheumatology." *Reports on the Rheumatic Disease*.

- A. Wilson, C. Schuch, R. Nitschke. 1987. "A Variable Volume Socket for Below-knee Prostheses." *Clinical Prosthetics and Orthotics* 11 - 19.
- Active_Robots. 2017. Actuator L12-30-50-06-R. Accessed March 2017. <http://www.active-robots.com/linear-actuator-112-30-50-06-r>.
- Agale, A. V. 2013. "Chronic Leg Ulcers: Epidemiology, Aetiopathogenesis, and Management." *Ulcers* 1 - 9.
- Arduino. 2020. Arduino Boards & Modules. Accessed July 14th, 2020. <https://store.arduino.cc/>.
- Arkin, R. C. 1991. "Reactive Control as a substrate for Telerobotic Systems." *Institute of Electrical and Electronic Engineers* 309 - 314.
- AspenCore. 2014. Electronics Tutorials. Accessed April 2021. <https://www.electronicstutorials.ws/electromagnetism/hall-effect.html>.
- B. J. Parmar, X. Yang, A. Chaudhry, P. S. Shajudeen, S. P. Nair, B. K. Weiner, E. Tasciotti, T. A. Krouskop, R. Righetti. 2016. "Ultrasound elastography assessment of bone/soft tissue interface." *Physics in Medicine & Biology* 61 131 - 150.
- B. J. Ranger, M. Feigin, X. Zhang, A. Mireault, R. Raskar, H. M. Herr, B. W. Anthony. 2016. "3D optical imagery for motion compensation in a limb ultrasound system." *Medical Imaging 2016: Ultrasonic Imaging and Tomography*. San Diego.
- B. Johnson, C. A. Mushett, K. Richter, G. Peacock. 2004. *Sport for Athletes with Physical Disabilities: Injuries and Medical Issues*. Review, Atlanta: Blaze Sports America.
- B. Ludescher, P. Martirosian, S. Lenk, J. Machann, F. Dammann, F. Schick, C. Claussen & H. Schlemmer. 2005. "High-Resolution Magnetic Resonance Imaging of Trabecular Bone in the Wrist at 3 Tesla: Initial Results." *Acta Radiologica* 306-309.

- B. M. Isaacson, T. M. Swanson, P. F. Pasquina. 2013. "The use of a computer-assisted rehabilitation environment (CAREN) for enhancing the wounded warrior rehabilitation regimens." *The Journal of Spinal Cord Medicine* 296 - 299.
- B. Parmar, X. Yang, A. Chaudhry, P. Shafeeq, S. P. Nair, B. K. Weiner, E. Tasciotti, T. A. Krouskop, R. Righetti. 2016. "Ultrasound elastography assessment of bone/ soft tissue interface." *Physics in Medicine & Biology* 131-150.
- B. Sonies, C. Wang, D. J. Sapper. 1996. "Evaluation of Normal and Abnormal Hyoid Bone Movement During Swallowing By Use of Ultrasound Duplex-Doppler Imaging." *Ultrasound in Medicine & Biology* 1169-1175.
- Bagwell, J. 2016. "The development of an adaptive and reactive interface system for lower limb prosthetic application." EngD Summer Project, Glasgow.
- Banzai, M. 2008. *Getting Started with Arduino*. Sebastopol: Make:Books.
- Bionics, Open. 2018. Hero Arm - User Guide. Accessed June 12, 2020. <https://openbionics.com/hero-arm-user-guide/>.
- C. Garcia, D. M. Prett, M. Morari. 1989. "Model Predictive Control: Theory and Practice - a Survey." *Automatica* Vol. 25 335-348.
- C. Nayak, A. Singh, H. Chaudhary. 2014. "Customised prosthetic socket fabrication using 3D scanning and printing." *Additive Manufacturing Society of India*. Bangalore. 1 - 10.
- C. Twist, Y. Kimyogo, R. L. Solis, K. V. Mushahwat. 2012. "Reversal of Deep Tissue Injury using Intermittent Electrical Stimulation." *International Functional Electrical Stimulation Society*.

- Ceramic, PI. 2017. P-080 PICMA® Stack Multilayer Ring Actuator. Accessed 2017. <https://www.piceramic.com/en/products/piezoceramic-actuators/linear-actuators/p-080-picma-stack-multilayer-ring-actuator-100820/>.
- Childress, D. S. 1985. "Historical Aspects of Powered Limb Prostheses." *Clinical Prosthetics & Orthotics* 2 - 13.
- Coalition, Amputee. 2017. Limb Loss Statistics. Accessed March 2017. <http://www.amputee-coalition.org/limb-loss-resource-center/resources-by-topic/limb-loss-statistics/limb-loss-statistics/>.
- D. A. Nowak, J. Hermsdorfer, K. Rost, D. Timmann, H. Topka. 2004. "Predictive and reactive finger force control during catching in cerebellar degeneration." *The Cerebellum* 227 - 235.
- D. Boone, T. Kobayashi, T. Chou, A. Arabian, K. Coleman, M. Orenduff, M. Zhang. 2013. "Influence of malalignment on Socket reaction moments during gait in amputees with transtibial prostheses." *Gait & Posture* 620 - 626.
- D. Felix, S. Tanriverdi, C. Trivedi, E. Wenzlaff. 2016. Designing a Dynamic Prosthetic Socket for Transtibial Amputees. Dissertation: Degree of Bachelor of Science in Biomedical Engineering, Robotics Engineering and Mechanical Engineering, Design concentration, Worcester, Massachusetts: Worcester Polytechnic Institute.
- D. Gouwanda, A. Senanayake. 2011. "Identifying gait asymmetry using gyroscopes - A cross-correlation and normalized symmetry index approach." *Journal of Biomechanics* 972 - 978.
- D. Ho, E. Kim. 2009. "Optical Skin-fat Thickness Measurement Using Miniaturized Chip LEDs: A Preliminary Human Study." *Journal of the Optical Society of Korea* 304-309.

- D. J. Brenner, E. J. Hall. 2007. "Computed Tomography - An Increasing Source of Radiation Exposure." *The New England Journal of Medicine* 2277-2284.
- D. Landau, R. Lozano, M. M'Saad, A. Karimi. 2011. *Adaptive Control: Algorithms, Analysis and Applications*. Springer Science & Business Media .
- D. M. Sengeh, H. Herr. 2013. "A Variable-Impedance Prosthetic Socket for a Transtibial Amputee Designed from Magnetic Resonance Imaging Data." *Journal of Prosthetics and Orthotics* Volume 25 Number 3.
- D. M. Sengeh, K. M. Moerman, A. Petron, H. Herr. 2016. "Multi-Material 3-D Viscoelastic Model of a Transtibial Residuum from In-vivo Indentation and MRI Data." *Journal of the Mechanical Behaviour of Biomedical Materials* 1 - 24.
- D. R. Berlowitz, D. M. Brienza. 2007. "Are All Pressure Ulcers the Result of Deep Tissue Injury? A Review of the Literature." *Wound Management and Prevention* 53(10):34:38.
- D. Xia, C. Yu, L. Kong. 2014. "The Development of Micromachined Gyroscope Structure and Circuitry Technology." *Sensors* 1394 - 1473.
- Derman, W. *Stump-Socket Interface and Effect on Injury & Illness in Athletes with Amputations: A Team-Physicians Perspective*. Presentation, Cape Town: Clinical Sports & Exercise Medicine Research Group & IOC Research Centre.
- E. A. Al-Fakih, N. A. A. Osman, F. R. M. Adikan. 2016. "Techniques for Interface Stress Measurements within Prosthetic Sockets of Transtibial Amputees: A Review of the Past 50 Years of Research." *Sensors* 1 - 30.
- E. Antonsson, R. W. Mann. 1985. "The Frequency Content of Gait." *Journal of Biomechanics* 39 - 47.

- E. Baklouti, N. B. Amor, M. Jallouli. 2017. "Reactive control architecture for mobile robot autonomous navigation." *Robotics and Autonomous Systems* 89 9 - 14.
- E. Ceseracciu, Z. Sawacha, C. Cobelli. 2014. "Comparison of Marker less and Marker - Based Motion Capture Technologies Through Simultaneous Data Collection during Gait: Proof of Concept." *PLOS ONE* 9 1 - 7.
- E. E. Drakonaki, G. M. Allen, D. J. Wilson. 2012. "Ultrasound elastography for musculoskeletal applications." *The British Journal of Radiology* 85 1435 - 1445.
- E. J. Chen, J. Novakofski, W. K. Jenkins, W. D. O'Brien. 1996. "Young's Modulus Measurement of Soft Tissues with Application to Elasticity Imaging." *IEEE Transactions on Ultrasonics, Ferroelectrics and Frequency Control* 191 - 194.
- E. Kim, R. Leesungbok, S. Lee, J. Hong, E. Ko, S. Ahn. 2017. "Effects of static magnetic fields on bone regeneration of implants in the rabbit: micro-CT, histologic, microarray, and real-time PCR analyses." *Clinical Oral Implants Research* 396 - 405.
- Ertl, C. 2018. "Lower Extremity traumatic amputations - brief review of reconstruction, wound and soft tissue management, alternatives to conventional practice." *Journal of Emergency and Critical Care Medicine* 1 - 7.
- F. Crespi, S. Cattani, M. Donini, A. Bandera, L. Rovati. 2016. "In vivo real time non invasive monitoring of brain penetration of chemicals with near-infrared spectroscopy: Concomitant PK/PD analysis." *Journal of Neuroscience Methods* 79-86.
- F. Cui, Y. Pan, H. Xie, X. Wang, H. Shi, J. Xiao, H. Zhang, H. Chang, L. Jiang. 2016. "Pressure Combined with Ischemia/Reperfusion Injury Induces Deep Tissue Injury via Endoplasmic Reticulum Stress in a Rat Pressure Ulcer Model." *International Journal of Molecular Sciences* 17(3):284.

- Fricke, G. 1996. "Successful Individual Approaches in Engineering Design." *Research in Engineering Design* 151 - 165.
- G. Bennett, C. Dealey, J. Posnett. 2004. "The cost of pressure ulcers in the UK." *Age and Aging* 33: 230 - 235.
- G. Bradskit, A. Kaehler. 2008. *Learning OpenCV: Computer Vision with the OpenCV Library*. Sebastopol: O'Reilly Media Inc.
- G. Hurley, R. Mckenney, M. Robinson, M.Zadravec, M. Pierrynowski. 1990. "The role of the contralateral limb in below-knee amputee gait." *Prosthetics and Orthotics International* 33 - 42.
- G. Katti, S. Ara, A. Shireen. 2011. "Magnetic Resonance Imaging (MRI) - A Review." *International Journal of Dental Clinics* 65-70.
- G. Kim, Y. Z. Cho, S. K. Baik, M. Y. Kim, W. K. Hong, S. O. Kwon. 2015. "The Accuracy of Ultrasonography for the Evaluation of Portal hypertension in Patients with Cirrhosis: A Systematic Review." *Korean Journal of Radiology* 314-325.
- G. Li, T.A. Kuiken. 2008. "Modelling of Prosthetic Limb Rotation Control by Sensing Rotation of Residual Arm Bone." *IEEE Transactions on Biomedical Engineering* 2134-2142.
- G. M. Hefferman, F. Zhang, M. J. Nunnery, H. Huang. 2015. "Integration of surface electromyographic sensors with the transfemoral amputee socket: A comparison of four differing configurations." *Prosthetics and Orthotics International* 166 - 173.
- G. Mantovani, M. Lamontagne. 2017. "How Different Marker Sets Affect Joint Angles in Inverse Kinematics Framework." *Journal of Biomechanical Engineering* 044503.1-044503.7.

- G. Pahl, W. Beitz. 2013. *Engineering Design: A Systematic Approach*. Springer Science & Business Media.
- G. Pirouzi, N. A. Abu Osman, A. Eshraghi, S. Ali, H. Gholizadeh, W. A. B Wan Abas. 2014. "Review of the Socket Design and Interface Pressure Measurement for Transtibial Prosthesis." *The Scientific World Journal* 1 - 9.
- G. T. Clement, H. Nomura, H. Adachi, T. Kamakura. 2013. "The feasibility of non-contact ultrasound for medical imaging." *Physics in Medicine and Biology* 58 6263 - 6278.
- G. Kim, Y. Z. Cho, S. K. Baik, M. Y. Kim, W. K. Hong, S. O. Kwon. 2015. "The Accuracy of Ultrasonography for the Evaluation of Portal hypertension in Patients with Cirrhosis: A Systematic Review." *Korean Journal of Radiology* 314-325.
- Geethanjali, P. 2016. "Myoelectric control of prosthetic hands: state-of-the-art review." *Medical Devices: Evidence and Research* 247 - 255.
- Gefen, A. 2011. "How do microclimate factors affect the risk of superficial pressure ulcers: a mathematical modelling study." *Journal of Tissue Viability* 81 - 88.
- Gefen, A. 2007. "Risk factors for pressure-related deep tissue injury: a theoretical model." *Medical & Biological Engineering & Computing* 563 - 573.
- Gonzalez, C. 2015. *Pneumatic, Hydraulic, and Electrical Actuators?* Accessed July 14, 2020. <https://www.machinedesign.com/mechanical-motion-systems/linear-motion/article/21832047/whats-the-difference-between-pneumatic-hydraulic-and-electrical-actuators>.
- Goulding, V. 2015. "The effects of diabetes on collagen within wound healing." *The Diabetic Foot Journal* 75 - 80.

- H. E. Harding, R. Langdale-Kelham. 1957. "Amputation Stumps." *The Journal of Bone and Joint Surgery* 221 - 223.
- H. E. Meulenbelt, J. H. Geertzen, M. F. Jonkman, P.U. Dijkstra. 2009. "Determinants of Skin Problems of the Stump in Lower-limb Amputees." *Archives of Physical Medicine and Rehabilitation* 74 - 81.
- H. Gholizadeh, N. A. Abu Osman, M. Kamyab, A. Eshraghi, W. A. B. Wan Abas, M. N. Azam. 2012. "Transtibial prosthetic socket pistoning: Static evaluation of Seal-In X5 and Dermo Liner using motion analysis system." *Clinical Biomechanics* 34-39.
- H. J. Kim, D. H. Shim. 2003. "A flight control system for aerial robots: algorithms and experiments." *Control Engineering Proactive* 11 1389 - 1400.
- Honeywell. 2013. Hall Effect Sensing and Application. Illinois: honeywell.com/sensing.
- Hrdlicka, A. 1898. "Study of the Normal Tibia." *American Anthropologist* 307 - 312.
- I. K. Kuder, A. F. Arrieta, W. E. Raither, P. Ermanni. 2013. "Variable stiffness material and structural concepts for morphing applications." *Journal of Progress in Aerospace Sciences* 63 33-55.
- I. Kovac, V. Medved, L. Ostojic. 2009. "Ground Reaction Force Analysis in Traumatic Transtibial Amputees' Gait." *Collegium Antropologicum* 107 - 114.
- Ialzzo, P. A. 2004. "Temperature modulation of pressure ulcer formation: using a swine model." *WOUNDS* 37 - 43.
- J. Goh, P. Lee, S. Chong. 2003. "Stump/socket pressure profiles of the pressure cast prosthetic socket." *Clinical Biomechanics* 18 237 - 243.

- J. Alberts, J. Hirsch, M. Koop, D. Schindler, D. Kana, S. Linder, S. Campbell, A. Thota. 2015. "Using Accelerometer and Gyroscopic Measures to Quantify Postural Stability." *Journal of Athletic Training* 578 - 588.
- J. B. Kosasih, M. B. Silver-Thorn. 1998. "Sensory Changes in Adults with Unilateral Transtibial Amputation." *J. Rehabil Res Dev* 35(1):85-90. PMID 9505256.
- J. Bramley, P. Worsley, D. Bader, C. Everitt, A. Darekar, L. King, A. Dickinson. 2021. "Changes in Tissue Composition and Load Response After Transtibial AMputation Indicate Biomechanical Adaptation." *Annals of Biomedical Engineering* 3176 - 3188.
- J. Buchanan, P. Sheppard, D. V. Lamsade. 1999. "Project ranking using ELECTRE III." *Journal of Multi-Criteria Decision Analysis*.
- J. Buijs, H. Hansen, R. Lopata, C. de Korte, S. Misra. 2011. "Predicting Target Displacements Using Ultrasound Elastography and Finite Element Modelling." *IEEE Transactions on Biomedical Engineering* 3143 - 3155.
- J. D. Carrico, T. Tyler, K. K. Leang. 2018. "A comprehensive review of select smart polymeric and gel actuators for soft mechatronics and robotics applications: fundamentals, freeform fabrication, and motion control." *International Journal of Smart and Nano Materials* 144 - 213.
- J. D. Stroncek, W. M. Reichert. 2008. *Indwelling Neural Implants: Strategies for Contending with In Vivo Environment*. Boca Raton: CRC Press/ Taylor & Francis.
- J. E. Sanders, S. Fatone. 2011. "Residual limb volume change: Systematic review of measurement and management." *Journal of Rehabilitation Research & Development* 949 - 986.

- J. E. Sanders, S. G. Zachariah, A. B. Baker, J. M. Greve, C. Clinton. 2000. "Effects of changes in cadence, prosthetic componentry, and time on interface pressures and shear stresses of three trans-tibial amputees." *Clinical Biomechanics* 15 684 - 694.
- J. Engsborg, A. Lee, K. Tedford, J. Harder. 1993. "Normative ground reaction force data for able-bodied and trans-tibial amputee children during running." *Prosthetics and Orthotics International* 83 - 89.
- J. Jezny, M. Curilla. 2013. "Position Measurement with Hall Effect Sensors." *American Journal of Mechanical Engineering* 231-235.
- J. Kahle, T. Klenow, M. Highsmith. 2016. "Comparative Effectiveness of an Adjustable Transfemoral Prosthetic Interface Accommodating Volume Fluctuation: Case Study." *Technology and Innovation* 175 - 183.
- J. L. Gennisson, T. Deffieux, M. Fink, M. Tanter. 2013. "Ultrasound elastography: Principles and techniques." *Diagnostic and Interventional Imaging* 94 487 - 495.
- J. Larsson, J. Apelqvist. 1995. "Towards less amputations in diabetic patients." *Acta Orthop Scand* 181 - 192.
- J. R. Figueira, V. Mousseau, B. Roy. 2016. "Electre Methods." In *Multiple Criteria Decision Analysis*, by Greco, Matthias, Ehrgott, Jose Rui, Figueira Salvatore, 155 - 185. New York: Springer.
- J. Saunders, B. Nicholson, S. Zachariah, D. Cassisi, A. Karchin, J. Ferguson. 2004. "Testing of elastomeric liners used in limb prosthetics: Classification of 15 products by mechanical performance." *Journal of Rehabilitation Research & Development* 175 - 186.
- J. T. Peery, W. R. Ledoux, G. K. Klute. 2005. "Residual - limb skin temperature in transtibial sockets." *Journal of Rehabilitation Research & Development* 147 - 154.

- J. ten Kate, G.Smit, P. Breedveld. 2017. "3D-printed upper limb prostheses: a review."
Disability and Rehabilitation: Assistive Technology 300 - 314.
- J. Ten Kate, G.Smit, P. Breedveld. 2017. "3D-printed upper limb prostheses: a review."
Disability and Rehabilitation: Assistive Technology 300 - 314.
- J. W. Nieves, C. Formica, J. Ruffing, M. Zion, P. Garrett, R. Lindsay, F. Cosman. 2005. "Males
Have Larger Skeletal size and Bone Mass Than Females Despite Comparable Body
Size." Journal of Bone and Mineral Research 529 - 535.
- J. Xiaohong, W. Rencheng, Z. Ming, L. Xiaobing. 2008. "Influence of Prosthetic Sagittal
Alignment on Trans-Tibial Amputee Gait and Compensating Pattern: A Case Study."
Tsinghua Science and Technology 581 - 586.
- S. L. Jacques, 2013. "Optical properties of biological tissues: a review." Physics in Medicine
and Biology 37-61.
- K. D. Murray, P. Convery. 2000. "The calibration of ultrasound transducers used to monitor of
the residual femur within a trans-femoral socket during gait." Prosthetics and Orthotics
International 24 55 - 62.
- K. Dermitzakis, A. H. Arieta, R. Pfeifer. 2011. "Gesture recognition in upper-limb prosthetics:
A viability study using Dynamic Time Warping and gyroscopes." 33rd Annual
International Conference of the IEEE EMBS. Boston: IEEE. 4530 - 4533.
- K. Kristjansson, J. S. Sigurdardogvarsson, A. O. Sverrisson, S. P. Sigurthosson, O. Sverisson,
A. Einarsson, K. Lechler, T. Ingarvarsson, M. Oddsson. 2017. "Prosthetic Control by
Lower Limb Amputees Using Implantable Myoelectric Sensors." Converging Clinical
and Engineering Research on Neurorehabilitation II 571- 574.

- K. M. Harmatys, E. L. Cole, B. D. Smith. 2013. "In Vivo Imaging of Bone Using a Deep-red Fluorescent Probe Bearing Multiple Iminodiacetates Groups." *Molecular Pharmaceutics* 4263-4271.
- K. Tong, M. Granat. 1999. "A practical gait analysis system using gyroscopes." *Journal of Medical Engineering & Physics* 87 - 94.
- K. Wolff, L. Goldsmith, S. Katz, B. Gilchrest, AS. Paller, D. Leffell. 2011. *Fitzpatrick's Dermatology in General Medicine*, 8th Edition. New York: McGraw-Hill.
- L. J. Marks, J. W. Michael. 2001. "Artificial limbs." *British Medical Journal* 732 - 735.
- L. O. Dissabandara, S. N. Nirthanan, T. K. Khoo, R. Tedman. 2015. "Role of cadaveric dissections in modern medical curricula: a study on student perceptions." *Anatomy & Cell Biology* 205 - 212.
- L. Shapiro, M. Harish, B. Hargreaves, E. Staroswiecki, G. Gold. 2012. "Advances in musculoskeletal MRI: Technical considerations." *Journal of Magnetic Resonance Imaging* 775 - 787.
- L. Yan, B. Zho, Z. Jiao, C. Chen, I. Chen. October 2014. "An Orientation Measurement Method Based on Hall-effect Sensors for Permanent Magnet Spherical Actuator with 3DMagnet Array." *Scientific Reports* 1-8.
- L. Yan, B. Zhu, Z. Jiao, C. Chen, I. Chen. 2014. "An Orientation Measurement Method Based on Hall-effect Sensors for Permanent Magnet Spherical Actuators with 3D Magnet Array." *Scientific Reports*.
- G. S. Leadstone, 1979. "The discovery of the Hall effect." *Physics Education* Volume 14 374 - 379.

- Loon, H. E. 1962. "Below-Knee Amputation Surgery." Orthotics and Prosthetics Library: Artificial Limbs 86 - 99.
- M. Ali, D. Magee, U. Dasgupta. 2008. "Signal Processing Overview of Ultrasound Systems for Medical Imaging." Journal of the Acoustical Society of America 1-26.
- M. Bey, S. Kline, S. Tashman, R. Zael. 2008. "Accuracy of biplane x-ray imaging combined with model-based tracking for measuring in-vivo patellofemoral joint motion." Journal of Orthopaedic Surgery and Research 1 - 8.
- M. Blagojević, U. Jovanović, I. Jovanović, D. Mancić, R. S. Popović. 2016. "Coreless Open-Loop Current Transducers Based on Hall Effect Sensor CSA-1V." Electronics and Energetics 489 - 507.
- M. C. Faustini, R. R. Neptune, R.H. Crawford, W. E. Rogers, G. Bosker. 2006. "An Experimental and Theoretical Framework for Manufacturing Prosthetic Sockets for Transtibial Amputees." IEEE Transactions on Neural and Rehabilitation Engineering 304 - 310.
- M. Clifford, L. Gomez. 2005. Measuring Tilt with Low-g Accelerometers. Tempe: NXP Freescale Semiconductor.
- M. F. Eilenberg, H. Geyer, H. Herr. 2010. "Control of a Powered Ankle-Foot Prosthesis Based on a Neuromuscular Model." Transactions on Neural Systems and Rehabilitation Engineering 18 164 - 173.
- M. Graser, S. Day, A. Buis. 2020. "Exploring the role of transtibial prosthetic use in deep tissue injury development: a scoping review." Biomedical Engineering.

- M. Gujjalapudi, C. Anam, P. Mamidi, R. Chiluka, A. G. Kuamr, R. Bibinagar. 2016. "Effect of Magnetic Field on Bone Healing around Endosseoud Implants - An In-vivo Study." *Journal of Clinical and Diagnostic Research* 1 - 4.
- M. H. J. Romanycia, F. J. Pelletier. 1985. "What is heuristic?" *Computational Intelligence* 47 - 58.
- M. J. Highsmith, J. T. Kahle, T. D. Klenow, C. R. Andrews, K. L. Lewis, R. C. Bradley, J. M. Ward, J. J. Orriola, J. T. Highsmith. 2016. "Interventions to manage residual limb ulceration due to prosthetic use in individuals with lower extremity amputation: A systematic review." *Tecnol Innov* 18: 115 - 123.
- M. J. Highsmith, J. T. Kahle, T. D. Klenow, C. R. Andrews, K. L. Lewis, R. C. Bradley, J. M. Ward, J. J. Orriola, J. T. Highsmith. 2016. "Interventions to Manage Residual Limb Ulceration due to Prosthetic use in Individuals with Lower Extremity Amputation: A Systematic Review of the Literature." *Journal of Technology and Innovation* 115 - 123.
- M. Lilja, T. Johansson, T. Oberg. 1993. "Movement of the tibial end in a PTB prosthesis socket: a sagittal X-ray study of the PTB prosthesis." *Prosthetics and Orthotics International* 21 - 26.
- M. Meißner, L. Blessing. 2006. "Defining an Adaptive Product Development Methodology." *International Design Conference* 69 - 78.
- M. R. Tucker, J. Oliver, A. Pagel, H. Bleuler, M. Bouri, O. Lamercy, J. Milian, R. Riener, H. Vallery, R. Gassert. 2015. "Control strategies for active lower extremity prosthetics and orthotics: a review." *Journal of Neuroengineering and Rehabilitation* 1 - 29.

- M. Reddy, S. S. Gill, S. R. Kalkar, W. Wu, P. J. Anderson, P. A. Rochon. 2008. "Treatment of Pressure Ulcers: A Systematic Review." *Journal of American Medical Association* 2647 - 2662.
- M. Stoppa, A. Chiolerio. 2014. "Wearable Electronics and Smart Textiles: A Critical Review." *Sensors* 11957 - 11992.
- M. Zhang, A. F. T. Mak. 1999. "In vivo friction properties of human skin." *Prosthetics and Orthotics International* 135 - 141.
- Mahajan, I. K. Moppett. R. P. 2004. "Transcranial Doppler ultrasonography in anaesthesia and intensive care." *British Journal of Anaesthesia* 710-724.
- Manucharian, S. R. 2011. "An Investigation of Comfort Level Trend Differences Between the Hands-On Patellar Tendon Bearing and Hands-off Hydrocast Transtibial Prosthetic Sockets." *Journal of Prosthetics and Orthotics* 23 124 - 140.
- Medicine, British Society of Rehabilitation. 2003. *Rehabilitation - Standards and Guidelines* (2nd Edition). London: British Society of Rehabilitation Medicine.
- Medicine, Netherlands Society of Physical and Rehabilitation. 2012. *Guideline Amputation and Prosthetics of the Lower Extremities. Guidelines*, Utrecht: Postbus.
- Melexis. 2016. Triaxis®: Unique position sensing solution. November. Accessed March 13th, 2017. <https://www.melexis.com/en/insights/knowhow/triaxis-position-sensing-solution>.
- MHRA. 2021. *Clinical investigations of medical devices - guidance for manufacturers*. Medicines & Healthcare products Regulatory Agency.
- Mollano, A. V. 2013. "Standard Below Knee Amputation." In *Operative Dictations in Orthopaedic Surgery*, by A. V. Mollano, 177-179. New York: Springer.

- N. Ahmad, G. N. Thomas, P. Gill, C. Chan, F. Torella. 2014. "Lower limb amputation in England: prevalence, regional variation and relationship with revascularisation, deprivation and risk factors. A retrospective review of hospital data." *Journal of the Royal Society of Medicine* 483 - 489.
- N. Mathur, I. Glesk, A. Buis. 2014. "Skin Temperature Prediction in Lower Limb Prostheses." *Journal of Biomedical and Health Informatics* 1 - 8.
- N. Ogawa, M. Hashimoto, M. Takasaki, T. Hirai. 2009. "Characteristics Evaluation of PVC Gel Actuators." *International Conference on Intelligent Robots and Systems*. St. Louis: IEEE. 2898 - 2903.
- N. Shanks, R. Greek, J. Greek. 2009. "Are animal models predictive for humans?" *Philosophy, Ethics, and Humanities in Medicine* 2009 1 - 20.
- NHS. 2023. *Prosthetic Service Review*. Accessed 2023. <https://www.england.nhs.uk/commissioning/spec-services/npc-crg/group-d/rehabilitation-and-disability/prosthetics-review/>.
- NPUAP. 2007. *NPUAP Pressure Ulcer Stages/Categories*.
- O. Bai, R. Atri, J. S. Marquez, D. Fei. 2017. "Characterization of lower limb activity during gait using wearable, multi-channel surface EMG and IMU sensors." *5th International Electrical Engineering Congress* 1 - 4.
- O. Cardin, D. Trentesaux, A. Thomas, P. Castagna, T. Berger, H. B. El-Haouzi. 2015. "Coupling predictive scheduling and reactive control in manufacturing hybrid control architecture: state of the art and future challenges." *Journal of Intelligent Manufacturing* 1 - 15.

- O. Fliegel, S. G. Feuer. 1966. "Historical Development of Lower-Extremity Prostheses." Orthopedic & Prosthetic Appliance Journal 313 - 324.
- Online, RS. 2017. Push Pull Action DC D-Frame Solenoid, 20mm stroke, 80W, 12 V dc . April. Accessed 2017. <http://uk.rs-online.com/web/p/dc-d-frame-solenoid/3073708/>.
- OWM, Ostomy Wound Management. 2014. Highlights from the International Forum on Deep Tissue Injury Evolution: A Research-based Scientific Collaborative. February. Accessed May 2017. www.o-wm.com.
- P. Convery, A. Buis. 1999. "Socket/stump interface dynamic pressure distribution recorded during the prosthetic stance phase of gait of a trans-tibial amputee wearing a hydrocast socket." Prosthetics and Orthotics International 107-112.
- P. Convery, K. D. Murray. 2001. "Ultrasound study of the motion of the residual femur within a trans-femoral socket during daily living activities other than gait." Journal of Prosthetics and Orthotics 25 220-227.
- P. Cortes, M. P. Kazmierkowski, R. M. Kennel, D. E. Quevedo, J. Rodriguez. 2008. "Predictive Control in Power Electronics and Drives ." IEEE Transactions on Industrial Electronics 4312 - 4324.
- P. F. Pasquina, M. Evangelista, A. J. Carvalho, J. Lockhart, S. Griffin, G. Nanos, P. McKay, M. Hansen, D. Ipsen, J. Vandersea, J. Butkus, M. Miller, I. Murphy, D. Hankin. 2015. "First-in-man demonstration of a fully implanted myoelectric sensors system to control an advanced electromechanical prosthetic hand." Journal of Neuroscience Methods 85 - 93.
- P. J. Kyberd, P. H. Chappell. 1993. "A force sensor for automatic manipulation based on the Hall effect." Measurement Science and Technology 281 - 287.

- P. Martins, F. Ferreira, R. N. Jorge, M. Parente, A. Santos. 2015. "Necromechanics: Death-induced changes in the mechanical properties of human tissue." *Journal of Engineering in Medicine* 343 - 349.
- Pedley, M. 2013. *Tilt Sensing Using a Three-Axis Accelerometer*. Tempe: NXP Freescale Semiconductor.
- Prawoto, Y. 2012. "Seeing auxetic materials from the mechanics point of view: A structural review on negative Poisson's ratio." *Computational Materials Science* 140 - 153.
- S. Pugh, 1991. *Total Design: Integrated Methods for Successful Product Engineering*. Essex: Prentice Hall.
- R. Bannatyne, G. Viot. 1998. "Introduction to Microcontrollers - Part 1." *Institute of Electrical and Electronics Engineers* 350 - 360.
- R. Morley, A. Sharma, A. Horsch, R. Hinchliffe. 2018. "Peripheral artery diseases." *BMJ* 1 - 8.
- R. Safari, A. McFadyen, P. Rowe, A. Buis. 2013. "Hands-off and Hands-on Casting Consistency of Amputee below Knee Sockets Using Magnetic Resonance Imaging." *The Scientific World Journal* 1 - 13.
- Research and Governance Integrity Team. 2021. *How to submit a clinical investigation for a non-CE marked device or a CE marked Device for a new purpose to the MHRA*. Imperial College Healthcare.
- Roszkowska, E. 2013. "Rank Ordering Criteria Weighting Methods - A Comparative Overview." *Optimum Studia Ekonomiczne* 5 14 - 31.

- RS-Online. 2017. Festo Double Action Pneumatic Compact Cylinder 12mm Bore, 30mm stroke. Accessed April 2017. <http://uk.rs-online.com/web/p/pneumatic-compact-cylinders/1215714/>.
- Festo Single Action Pneumatic Compact Cylinder 16mm Bore, 25mm stroke. Accessed April 2017. <http://uk.rs-online.com/web/p/pneumatic-compact-cylinders/1215492/>.
- S. Bohm, L. Mademli, F. Mersmann, A. Arampatzis. 2015. "Predictive and Reactive Locomotor Adaptability in Healthy Elderly: A Systematic Review and Meta-Analysis." *Journal of Sports Medicine* 1759 - 1777.
- S. D. Gupta, I. M. Shahinur, A. A. Haque, A. Ruhul, S. Majumder. 2012. "Design and Implementation of Water Depth Measurement and Object Detection Model Using Ultrasonic Signal System." *International Journal of Engineering Research and Development* 62-69.
- S. G. Zachariah, R. Saxena, J. R. Ferguson, J. E. Sanders. 2004. "Shape and volume change in the transtibial residuum over the short term: Preliminary investigation of six subjects." *Journal of Rehabilitation Research & Development* 683 - 694.
- S. Kim, J. Soh, K. Shin, J. Jeong, S. Myung. 2010. "Magnetic Shielding Performance of Thin Metal Sheets Near Power Cables." *IEEE Transactions on Magnetics* 682 - 685.
- S. Laing, P. Lee, J. Goh. 2011. "Engineering a Trans-Tibial Prosthetic socket for Lower Limb Amputee." *Annals Academy of Medicine* 252 - 259.
- S. Nayak, R. Das. 2020. "Application of Artificial Intelligence (AI) in Prosthetic and Orthotic Rehabilitation." In *Service Robotics*, by S. Oncu, P. Baykas V. Sezer.
- S. Pasco, O. Tolo. n.d. *The Doppler effect in medical ultrasound. Information Booklet*, Blackburn: Ultrasound Training Solutions.

- S. Portnoy, A. Kristal, A. Gefen, I. Siev-Ner. 2011. "Outdoor dynamic subject-specific evaluation of internal stresses in the residual limb: Hydraulic energy-stored prosthetic foot compared to conventional energy-stored prosthetic feet." *Gait & Posture* 1 - 5.
- S. Portnoy, G. Yamitzky, Z. Yizhar, A. Kristal, U. Oppenheim, I. Siev-Ner, A. Gefen. 2007. "Real-time patient-specific finite element analysis of internal stresses in the soft tissues of a residual limb: a new tool for prosthetic fitting." *Annals of Biomedical Engineering* 120 - 135.
- S. Portnoy, I. Siev-Ner, N. Shabshin, A. Gefen. 2010. "Effects of sitting postures on risks for deep tissue injury in the residuum of a transtibial prosthetic-user: a biomechanical case study." *Computer Methods in Biomechanics and Biomedical Engineering* 1 - 11.
- S. Portnoy, I. Siev-Ner, N. Shabshin, A. Kristal, Z. Yizhar, A. Gefen. 2009. "Patient-specific analyses of deep tissue loads post transtibial amputation in residual limbs of multiple prosthetic users." *Journal of Biomechanics* 42 2686-2693.
- S. Portnoy, J. van Haare, R. Geers, A. Kristal, I. Siev-Ner, H. Seelen, C. Oomens, A. Gefen. 2010. "Real-time subject-specific analyses of dynamic internal tissue loads in the residual limb of transtibial amputees." *Medical Engineering & Physics* 32 312-323.
- S. Portnoy, Z. Yizhar, N. Shabshin, Y. Itzchak, A. Kristal, Y. Dotan-Marom, I. Siev-Ner, A. Gefen. 2008. "Internal mechanical conditions in the soft tissues of a residual limb of a trans-tibial amputee." *Journal of Biomechanics* 1897-1909.
- S. Reinfeldt, B. Hakansson, H. Taghavi, M. Eeg-Olofsson. 2015. "New developments in bone-conduction hearing implants: a review." *Medical Devices: Evidence and Research* 79-93.

- S. S. Aher, A. Desarda, J. A. Shelke, M. Chaudhari. 2015. "A Review on Smart Materials: Future Potentials in Engineering." *International Journal of Science Technology and Management* Vol. No. 4, Issue 10, 7-16.
- S. S. S. Shikh, N. A. A. Osman, L. A. Latif. 2008. "Development of an Alternative Socket Fabrication Method Using Hydrostatic Cast System: A Preliminary Study." *Biomed* 2008, Proceedings 21. Berlin: Springer. 766 - 768.
- S. Shacham, D. Castel, A. Gefen. 2010. "Measurements of the Static Friction Coefficient Between Bone and Muscle Tissues." *Journal of Biomechanical Engineering* 084502-1 - 084502-4.
- S. Tashman, W. Anderst. 2003. "In-Vivo Measurement of Dynamic Joint Motion Using High Seed Biplane Radiography and CT: Application to Canine ACL Deficiency." *Journal of Biomechanical Engineering* 238 - 245.
- S. Leung, K. Zhao, M. Qu, K. An, R. Berger, C. H. McCollough. 2011. "Dynamic CT technique for assessment of wrist joint instabilities." *Journal of Medical Physics* 38 51-56.
- Safari, R. 2020. "Lower limb prosthetic interfaces: Clinical and technological advancement and potential future direction." *International Society for Prosthetics and Orthotics* 384 - 401.
- Segway. n.d. "A balanced approach to transport." Segway. www.segway.com.
- . n.d. "Designing magic." Segway. www.segway.com.
- Sengeh, D. M. 2013. "Design of a Variable-impedance Prosthetic Socket." *Journal of Prosthetics and Orthotics* 129 - 137.
- Sentron. 2008. *Current Sensing with the CSA-1V*. Application Note, Sentron.

- SMC. 2017. Electric Actuators. Accessed March 2017.
http://www.smcworld.com/actuator/en/mini.do?se_id=1672.
- T. Douglas, S. Solomonidis, W. Sandham, W. Spence. 2002. "Ultrasound Imaging in Lower Limb Prosthetics." *IEEE Transactions on Neural Systems and Rehabilitation Engineering* 11-21.
- T. Dumbleton, A. W. P. Buis, A. Mcfaden, B. F. McHugh, G. Mckay, K. D. Murray, S. Sexton. 2009. "Dynamic interface pressure distributions of two transtibial prosthetic socket concepts." *Journal of Rehabilitation Research & Development* 405 - 416.
- T. Jiang, H. Gradus, A. Rosellini. 2020. "Supervised machine learning: A brief primer." *Behaviour Therapy* 675 - 687.
- T. Kobayashi, M. Orendurff, M. Zhang, D. Boone. 2016. "Socket reaction moments in transtibial protheses during walking at clinically perceived optimal alignment." *Prosthetics and orthotics International* 503 - 508.
- T. L. Szabo, P. A. Lewin. 2013. "Ultrasound Transducer Selection in Clinical Imaging Practice." *Journal of Ultrasound in Medicine* 573-582.
- T. Leong, M. Ashok Kumar, S. Kentish. 2011. "The Fundamentals of Power Ultrasound - A Review." *Acoustic Australia* 39 54 - 63.
- T. P. Chenal, J. C. Case, J. Paik, R. K. Kramer. 2014. "Variable Stiffness Fabrics with Embedded Shape Memory Materials for Wearable Applications." *International Conference on Intelligent Robots and Systems* 2827-2831.
- T. P. Tomo, S. Somlor, A. Schmitz, L. Jamone, W. Huang, H. Kristanto, S. Sugano. 2016. "Design and Characterisation of a Three - Axis Hall Effect - Based Soft Skin Sensor." *Sensors* 1 - 11.

- T. Shina, K. R. Nightingale, M. L. Palmeri, T. J. Hall, J. C. Bamber, R. G. Barr, L. Castera, B. I. Choi, Y. Chou, D. Cosgrove, C. F. Dietrich, H. Ding, D. Amy, A. Farrokh, G. Ferraioli, C. Filice, M. Friedrich-Rust, K. Nakashima, F. Schafer, I. Sporea. 2015. "Wfumb Guidelines and Recommendations for Clinical use of Ultrasound Elastography: Part 1: Basic Principles and Terminology." *Ultrasound in Medicine & Biology* (41) 1126 - 1147.
- Tekscan. 2020. F-Scan System. June. Accessed June 11, 2020. <https://www.tekscan.com/products-solutions/systems/f-scan-system>.
- Therapy, MIST Ultrasound Healing. 2013. Early Intervention for Deep Tissue Injuries. Celleration.
- Ullman, G. G. 2006. *Making Robust Decisions*. Bloomington: Trafford Publishing.
- V. Rajtukova, R. Hudak, J. Zivcak, P. Halfarova, R. Kudrikova. 2014. "Pressure Distribution in Transtibial Prostheses Socket and the Stump Interface." *Procedia Engineering* 374 - 381.
- V. Stuphorn, E. E. Emeric. 2012. "Proactive and reactive control by the medial frontal cortex." *Frontiers in Neuroengineering* 1 - 11.
- Vanderwerker, E. E. 1976. "A Brief Review of the History of Amputations and Prostheses." *Inter-Clinic Information Bulletin* Vol 15, 15 - 16.
- VICON. 2013. "MOTEK Medical CAREN System." VICON. 05 March. Accessed March 12, 2018. <https://www.vicon.com/case-studies/life-sciences/motek-medical-caren-system>.
- Vougioukas, S. G. 2007. "Reactive Trajectory Tracking for Mobile robots based on Non-Linear Model Predictive Control." *IEEE International Conference on Robotics and Automation* 3074 - 3079.

- W. L. Childers, S. Siebert. 2016. "Marker-based method to measure movement between the residual limb and a transtibial prosthetic socket." *Prosthetics and Orthotics International* 720 - 728.
- Wake, W. T. 2010. "Pressure Ulcers: What Clinicians Need to Know." *The Permanente Journal* 56 - 61.
- Woodman, O. J. 2007. *An introduction to inertial navigation*. Cambridge: University of Cambridge Computer Laboratory.
- X. Chen, S. Chen, G. Dan. 2011. "Control of Powered Prosthetic Hand Using Multidimensional Ultrasound Signals: A Pilot Study." *Universal Accessing Human-Computer Interaction. Applications and Services*. Orlando: Springer. 688.
- X. Chen, S. Chen, G. Dan. 2011. "Control of Powered Prosthetic Hand Using Multidimensional Ultrasound Signals: A Pilot Study." *6th International Conference: Universal Access in Human-Computer Interaction. Applications and Services*. Orlando: Springer - Verlag. 322 - 327.
- X. Zhang, X. Chen, Y. Li, V. Lantz, K. Wang, J. Yang. 2011. "A Framework for Hand Gesture Recognition Based on Accelerometer and EMG Sensors." *IEEE Transactions On Systems, Man, And Cybernetics - Part A: Systems And Humans* 1064 - 1076.
- Y. Do, J. Kim. 2013. "Infrared Range Sensor Array for 3D Sensing in robotic Applications." *International Journal of Advanced Robotic Systems* 1-9.
- Y. Li, M. Hashimoto. 2016. "Development of a Lightweight Walking Assist Wear using PVC Gel Artificial Muscles." *International Conference on Biomedical Robotics and Biomechatronics*. Singapore: IEEE. 686 - 691.

- Y. Liu, H. Hu, J. K. C. Lam, S. Liu. 2010. "Negative Poisson's Ratio Weft-knitted Fabrics." *Textile Research Journal* 856 - 863.
- Y. Risodkar, G. Shirsath, M. Holkar, M. Amle. 2015. "Designing the Self - Balancing Platform (Segway)." *International Journal of Science, Engineering and Technology Research* 3033 - 3038.
- Y. Wu, D. W. J. Van de Schaft, F. P. Baaijens, C. W. J. Oomens. 2016. "Cell death induced by mechanical compression on engineered muscle results from a gradual physiological mechanism." *Journal of Biomechanics* 1071- 1077.
- Z. Ge, H. Hu, S. Liu. 2016. "A novel plied yarn structure with negative Poisson's ratio." *The Journal of The Textile Institute* 578 - 588.

Appendix - A

Circuit diagram for proof of concept device

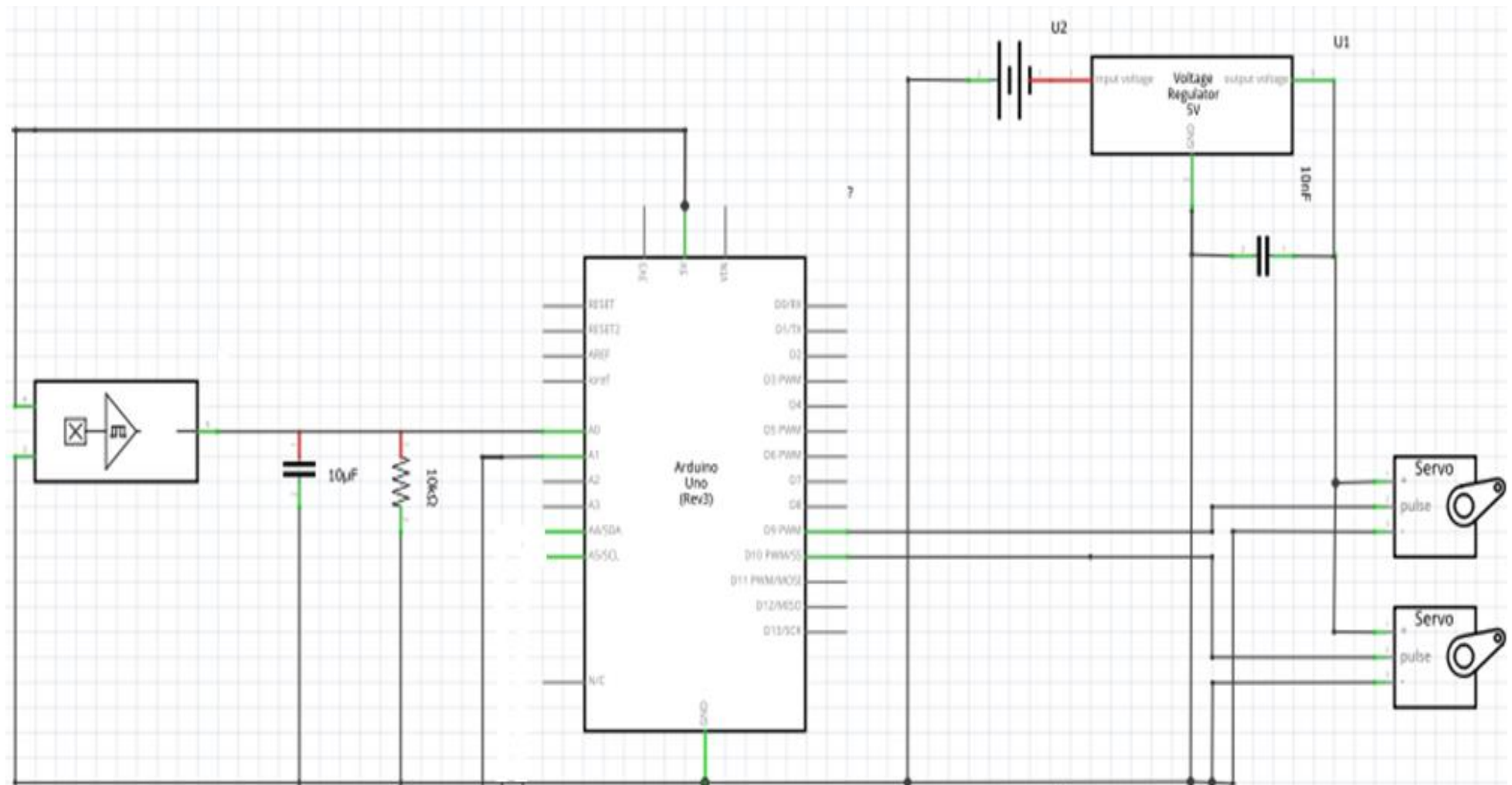


Figure 77: Circuit design, showing connections between the Hall effect sensing circuit, Arduino Uno and Futaba servos

Appendix – B

Ethics application for participant trialling

GENERAL RISK ASSESSMENT FORM (S20)



Persons undertaking risk assessments must have a level of competence commensurate with the significance of the risks they assess. Each Head of Department or Director of Service is responsible for ensuring that all staff are adequately trained in risk assessment techniques. In due course, the University document “Guidance on Carrying Out Risk Assessments” will be available to remind assessors of the current practice used by the University. However, reading the document above will not substitute suitable training.

Before the commencement of any work involving non-trivial hazards, a suitable and sufficient assessment of risks should be made, and effective measures taken to control those risks.

Individuals working under this risk assessment have a legal responsibility to ensure they follow the control measures stipulated to safeguard the health and safety of themselves and others.

SECTION 1

1.1 OPERATION / ACTIVITY		Complete the relevant details of the activity being assessed.	
Title:	A pilot study to investigate the effectiveness of a tibial stabilisation device designed to be implemented below the knee prosthesis.		
Department:	Biomedical Engineering		
Location(s) of work:	Biomechanics gait lab	Ref No.	
Brief description:			

To test a prosthetic socket stabilisation system designed to reduce injury and increase socket comfort and fit.

1.2 PERSON RESPONSIBLE FOR MANAGING THIS WORK

Name:	Dr Arjan Buis	Position:	Senior Research Fellow
Signature:		Date:	23-06-2015
Department:	Biomedical Engineering		

1.3 PERSON CONDUCTING THIS ASSESSMENT

Name:	Dr Arjan Buis	Signature:	
A date risk assessment is undertaken:	23-06-2015		

1.4 ASSESSMENT REVIEW HISTORY

This assessment should be reviewed immediately if there is any reason to suppose the original assessment is no longer valid. Otherwise, the assessment should be reviewed annually. The responsible person must ensure that this risk assessment remains valid.

	Review 1	Review 2	Review 3	Review 4
Due date:				
Date conducted:				
Conducted by:				

SECTION 2

Work Task Identification and Evaluation of Associated Risks					Page 2 of 6		Ref No.		
Component Task / Situation	Hazards Identified	Hazard Ref No.	Who Might Be Harmed and How?	Existing Risk Control Measures (RCM)	Likelihood	Severity	Risk Rating	Risk	RCM's
Gait trial on Motek Caren system	Could trip/fall	1	Prosthetic user	The volunteer will be secured with a safety harness that is part of the Caren system	1	1	1	L	Y
Gait trial on Motek Caren system	Component failure	2	Prosthetic user	The volunteer will be secured with a safety harness that is part of the Caren system	1	1	1	L	Y
Gait trial on Motek Caren system	Volunteer Fatigue	3	Prosthetic user	Regular breaks will be scheduled between trials to allow the volunteer to recover. The trial will be stopped immediately if the volunteer feels fatigued during the study.	1	1	1	L	Y
Load application	Excessive pressure (system measured)	4	Prosthetic user	The device will be fitted with a force sensor feedback system. This will immediately cut off the electrical supply to	1	1	1	L	Y

				the actuators, thus removing all loading from the participant's leg if the measured forces exceed a pre-set limit of 40N. The device shutdown will also be programmed to require a full reset if this eventuality occurs, meaning the participant will no longer be at risk of allowing the device to be checked before continuing.					
Load Application	Excessive pressure (volunteer feedback)	5	Prosthetic user	If the participant indicates discomfort from too great a pressure that the sensor feedback system does not detect. An external volunteer-held kill switch will be fitted to the device, allowing direct intervention from the volunteer in shutting down the device at the first indication of discomfort.	1	1	1	L	Y
Conventional socket casting	Volunteer discomfort	6	Participant	With the casting being carried out by an experienced prosthetist, the process can be	1	1	1	L	Y

				stopped and adjusted quickly and easily if the participant indicates any discomfort.					
Pressure socket casting	Volunteers Discomfort	7	Participant	The casting device can be stopped immediately at any sign of discomfort. The device has already passed the necessary health and safety requirements for use.	1	1	1	L	Y

SECTION 4

RECORD OF SIGNIFICANT FINDINGS

Page 5 of 6

Ref No.

Where this Section is to be given to staff etc., without Sections 2 & 3,
please attach a copy of the relevant Section 1 details to the front of this page.

The significant findings of the risk assessment should include details of the following:

- The identified hazards
- Groups of persons who may be affected
- An evaluation of the risks
- The precautions that are in place (or should be taken) with comments on their effectiveness
- Identified actions to improve control of risks, where necessary

Alternatively, where the work activity/procedure is complex or hazardous, then a written Safe System of Work (SSOW) or Standard Operating Procedure (SOP) is advised that should incorporate the significant findings. Such documents should, again, have the relevant Section 1 attached. Please state below whether either an SSOW or SOP is available in this case.

Relevant SSOW available

Yes

No

Relevant SOP available

Yes

No

Significant Findings: (Please use additional pages if further space is required)

Volunteers could trip/fall during gait trials on the Motek Caren system. This is a low risk (Likelihood 1; Severity 1; risk rating 1). As a precaution, the volunteer will be secured with a safety harness that is part of the Caren system reducing the risk of falls and personal injury.

The stabilisation system implemented could apply too much force to the volunteer's limb if it malfunctions. However, this is a low risk (Likelihood 1; Severity 1; risk rating 1). As a precaution, the device will be fitted with a kill switch feedback system that will shut off the device's power if pressure exceeds a predetermined value.

SECTION 5

RECEIPT OF SIGNIFICANT FINDINGS OF RISK ASSESSMENT

Page 6 of 6

Please copy this page if further space is required.

Ref No.

All individuals working on the risk assessment with the Ref. No. As shown, you must sign and date this Section to acknowledge that they have read the relevant risk assessment and are aware of its contents, plus the measures taken.

(or to be taken by them) to safeguard their health and safety and that of others.

If the following review of the assessment revisions is minor, signatories may initial these where they occur in the documentation to indicate they are aware of the changes made. If revisions are major, producing a new risk assessment and signature page is advisable.

NAME (Print)	SIGNATURE	DATE
Dr Arjan Buis		23-06-2015

Appendix - C

Open CV Code

The following section will show the initial code, broken down into sections, with comments on their content and general function.

```
from collections import deque  
from imutils.video import VideoStream  
import numpy as np  
import argparse  
import cv2  
import imutils  
import time  
From scipy.spatial import distance as dist
```

```
from an imutils import perspective
```

```
from imutils import contours
```

At the outset, the code establishes which packages and libraries must be called upon to allow access to the specific features, calculations and triggers made available through OpenCV. The main packages revolved around accessing and processing the video feed, with other packages designed to identify the key features of an image ready for further processing by written code instructions.

```
def midpoint(ptA, ptB):
```

```
    return ((ptA[0] + ptB[0]) * 0.5, (ptA[1] + ptB[1]) * 0.5)
```

A small calculation used in a later stage of the programme, in which a straight line joined the midpoints of two lines, was used to help establish the centre point of a bounding rectangle.

```
ap = argparse.ArgumentParser()
```

```
ap.add_argument("-v", "--video",
```

```
    help="path to the (optional) video file")
```

```
ap.add_argument("-b", "--buffer", type=int, default=32,
```

```
    help="max buffer size")
```

```
ap.add_argument("-w", "--width", type=int, default=20,
```

```
    help="width of the left-most object in the image (in millimetres)")
```

```
args = vars(ap.parse_args())
```

Parsing of the available command lines made the code more versatile, opening up the possibility of using it in conjunction with either a video or webcam, if necessary, with other lines generating values for the number of points available for tracking and specifying the set width of the reference object used in the distance calculations.

```
green lower = (159, 71, 0)
greenUpper = (255, 168, 111)
```

Although seen as greenLower and greenUpper here, this line of code defines the upper and lower bounds for the colour detected in the RGB scale, a value that could refer to any colour inputted by the code user.

```
if not args.get("video", False):
    vs = VideoStream(src=0).start()

Else:
    vs = cv2.VideoCapture(args["video"])

time.sleep(2.0)
```

The 'if' statement makes it possible to initialise the program whether a video file was supplied or not. In this way, the webcam feed could be selected following a brief warm-up period of the camera itself.

```
While True:

    frame = vs.read()

    frame = frame[1] if args.get("video", False) else frame
    If the frame is None:
        break

    frame = imutils.resize(frame, width=400)
    blurred = cv2.GaussianBlur(frame, (11, 11), 0)
    hsv = cv2.cvtColor(blurred, cv2.COLOR_BGR2HSV)
```

This loop begins processing each frame from either the video or webcam supply, sizing the frame ready for viewing at later stages and processing it into the chosen colour space. This made it possible to identify each frame's specific contours of interest.

```
mask = cv2.inRange(hsv, greenLower, greenUpper)
mask = cv2.erode(mask, None, iterations=2)
mask = cv2.dilate(mask, None, iterations=2)

cnts = cv2.findContours(mask.copy(), cv2.RETR_EXTERNAL,
                        cv2.CHAIN_APPROX_SIMPLE)
cnts = imutils.grab_contours(cnts)
cnts = sorted(cnts, key=cv2.contourArea, reverse=True)[:2]
```

'mask' refers to creating a new image in which only a specific range of colours appears. Further post-processing of this mask helped smooth and sharpen the detected areas by removing smaller interference blobs, leaving only larger, more significant contours. The various forms of 'cnts' is the process of identifying and targeting the specific contours within the mask, with the final line making it possible to choose only the two largest contours in the frame for final calculations. This process can be altered if more than one significant contour is needed for comparison against the reference contour.

```
cv2.imshow("mask", mask)

(cnts, _) = contours.sort_contours(cnts)
colours = ((0, 0, 255), (240, 0, 159), (0, 165, 255), (255, 255, 0),
           (255, 0, 255))
refObj = None
```

'Cv2.imshow' allows a monitoring screen displaying the coloured mask to be produced. Although not important to the code's functionality, it was inputted as a check to ensure the correct colours/objects in the image were being detected. The remaining code sorted the detected contours, allowing them to be read from left to right, meaning that the reference object used for the primary calculations needed to be placed on the left-hand side of the image.

```
For c in (cents):
```

```
if cv2.contourArea(c) < 100:  
    continue
```

```
    box = cv2.minAreaRect(c)  
    box = cv2.cv.BoxPoints(box) if imutils.is_cv2() else cv2.boxPoints(box)  
    box = np.array(box, dtype="int")
```

```
    box = perspective.order_points(box)
```

```
    cX = np.average(box[:, 0])  
    cY = np.average(box[:, 1])
```

This section controls the initial handling of the contours, with a minimum size helping reduce the potential jittery nature of the contour identification. The remaining lines coordinate the generation of the minimally-sized bounding rectangles, identifying the corner locations and generating the midpoints of the bounding lines.

```
If refObj is None:
```

```
    (tl, tr, br, bl) = box  
    (tlbX, tlbY) = midpoint(tl, bl)  
    (trbrX, trbrY) = midpoint(tr, br)
```

```
    D = dist.euclidean((tlbX, tlbY), (trbrX, trbrY))  
    refObj = (box, (cX, cY), D / args["width"])  
    continue
```

This part of the code assumes that the contour featured closest to the top-left of the zone would be the reference object for the calculation while establishing the distances between the bounding rectangle corners and the computed midpoint about the inputted reference object width specified at the beginning of the code.

```
orig = frame.copy()  
cv2.drawContours(orig, [box.astype("int")], -1, (0, 255, 0), 2)  
cv2.drawContours(orig, [refObj[0].astype("int")], -1, (0, 255, 0), 2)  
  
refCoords = np.vstack([refObj[0], refObj[1]])  
objCoords = np.vstack([box, (cX, cY)])
```

This section draws the contour-bounding box on the viewing screen while generating coordinates for the boxes bounding both the reference and target objects, including the centre point of the rectangle.

```
for ((xA, yA), (xB, yB), color) in zip(refCoords, objCoords, colors):
```

```
    cv2.circle(orig, (int(xA), int(yA)), 3, color, -100)
    cv2.circle(orig, (int(xB), int(yB)), 3, color, -100)
    cv2.line(orig, (int(xA), int(yA)), (int(xB), int(yB)),
            colour, 2)
```

```
    D = dist.euclidean((xA, yA), (xB, yB)) / refObj[2]
    (mX, mY) = midpoint((xA, yA), (xB, yB))
    cv2.putText(orig, "{:.1f}mm".format(D), (int(mX), int(mY - 10)),
            cv2.FONT_HERSHEY_SIMPLEX, 0.5, colour, 2)
```

This section increases the visual appeal of the display, marking the corners and centre points with dots and joining the corresponding corner markers with straight lines, for easier interpretation, before calculating the distance between the corner markers of the reference and targets objects and also the distances between the two bounding rectangles' centre points. These distances are later displayed on the corresponding lines drawn on the final virtual image.

```
cv2.imshow("frame", Orig)
cv2.waitKey(1)

cv2.destroyAllWindows()
```

Finally, the last display is called on to produce a real-time visual display of the two bounding rectangles with displacements marked in position before a final clean-up allows the programme to be closed and reset if required.